ACS OMEGA

Open Access

http://pubs.acs.org/journal/acsodf

Review

Recent Advances in Mesoporous Carbon Nitride-Based Materials for Electrochemical Energy Storage and Conversion and Gas Storage

Mustapha Balarabe Idris,* Zaharaddeen Musa Mohammed, Sadiya Nuhu, Halima Aliyu, Habu Abba, Bhekie B. Mamba, Devaraj Sappani, and Fuku Xolile

Cite This: *ACS Omega* 2025, 10, 18184−18212

Read Online

ACCESS | Metrics & More | Article Recommendations

ABSTRACT: Mesoporous carbon nitride (MCN) is a fascinating material with enhanced textural properties, tailored morphology and enriched surface functionalities. Hence, it demonstrates promising performance in various applications. Over the years, various methods such as hard template, soft template, template-free, etc. have been adopted toward the preparation of MCN with controlled structural properties. Furthermore, the exciting properties of MCN have been fine-tuned by controlling the morphology and tuning the textural properties and surface functionalities, including the type and amount of nitrogen, via simple adjustment of the precursors, the carbonization temperature and the nature of the structure-directing agents/hard template. Besides these, the integration of conductive carbon, heteroatoms, metal-based materials, organic molecules, etc. was found to not only enhance MCN's performance in the already existing applications but also open up more exciting applications. The present Review begins by providing a general overview of the salient features of MCN, which dictate its performance in the various applications. Then, the Review discusses the trends in the applications of MCN-based material in the areas of electrochemical energy storage and conversion and gas storage in the past decade. The structure−property relationships of MCN-based materials in the above-mentioned applications are also discussed in detail. Emphasis is given to the role of the synthetic approach adopted and the nature of the precursor(s) used toward controlling the textural, morphological properties and chemical composition of MCN-based materials in obtaining the final product with improved performance. Moreover, the effects of modifications of key features of MCN on its electrochemical performance are also discussed. Finally, the current challenges and perspectives are provided, thereby guiding future research in the field of MCN-based materials for electrochemical energy storage and conversion and gas storage.

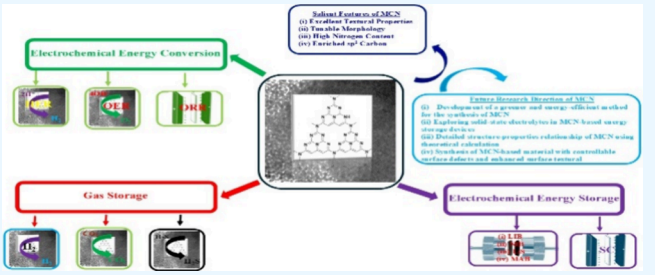

1. INTRODUCTION

Carbon nitrides (CNs) are emerging metal-free semiconducting materials with various applications owing to their fascinating properties such as superior mechanical strength, flexibility, chemical and thermal robustness, etc.[1−3] Primarily, CNs are made up of carbon and nitrogen, and the presence of nitrogen in their structural framework endows them with exceptional electronic and field emission properties. Indeed, five different structures of CNs have been predicted based on density functional calculations.[4−6] Among them, graphitic carbon nitride ($g\text{-}C_3N_4$, g-CN) is considered to be the most stable under ambient conditions. g-CN, prepared using various methods including ion implantation[7,8] and polycondensation of nitrogen-containing precursors,[9,10] is believed to consist of layered structures that are linked by weak intermolecular forces, forming an extended stacked structure similar to that of graphite.[11,12] Though the predicted stoichiometric ratio between C and N in g-CN is 0.75, it remains rather a herculean task to prepare g-CN without a trace of defects or hydrogen/oxygen or other elemental impurities, thereby creating a significant debate on naming g-CN.[1,13−15] In an attempt to address this concern, other compounds exhibiting lower or higher amounts of nitrogen content have been included in the family of g-CN.[3] It is worth mentioning that the imperfection in the stoichiometric ratio of g-CN arises from structural defects introduced during the reaction process and the extent of polycondensation of precursor(s). In general, using a lower polycondensation temperature and a single precursor allows the preparation of g-CN with higher nitrogen content and thus a C/N ratio close to the ideal for g-CN. Although there are various methods available for the synthesis of g-CN, thermal polycondensation of precursor(s) containing a high amount of nitrogen receives more attention owing to its

Received: January 22, 2025
Revised: March 21, 2025
Accepted: March 27, 2025
Published: May 1, 2025

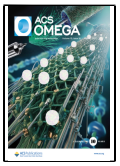

simplicity, cost-effectiveness and, most importantly, the ability to fine-tune the chemical composition of the final products.[16,17] One major limitation of direct thermal polycondensation of nitrogen-rich precursor(s) into g-CN is the formation of bulk and nonporous byproducts with extremely low specific surface area. Therefore, the utilization of bulk and nonporous g-CN in applications where textural properties play a significant role, such as adsorption, catalysis, electrochemical energy storage and conversion, etc., is quite limited. A pioneering work credited to Vinu et al. in 2005 is considered a turning point in the space of g-CN.[15] The work presented a novel approach for the introduction of mesoporosity into the structural framework of g-CN without noticeably changing its unique properties. Thereafter, various researchers reported the preparation and functionalization of mesoporous carbon nitride (MCN) for various applications utilizing different approaches, as comprehensively discussed in a review by the Vinu group.[1] On the other hand, improvements in the textural properties of MCN not only enhanced its performance in the previously explored applications but also opened up more exciting applications. In the past few decades, a large number of review articles have been published in the areas of synthesis, properties and applications of g-CN and its composites for various applications. For instance, Das et al.[18] discussed the electrochemical energy storage applications of g-CN nanosheets systems, Chaluvachar et al.[19] and Thomas and his coworkers[20] provided overviews of the utilization of 2D g-CN as an electrode material for rechargeable batteries as well as electrolyte fillers, and Sajid et al.[21] highlighted the challenges and prospects of utilization of g-CN for lithium ion batteries. The review articles by Iqbal et al.[22] and Safaei et al.[23] discussed the electrochemical energy storage of g-CN systems, whereas Ghaemmaghami et al.[24] and Govindaraju et al.[25] highlighted the supercapacitive performance of g-CN and the electrocatalytic properties of g-CN and its composites, respectively. Furthermore, Pachaiappan et al.[26] reviewed the recent advances in the photocatalytic applications of g-CN, including hydrogen production and storage. The influences of synthetic conditions on the electronic structure and photocatalytic properties of g-CN have also been discussed. Recent advances in the synthesis and modification of g-CN toward photocatalytic-related conversation applications, including photocatalytic hydrogen generation, CO_2 reduction and N_2 fixation, were reported by Tang et al.[27] It is worth mentioning that the above reviews mainly focused on the photocatalytic energy conversion applications of pristine g-CN and either provided a limited discussion on electrochemical energy storage or did not discuss the electrocatalytic and gas storage applications of g-CN. Very recently, Ajmal et al.[28] overcame the limitations of the above reviews by comprehensively discussing the synthetic strategies and various applications of g-CN, including supercapacitors, photo(electro)catalysis and batteries. Of special interest, the textural properties (surface area, pore volume, pore diameter), morphology and surface chemistry of g-CN play interesting roles in the numerous applications of g-CN. Nevertheless, a review article that exclusively and comprehensively discusses the applications of MCN and its composites in the field of electrochemical energy storage and conversion and gas storage is lacking. It is worth noting that the biosensing applications of MCN have already been reported by the Vinu group in 2023.[29] Therefore, the present Review begins by providing a general overview of the salient features of MCN, which dictate its performance in the various applications. Then, the Review discusses the trends in the applications of MCN-based materials in the areas of electrochemical energy storage and conversion and gas storage in the past decade. The structure−property relationships of MCN-based materials in the above-mentioned applications are also discussed in detail. Emphasis is given to the role of the synthetic approach adopted and the nature of the precursor(s) used toward controlling the textural and morphological properties and chemical composition of MCN-based materials in obtaining the final product with improved performance. Moreover, special consideration is given to the key features of MCN and the effect of modification of those key features on the electrochemical performance of the final product. Finally, the current challenges and perspectives are provided, thereby guiding future research in the field of MCN-based materials for electrochemical energy storage and conversion and gas storage. It is worth mentioning that only articles in which mesoporosity is intentionally introduced by either hard template, soft template or template-free methods into the structural framework of MCN-based materials are reviewed. This Review is expected to provide new avenues for the advancement of MCN-based materials toward electrochemical energy storage and conversion and gas storage and act as a starting point for new researchers who want to step into the spaces of MCN-based materials.

2. GRAPHITIC CARBON NITRIDE

Graphitic carbon (g-CN) is a solid semiconducting material that exists as a stacked structure similar to that of graphite, in which two-dimensional (2D) layers of g-CN are held together by weak intermolecular forces.[7−10,12,30] g-CN has been extensively investigated for various applications such as photocatalysis,[31−33] adsorption,[1,13] sensing, drug delivery,[34] etc. Over the years, various strategies have been adopted to further improve its performance and open up more exciting applications. Nevertheless, the ultimate utilization of bulk and nonporous g-CN for electrochemical energy storage and conversion and gas storage has not been widely explored, despite its key attributes that could trigger promising performance.

2.1. Salient Properties of Graphitic Carbon Nitride toward Electrochemical Energy Storage and Conversion and Gas Storage. The presence of carbon and nitrogen atoms in the structural framework of g-CN imparts distinctive surface properties toward its applications in electrochemical energy storage and conversion and gas storage. Moreover, surface modifications and introduction of mesoporosity also play crucial roles in improving its performance. Besides the elemental building blocks, carbon and nitrogen, the presence of hydrogen as an inevitable elemental impurity provides a dangling bond within the layered structures, thereby creating periodic vacancies in the lattice, which act as sites for ion adsorption and storage. In this section, the salient features of g-CN that could make it an ideal candidate for electrochemical energy storage and conversion are discussed.

2.1.1. Two-Dimensional Layer Structure of Graphitic Carbon Nitride. g-CN is made up of triazine subunits and/or tri-s-triazine units connected by planar tertiary amino groups that form stacked-layered 2D structures. The layers are connected via weak intermolecular forces such as hydrogen bonds, van der Waals forces, etc. The 2D layered structure of g-CN reversibly hosts guest ions during the charging and discharging process of rechargeable batteries and super-

https://doi.org/10.1021/acsomega.5c00679
ACS Omega 2025, 10, 18184−18212

capacitors via an intercalation/deintercalation mechanism. In addition, the electron confinement effect in 2D layered structures has been identified as an opportunity for making improvements in the electrical properties of g-CN, in turn providing platforms for the fast transport of electrons/ions during the charge/discharge process. The interlayer distance of 0.315 nm in g-CN is slightly lower than that of graphite (0.335 nm) owing to the localization of electrons caused by the substitution of carbon atoms with nitrogen atoms. This denser packing introduced by nitrogen substitution is expected to provide stronger binding energy along the perpendicular direction, thereby enhancing the charge transfer storage performance of the material. Furthermore, the 2D layered configuration with a sheet-like morphology and lateral size of less than 100 nm offers a large surface area with abundant active sites for the adsorption of reactants and ions, which makes g-CN an attractive candidate for electrochemical energy storage and conversion. It is worth mentioning that the interlayer distance of 0.315 nm in g-CN is not sufficient to intercalate larger electrolyte ions such as Na^+, K^+, etc. However, it has been documented that the interlayer spacing can be tailored by the insertion of foreign substances such as amorphous carbon, organic molecules, functional groups, solvent ions, etc.[1,35,36] For instance, the intercalation of amorphous carbon into the layered structure of g-CN enlarges the spacing, thereby improving its supercapacitive performance and electrocatalytic hydrogen evolution reaction.[36,37] Also, the interaction of the foreign species, particularly conductive substrates, not only makes it possible to overcome difficulties related to the storage of large ions but also provides conductive pathways, thereby improving the kinetics of the ion transport.[35]

2.1.2. Mechanical Stability of Graphitic Carbon Nitride. The mechanical stability of materials used for the fabrication of energy storage and conversion devices plays a crucial role toward their durability during operation and real-time application. Continuous volume expansion and contraction may lead to structural changes, cracking and even delamination of the electroactive material from the surface of the current collector, thereby causing the deterioration of capacitance/capacity and cycling stability. Interestingly, g-CN demonstrates excellent mechanical properties, which make it a potential candidate for various electrochemical energy storage and conversion applications. Indeed, studies on the mechanical properties of both the triazine and tri-s-triazine structures of g-CN using first-principles calculation have shown that their tensile stress and elastic modulus can reach up to 40 and 25 GPa and 210 ± 5 and 320 ± 5 GPa, respectively.[38] The reported tensile strength and elastic modulus of g-CN are one-third those of defect-free graphene, a clear indication that g-CN is among the strongest known 2D materials. Furthermore, it has been established that, during the deformation of g-CN structure, the sheets expand uniformly and no crack or defect is observed up to the tensile strength point, a clear indication that g-CN could be explored as a promising electrode material for flexibile and wearable applications.[38]

2.1.3. Thermal Stability of Graphitic Carbon Nitride. The thermal stability of the electroactive material plays a crucial role in ensuring that electrochemical energy storage and conversion devices operate safely and reliably. The thermal stability of an electrode/electrocatalyst is one of the key considerations, especially for batteries and fuel cells that are deployed for long-term operation at elevated temperatures during which the internal temperature of the devices could potentially build up. In this regard, g-CN exhibits excellent thermal stability and only decomposes at a temperature above 600 °C and a pressure of 25 GPa,[39] suggesting that g-CN could be an ideal candidate for the development of next-generation batteries and fuel cells for electric vehicles and large grid applications.

2.1.4. Chemical and Electrochemical Stability of Graphitic Carbon Nitride. In electrochemical energy storage and conversion devices, electrode materials are exposed to various corrosive chemical environments, and their stability in the target electrolyte ensures long-term operation with no or only limited capacity fading. Notably, because of the presence of strong covalent bonds between C and N in its structural framework, g-CN exhibits excellent resistance to chemical attack; thereby, a prolonged lifespan of devices can be anticipated, which lowers the need for frequent replacement, saving costs and environmental impact.[40] On the other hand, g-CN demonstrates excellent structural integrity when subjected to continuous intercalation/deintercalation of ions, an indication that the volume changes experienced during the electrochemical processes do not result in phase changes.[41,42] In addition, owing to its excellent chemical stability, g-CN is not expected to undergo dissolution. Furthermore, delamination of the electroactive materials from the current collector during extended operation leads to capacity/capacitance fading and deactivation of electrocatalytic active sites. Therefore, the excellent chemical and electrochemical stabilities of g-CN make it an ideal candidate as an electroactive material for various electrochemical energy storage and conversion devices.

2.1.5. Surface Chemistry of Graphitic Carbon Nitride. The existence of heteroatoms in the structural framework of carbon-based materials has been reported to tune their electronic conductivity and wettability.[9,43−46] Therefore, several methods have been adopted for doping heteroatoms in carbon materials, which enhances their electrochemical properties. Among various heteroatoms, nitrogen doping has received extensive attention, mainly due to its capability to enhance the electrical properties and surface chemistry, which are crucial for energy storage and conversion applications. On the other hand, g-CN is made up of a substantial amount of nitrogen (an ideal g-CN contains 60%), and its surface chemistry is mainly controlled by the nitrogen atoms. Based on the deconvolution of the high-resolution X-ray photoelectron spectrum of N 1s of g-CN, four types of nitrogen were found.[24] While quaternary nitrogen (N-Q) is believed to be responsible for the electron transport properties of g-CN, pyrrolic, oxide pyridinic and pyridinic N act as the sites for electron donations. In addition, nitrogen-based functionalities present in g-CN were reported to participate in redox reactions in acidic media, thereby enhancing the energy storage capabilities of g-CN.[42,47] Furthermore, the nitrogen group bonded to neighboring carbon tends to create a spin density and charge distribution around the carbon atoms, thus creating favorable sites for electrocatalytic reactions.[48]

2.2. Challenges Faced by Graphitic Carbon Nitride. Although pristine g-CN demonstrates several attributes that could potentially ensure its excellent performance when deployed for various electrochemical energy storage and conversion applications, there are still some key challenges that limit its potential applications. The key challenges of g-CN are discussed below.

https://doi.org/10.1021/acsomega.5c00679
ACS Omega 2025, 10, 18184−18212

2.2.1. Low Electrical and Ionic Conductivity. The electrical and ionic conductivities of materials are among the key properties that ensure their superior electrochemical performance when deployed in the fields of energy storage and conversion. The fast transport of ions and electrons at the interface ensures accelerated kinetics of the electrochemical reactions. Unfortunately, bulk g-CN demonstrates low ionic and electrical conductivities due to the restricted movement of ions and electrons, respectively. Furthermore, the long diffusion path length of ions results in high resistance to the transport of ions, thereby deteriorating the rate performance. Thus, developing high-performance electrochemical energy storage and conversion devices based on bulk g-CN remains a major challenge. It is worth mentioning that some attempts, such as composite formation, surface functionalization, doping, etc., have been adopted in the past few decades to address the above-mentioned limitations. Nevertheless, rapid capacity fading and deactivation of electrocatalytic sites caused by the unstable boundary interphase between the g-CN and composite material is observed in most of the g-CN-based composites and surface-functionalized g-CN.[18,19,49] It has been reported that the weak intermolecular van der Waals forces are responsible for the unstable boundary interphase witnessed in g-CN-based composites.[25]

2.2.2. Poor Textural Properties. The state-of-the-art materials presently used in various electrochemical energy storage and conversion and gas storage suffer from inferior textural properties, including surface area, pore size, pore volume, etc., which inhibit the accumulation of ions at the interface, thereby limiting the formation of double-layers and also redox reactions.[50,51] Therefore, enhancing the textural properties of an electroactive material plays an indispensable role in dictating the performance of electrochemical energy storage and conversion devices. For instance, EDLCs, which are based on high surface area carbon materials, store charges primarily by the adsorption/desorption of ions at the electrode−electrolyte interface, and the capacitance has been found to increase linearly with an increase in surface area.[52,53] The increase in the capacitance as a function of surface area is mostly witnessed for mesoporous materials in contrast to microporous materials.[54] Also, the high surface area enhances the wettability and provides abundant electrochemical active sites to facilitate the rapid transport of ions to the electrode, thereby ensuring higher energy storage capability. In addition, other textural properties of the electrode materials, such as pore size, pore volume, pore shape, etc., play significant roles in tailoring the performance of electrochemical energy storage and conversion and gas storage.[54] For instance, materials with ordered mesopores and large pore volumes store more electrolyte ions and demonstrate better rate performance. Bulk and nonporous g-CN is known for having inferior textural properties which seriously impede its extensive utilization in the areas of energy storage and conversion and gas storage, considering that textural properties influence the performance of these devices significantly.[1] Hence, rational design, nanostructuring and surface engineering have been adopted to enhance the performance of bulk g-CN, and the introduction of mesoporosity, modifications and surface functionalization has been intensively explored as a promising strategy to not only improve the textural properties but also overcome some of the limitations of g-CN mentioned above.[1,55,56]

3. MESOPOROUS GRAPHITIC CARBON NITRIDE

Mesoporous graphitic carbon nitride (MGCN) is a nanoporous g-CN prepared through the deliberate introduction of mesoporosity into its structural matrix. MGCN, with enhanced textural properties and tailored morphology, demonstrates improved performance for various applications. For instance, the high nitrogen content provides important sites for electrochemical reactions, the enriched sp^2 hybridized carbon facilitates flow of electrons, and the large surface area and porosity provide abundant sites for the adsorption of a large volume of reactants and accessible channels for mass transport. Furthermore, MGCN, with adjustable textural and environmentally benign properties, excellent thermal and mechanical stability and high basicity, could be an exciting material for CO_2 and/or H_2S adsorption, separation and storage. Over the years, various methods have been adopted toward the preparation of MGCN with controlled structural properties. In general, three major strategies have been extensively explored, namely, hard template, soft template and template-free, as comprehensively discussed in a review article by Vinu and his co-workers.[1]

3.1. Mesoporous Carbon Nitride-Based Materials for Electrochemical Energy Storage Applications. The overdependency on nonrenewable energy sources including fossil fuels, coal and natural gas has posed serious major environmental and health impacts, thereby leading to unpleasant challenges such as global warming, air pollution, acid rain, ozone layer depletion, deforestation,[57] etc. These environmentally related issues need an urgent holistic approach if humanity is to realize a bright energy future with minimal environmental impacts. Renewable energy sources are alternative, nondepleting and cost-effective energy resources with sustainability potential. Therefore, the need for developing efficient energy conversion and storage systems for storing and integrating renewable energy resources is gaining significant attention.

3.1.1. Supercapacitors. Supercapacitors, also known as electrochemical capacitors (ECs), which bridge the gap between batteries and conventional capacitors, are gaining interest owing to their ability to deliver higher energy than traditional capacitors and higher power than rechargeable batteries.[58,59] Other attributes of ECs include long cycling stability, high safety, low cost of maintenance, etc.[60−62] ECs have been used as standalone devices for applications that require fast power impulses for short durations and as complementary energy storage devices where they are integrated with batteries for various applications.[63,64] At present, the energy density of the commercially available ECs (8−10 Wh kg^{-1}) is still far below the requirement for their utilization in applications where high energy density is essential.[62,65] Thus, the major bottleneck of the low energy density of ECs is currently at the forefront of research activity from both academia and industry. Considering that the energy density of ECs greatly depends on the specific capacitance of the electrode material and the voltage window of the electrolyte, the explosive number of investigations are geared toward the development of advanced electrode materials that can deliver enhanced specific capacitance and novel electrolytes with extended working voltage.[66,67] Based on the charge storage mechanism, ECs are categorized into electrical double-layer capacitors (EDLCs) and pseudocapacitors. In EDLCs, charges are stored based on the adsorption/desorption of ions

https://doi.org/10.1021/acsomega.5c00679
ACS Omega 2025, 10, 18184−18212

Table 1. Capacitance Performance of Various MGCN-Based Materials

Electrode material	Specific/aerial capacitance ($F\ g^{-1}$/$mF\ cm^{-2}$)	Current density ($A\ g^{-1}$ or $mA\ cm^{-2}$) or scan rate ($mV\ s^{-1}$)	Electrolyte used	Capacitance retention (%)/number of cycles	Energy density ($Wh\ kg^{-1}$/$mWh\ cm^{-3}$)/ power density ($W\ kg^{-1}$/$mW\ cm^{-3}$)	Ref
MGCN	244	0.5	1 M H_2SO_4	100/5,000	-	78
MGCN-T	279	0.5	1 M H_2SO_4	98.10/1,000	20.97/499.94	79
P2-g-CN	520.5	0.5	1 M H_2SO_4	1131.1/10,000	37.2/750	80
MGCN-SBA-15	322	0.5	1 M H_2SO_4	95.3/15,000	-	81
MCN-GA	240	5	1 M H_2SO_4	>94%/10,000	11.6/8,000	82
MGCN-E	394	0.75	1 M H_2SO_4	95.88/10,000	-	83
Ultrathin porous g-CN	936	1	1 M H_2SO_4	95/10,000	281.3/1	84
MGCN-0.3	252	0.5	1 M H_2SO_4	98/10,000	20.42/300	36
UMCN-$A_{1.25}$	520	0.1	1 M H_2SO_4	82.04/10,000	7/241.15	86
g-CN-2	235	10	6 M KOH	95/5,000	3.92/1,666	87
ZM-C-800	359.1	1	6 M KOH	89/10,000	11.4/498.5	88
NiCo-LDH/g-CN2	2933.3	0.5	6 M KOH	75.3/7,000	52.7/524	89
Porous ACN-700	185	0.5	6 M KOH	87.2/5,000	16.9, 650	90
MGCN-P-0.5	399	0.5	1 M H_2SO_4	83.10/10,000	17.22/500	91
B-g-CN_{800}	620	0.1	1 M H_2SO_4	101.3/2,500	86.1/100	92
$NiCo_2S_4$/NSs/P-g-CN	506	1	2 M NaOH	99/5,000	16.7/200	93
3D-Bi_2S_3@2D-g-CN	41.53 $\mu A\ h\ cm^{-2}$	1	1 KOH/PVA	94.86/5,000	3.17/1,495	94
GCN/Bio-C_{20}	300	1	0.5 M H_2SO_4	100/13,000	53.72/900	95
rGO-pg-CN/PPyNTs	803	0.5	1 M KCl	82/5,000	8.063/125.002	97
GCNNFS	275	0.5	0.1 M Na_2SO_4	93.6/2,000	-	98
NPGC	261	1	6 M KOH	97/2,000	6.53/28,400	99
Porous c-CN	333.8	5	6 M KOH	88/12,000	5.9/846	100

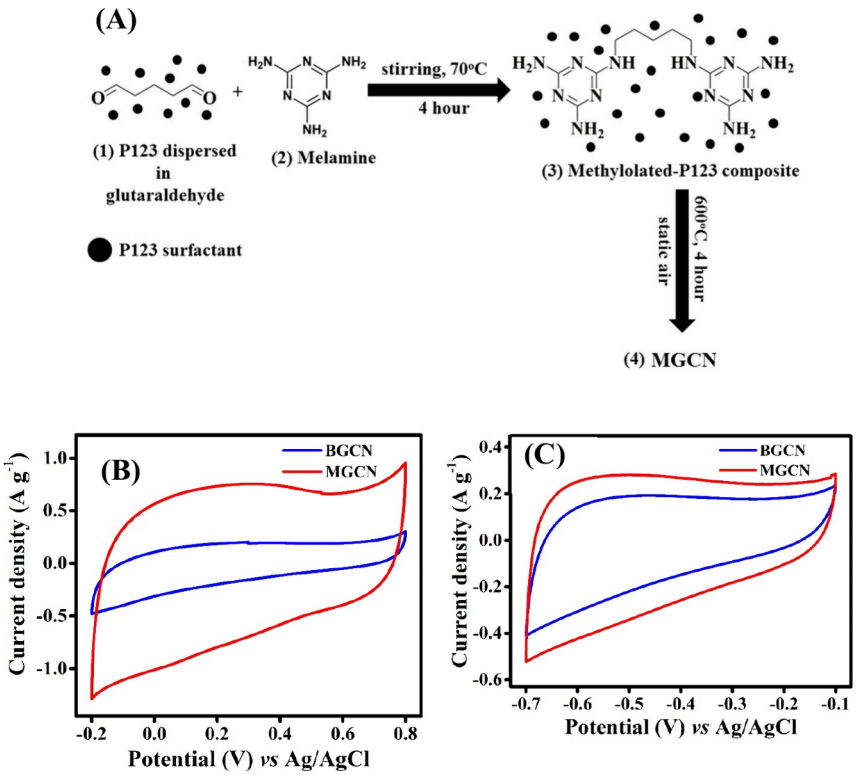

Figure 1. (A) Schematic illustration of the synthesis of MGCN. Cyclic voltammograms (CVs) of BGCN and MGCN recorded at a scan rate of 5 $mV\ s^{-1}$ in (B) 1 M H_2SO_4 and (C) 6 M KOH electrolytes. Reproduced with permission from ref 78. Copyright 2018 Wiley-VCH Verlag GmbH & Co. KGaA.

at the electrode−electrolyte interface during charging/discharging. The amount of charge stored is linearly related to the electrochemical accessible active surface area of electrode materials.[68,69] Furthermore, EDLCs are well known for their superior power density and extended cycle-life.[70,71]

On the other hand, pseudocapacitors store charges due to the fast Faradaic reactions in addition to double-layer capacitance and thus deliver higher specific capacitance than EDLCs.[65,72] Transition metal compounds and conducting polymers are the most commonly studied electrode materials for pseudocapa-

https://doi.org/10.1021/acsomega.5c00679
ACS Omega 2025, 10, 18184−18212

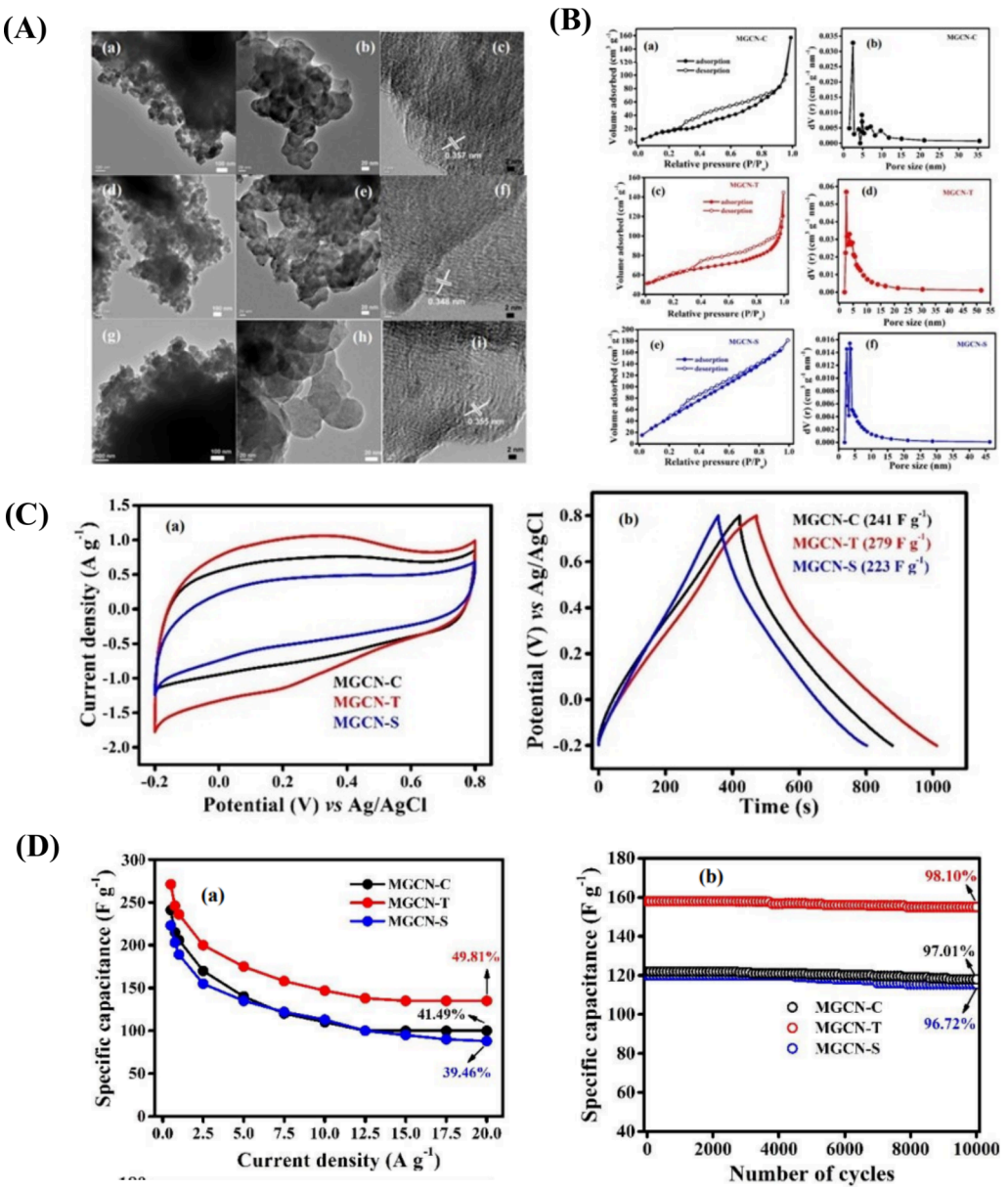

Figure 2. (A) TEM images of (a-c) MGCN-C, (d-f) MGCN-T and (g-i) MGCN-S. (B) Nitrogen sorption isotherms and BJH pore size distribution of (a,b) MGCN-C, (c,d) MGCN-T and (e,f) MGCN-S. (C) (a) CVs recorded at a scan rate of 5 mV s^{-1} and (b) GCD cycles recorded at a current density of 0.5 A g^{-1} of MGCN-C, MGCN-T and MGCN-S. (D) (a) Rate performance and (b) cycling stability at a current density of 7.5 A g^{-1} of MGCN-C, MGCN-T and MGCN-S electrodes. Reproduced with permission from ref 79. Copyright 2019 Elsevier Ltd.

citors.[66,73] The major limitations of this class of ECs include inferior cycling stability and limited power density.[74,75] Although various advancements in the field of ECs have occurred over the years in terms of fine-tuning the electrode materials and electrolytes, the need to develop ECs with energy density close to that of a battery is high.[76,77]

MGCN, with unique textural properties, morphology and abundant surface functionalities, could be a promising electroactive material for ECs. In the past few years, its potential application in the field of ECs has been explored, as highlighted in Table 1. Indeed, our group in 2018 unveiled MGCN as a promising electrode material for ECs.[78] A facile soft template method was adopted, and direct carbonization of a precursor/surfactant composite under limited oxygen resulted in the formation of MGCN with enhanced textural properties as compared to bulk g-CN (Figure 1A). The as-prepared MGCN demonstrates a typical combination of double-layer capacitance and pseudocapacitance properties in both acidic and alkaline electrolytes and outperforms bulk g-CN (BGCN) (Figure 1B). Quantitatively, MGCN delivers a specific capacitance of 244 F g^{-1} at a current density of 0.5 A g^{-1} in 1 M H_2SO_4 and 100% Coulombic efficiency over 5,000 cycles. The excellent capacitance properties of MGCN are largely due to the large surface area and uniform accessible mesopores, which provide abundant electrochemical active sites for the storage of ions at the electrode−electrolyte interface and facilitate rapid diffusion of ions, respectively. Also, the high pyridinic nitrogen content in MGCN acts as a center for fast Faradaic reactions, thereby enhancing the overall specific capacitance.

Although it is difficult to control the morphology of MGCN by the soft template method, the textural properties and

https://doi.org/10.1021/acsomega.5c00679
ACS Omega 2025, 10, 18184−18212

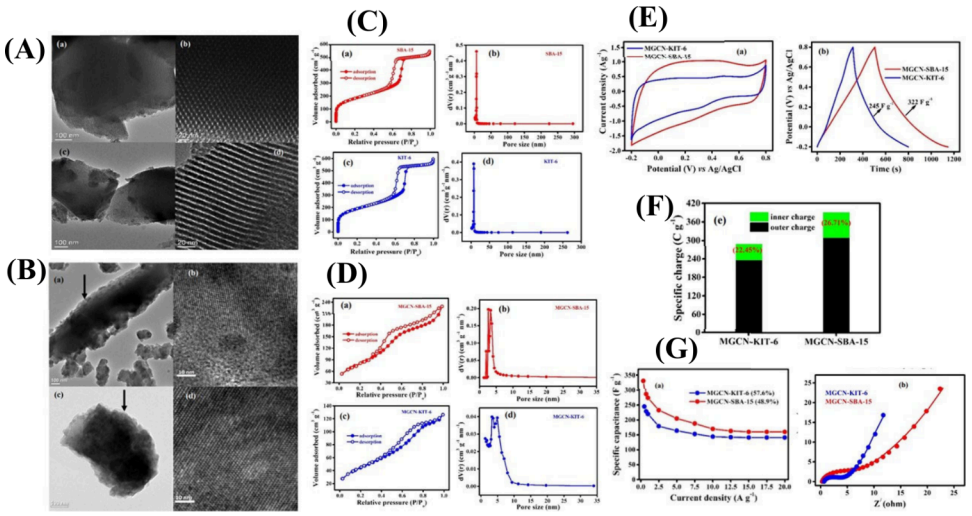

Figure 3. (A) TEM images of (a,b) SBA-15 and (c,d) KIT-6. (B) TEM images of MGCN-SBA-15 and MGCN-KIT-6. (C) (a,c) Nitrogen sorption isotherms and (b,d) the corresponding BJH pore size distributions of SBA-15 and KIT-6. (D) (a,c) Nitrogen sorption isotherms and (b,d) the corresponding BJH pore distributions of MGCN-SBA-15 and MGCN-KIT-6. (E) (a) CVs recorded at a scan rate of 5 mV s^{-1} and (b) GCD cycles recorded at a current density of 0.5 A g^{-1} of MGCN-SBA-15 and MGCN-KIT-6. (F) Inner and outer charge contributions of MGCN-SBA-15 and MGCN-KIT-6. (G) (a) Rate performance and (b) Nyquist plot of impedance spectra of MGCN-SBA-15 and MGCN-KIT-6 electrodes (open circles represent raw data, and solid lines represent fitted data). Reproduced with permission from ref 81. Copyright 2018 Elsevier Ltd.

chemical composition of MGCN can be tailored by controlling the nature of the interaction between the surfactant and the precursors. In this regard, we explored the role of surfactants in tuning the textural and electrochemical properties of MGCN.[79] Three different surfactants, namely, cetyltrimethylammonium bromide (CTAB), polyethylene glycol *p*-(1,1,3,3-tetramethylbutyl)phenyl ether (Triton X-100) and sodium dodecyl sulfate (SDS) as cationic, neutral and anionic surfactants, respectively, were used as porogen and structure directing agents. Owing to the difference in the nature of the interactions between the cross-linked product formed by the reaction between melamine and glutaraldehyde and surfactants, all the MGCN samples exhibited different textural properties and various amounts of sp^2 graphitic carbon domains (Figure 2A and 2B). Among all the samples, MGCN synthesized using Triton X-100 (MGCN-T) displayed the highest surface area and a higher number of mesopores, which is attributed to the ability of Triton X-100 surfactant to provide two sites for interaction with the precursor, namely polyethylene glycol moieties and ether groups. MGCN-T delivered the highest specific capacitance of 279 F g^{-1} at 0.5 A g^{-1} as compared to MGCN prepared using CTAB (MGCN-C) and SDS (MGCN-S), which offered 241 and 223 F g^{-1} at the same current density, respectively. Furthermore, MGCN-T demonstrated a good rate performance, retaining 49.81% of its initial specific capacitance value when the current density was increased 40 times, and exhibited excellent cycling stability over 10,000 cycles (Figure 2C and 2D). A symmetrical device fabricated using MGCN-T displayed a high energy density of 20.97 Wh kg^{-1} at a power density of 499.94 W kg^{-1} and an excellent cycle-life over 10,000 cycles. The superior electrochemical performance of MGCN-T is due to its better morphology and textural properties, the higher amount of pyridinic nitrogen and the sp^2 carbon domain originated from the decomposition of the surfactant during the thermal process. The residual carbon originating from the decomposition of soft templates not only enhances the electrical conductivity of MCN but also acts as a spacer to mitigate the stacking of layers brought about by strong $\pi-\pi$ interactions. Inspired by this, Xu et al.[80] used various amounts of P123, urea and glucose as structure-directing agents and precursors for the preparation of porous g-CN for high-performance supercapacitors. Due to the synergistic effect arising from the distinctive porous structure and the high level of nitrogen doping, the as-synthesized CN with 234 mg of P123 (P2-g-CN) exhibited the highest specific capacitances of 520.5 and 176.0 F g^{-1} at current densities of 0.5 and 50 A g^{-1}, respectively. Interestingly, symmetrical devices fabricated using P2-g-CN displayed an energy of 37.2 Wh kg^{-1} at a power density of 750 W kg^{-1} and could power a 3.2 V light-emitting diode.

Due to the difficulty experienced in tuning the morphology of MGCN to a larger extent by the soft template method and the inherently low nitrogen content of the final material, our group adopted the hard template approach using hexamethylenetetramine as a single precursor, thereby improving the supercapacitive performance of MGCN electrode.[81] Two different silica templates, namely, SBA-15 and KIT-6, were used during the synthesis. The morphology and textural parameters were well replicated in the parent MGCN, as evidenced by the microscopic and nitrogen adsorption/desorption studies (Figure 3A–D). Interestingly, the use of the hard template method resulted in the introduction of defects into the framework of MGCN, thereby providing more electroactive sites for charge storage. Furthermore, the nitrogen content of MGCN prepared using a hard template and a single precursor is higher than the amount obtained by the soft template method. Also, the choice of the template determines the amount of nitrogen content in the final product; thus, MGCN prepared using KIT-6 (MGCN-KIT-6) exhibited a higher nitrogen content than MGCN prepared using SBA-15 (MGCN-SBA-15), which is attributed to the smaller particle size of the KIT-6 template, thereby assisting in the retention of a higher amount of nitrogen during carbonization. It is worth mentioning that not only the amount but also the type of nitrogen influences the electrochemical performance of MGCN, and thus pyridinic

https://doi.org/10.1021/acsomega.5c00679
ACS Omega 2025, 10, 18184−18212

nitrogen offers better chances of undergoing fast Faradaic reactions in acid electrolyte. MGCN-SBA-15, which exhibited a higher surface area, a large pore volume and more mesopores and defect sites, delivered a specific capacitance of 322 F g^{-1} at a current density of 0.5 A g^{-1}, as compared to MGCN-KIT-6, which delivered 245 F g^{-1} at the same current density (Figure 3E). On the other hand, MGCN-KIT-6 displayed better rate performance, primarily due to the higher number of sp^2 carbon domains and the degree of crystallinity, which facilitate the rapid transport of ions at a higher current rate (Figure 3G). Furthermore, the decrease in the capacitance contribution from the inner charge storage mechanism in MGCN-SBA-15 at a higher current rate could have resulted in its inferior rate performance (Figure 3F).[81]

To enhance the electrical conductivity of MCN, a composite made up of graphene aerogel and MCN was prepared by Nazari et al. in 2021.[82] First, MCN and graphene oxide were prepared individually by a hard-templating nano approach using SBA-15 and a modified Hummers's method, respectively. Subsequently, an optimized amount of MCN (10 mg) was dispersed in a graphene oxide (GO) aqueous dispersion (10 mL, 1.0 mg mL^{-1}) and then subjected to ultrasonication-assisted hydrothermal treatment at 180 °C for 12 h to obtain the three-dimensional (3D) MCN−graphene aerogel composite (MCN-GA, Figure 4). The MCN-GA composite showed a

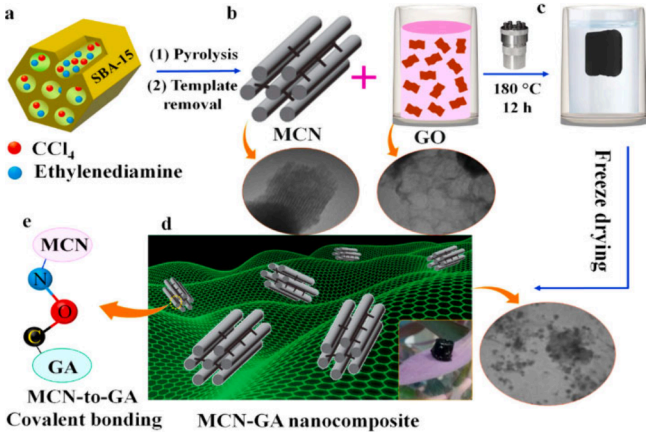

Figure 4. Schematic representation of the processes for the preparation of the mesoporous carbon nitride−graphene aerogel (MCN-GA) nanocomposite. Reproduced with permission from ref 82. Copyright 2021 Elsevier B.V.

specific capacitance of ∼240 F g^{-1} at 5 mV s^{-1} in 1.0 M H_2SO_4 electrolyte, which is higher compared to those of the pristine MCN (142 F g^{-1}) and graphene aerogel (174 F g^{-1}). Furthermore, the symmetric supercapacitors fabricated using MCN-GA exhibited an energy of 11.6 Wh kg^{-1} at a power density of 8.0 kW kg^{-1} and an excellent cycle-life with capacitance retention of >94% after 10,000 charge/discharge cycling tests. The as-synthesized MCN-GA composite is made up of MCN nanoparticles (NPs) encapsulated with graphene nanosheets (NSs) homogeneously, thereby forming a continuous conductive network, which is beneficial for the accelerated transport of ions and electrons even at a higher current rate. The surface functionalities of MCN primarily facilitate the strong interaction with the graphene aerogel through covalent bonding and thus mitigate the aggregation of MCN NPs, which is expected to offer the material a durable cycle-life. In addition, the high surface area for the formation of a double layer at the electrode−electrolyte interface and the existence of mesopores with a wide distribution of pore size in the range of 3.3−21.2 nm allow the material to deliver high specific capacitance and superior rate performance, respectively.

The layers of g-CN are held together by van der Waals forces, which results in the formation of a 3D stacked structure. In recent years, solvent-assisted ultrasonic or thermal exfoliation has been the most widely adopted strategy for the conversion of nonporous multilayered g-CN into a few-layers or a monolayer g-CN, which demonstrates better textural properties and improved performances. For the first time, our group reported the capacitance properties of a few-layered MGCN (MGCN-E), which is analogous to graphene, by the thermal exfoliation of multilayered MGCN.[83] Typically, the multilayered MGCN was prepared by a sol−gel method using commercially available colloidal silica and hexamethylenetetramine as a hard template and precursor, respectively. Thermal exfoliation under an air atmosphere resulted in a decrease in the number of layers from ∼11 to 2, as evidenced by microscopic images (Figure 5A and 5B), and a significant enhancement in textural properties (Figure 5C). As a consequence, MGCN-E outperformed its multilayered MGCN counterparts in terms of specific capacitance at a scan rate of 10 mV s^{-1} (Figure 5D). Quantitatively, MGCN-E delivered a specific capacitance of 394 F g^{-1} at a current density of 0.75 A g^{-1}, which is ∼1.5 times higher than that of MGCN (Figure 5D). Nevertheless, the rate performance of MGNC-E is slightly compromised, which could be due to a loss in the capacitance contribution from the fast Faradaic reactions of pyridinic nitrogen and carbonyl oxygen at higher current rates.[83]

Besides thermal exfoliation, a bottom-up strategy was adopted by Lu et al.[84] for the preparation of conductive ultrathin g-CN. Typically, a graphene-templated van der Waals epitaxial strategy was employed, and ultrathin g-CN was obtained with a large surface area, high electrical conductivity, narrow pore-size distribution and suitable level of nitrogen doping. Capacitance studies revealed that the material exhibited a high volumetric capacitance of 936 mF cm^{-2} at a current density of 1 mA cm^{-2} and showed excellent cycling stability of over 10,000 cycles. The excellent capacitance performance is attributed to the ultrathin structure and high nitrogen doping level that provides numerous active sites for charge storage besides unhindered channels for accelerated transport of ions.

In 2019, our group developed a simple and sustainable method for the synthesis of MGCN with improved capacitance properties. In this method, MGCN was synthesized using an environmentally friendly material, namely, the sodium salt of carboxymethyl cellulose (CMC), as a biotemplate.[36] It was reported that the chemical composition and the textural and electrochemical properties of MGCN could be easily fine-tuned by varying the ratio between the precursor and biotemplate. Notably, MGCN prepared using 0.3 g of CMC (MGCN-0.3) exhibited higher surface area, a larger pore volume and relatively more oxygen-based functionalities and thus demonstrated the highest specific capacitance of 252 F g^{-1} at a current density of 0.5 A g^{-1} as compared to MGCN synthesized using 0.1 g (MGCN-0.1) and 0.5 g (MGCN-0.5) of biotemplate, which deliver specific capacitance of only 182 and 222 F g^{-1}, respectively. A symmetrical supercapacitor device fabricated using MGCN-0.3 electrodes showed a high

https://doi.org/10.1021/acsomega.5c00679
ACS Omega 2025, 10, 18184−18212

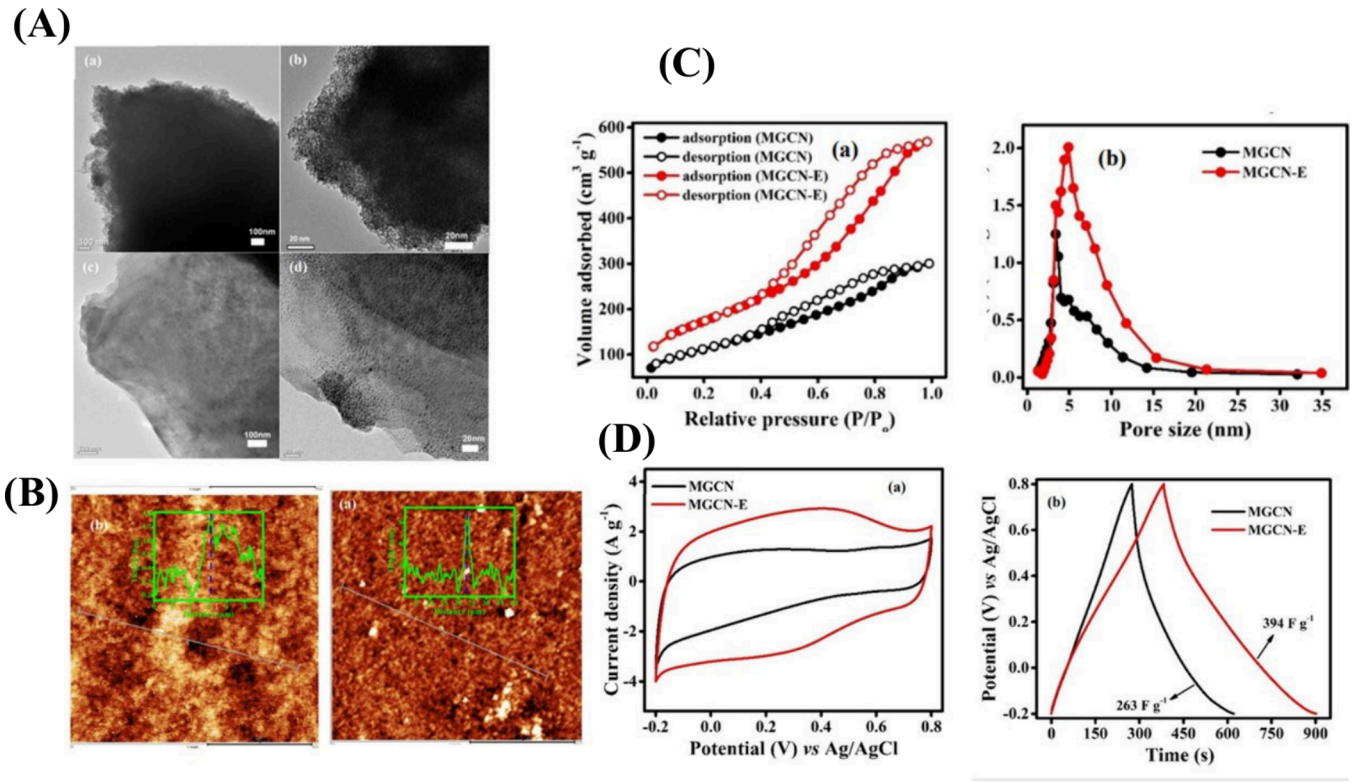

Figure 5. (A) TEM images of (a,b) MGCN and (c,d) MGCN-E. (B) Atomic force microscopic images of (a) MGCN and (b) MGCN-E, with their corresponding step height profiles inset. (C) (a) Nitrogen sorption isotherms and (b) BJH pore size distributions of MGCN and MGCN-E. (D) (a) CVs recorded at a scan rate of 10 mV s^{-1} and (b) GCD cycles recorded at a current density of 0.75 A g^{-1} of MGCN and MGCN-E. Reproduced with permission from ref 83. Copyright 2019 Centre National de la Recherche Scientifique (CNRS) and the Royal Society of Chemistry.

energy density of 20.42 Wh kg^{-1} at a power density of 300 W kg^{-1} and a good rate performance and retained more than 90% of its initial capacitance after 10,000 cycles. Carbonate-based materials were recently exploited for the generation of porosity into the building block of carbon material, thanks to their decomposition process, which releases gases that act as blowing agents.[85] In 2023, Wang et al.[86] reported the preparation of a hierarchical porous g-CN with a high nitrogen content for supercapacitor applications. Ammonium carbonate and glucose were used as pore generator and the source of carbon, respectively. On the other hand, melamine and urea were used as the binary precursors for the formation of a 3D interconnected g-CN structure after stepwise calcination at 550 and 800 °C. The effects of the loading level of the ammonium carbonate at values of 0.625, 1.25 and 2.5 g were investigated, and with the samples denoted as UMCN-A_X, where X indicates the amount of ammonium carbonate used during the synthesis. Although the formation of a distinct 3D network is favored by the use of a higher amount of ammonium carbonate (2.5 g, UMCN-$A_{2.5}$) due to the release of a higher amount of gases (NH_3 and CO_2), UMCN-$A_{1.25}$ exhibited higher surface area, interconnected mesoporous structures, higher nitrogen content and graphitic carbon domains. Consequently, the porous hierarchical structure and high nitrogen content of UMCN-$A_{1.25}$ enabled it to deliver specific capacitance values of 520 F g^{-1} at 0.1 A g^{-1} and 219.4 F g^{-1} at 20 A g^{-1} and steady cycling stability after 10,000 charge/discharge cycles. Inspired by the work of Wang, Shwetha et al.[87] reported the preparation of MGCN using two modified techniques, namely, a simple one-pot method (CN_1) and a hydrothermal method assisted by carbonated beverages (CN_2). In the first method, melamine and ammonium carbonate in a ratio of 1:1 were mixed and carbonized at 550 °C for 2 h. In the second method, 0.5 mL of Coca-Cola was introduced in place of ammonium carbonate. The mixture containing 10 g of melamine, 0.5 mL of Coca-Cola and 60 mL of deionized water was sonicated at room temperature for 5 min and then hydrothermally heated at 180 °C for 16 h. While the ammonium carbonate is presumed to be responsible for the generation of porous structures in the CN_1, the carbonated beverage acts as a porogen in the CN_2 method. The microscopic and surface area analyses indicated that g-CN prepared using CN_1 (g-CN-1) exhibited a combination of meso- and micropores with a surface area of 53.22 m^2 g^{-1}, whereas g-CN prepared by adopting the CN_2 (g-CN-2) strategy displayed ordered mesopores with a pore diameter and surface area of 4.5 nm and 68.66 m^2 g^{-1}, respectively. The electrochemical capacitance of both materials studied in 6 M KOH in the potential range of −0.1 to 0.6 V suggested that g-CN-2 delivered a specific capacitance of 235 F g^{-1} at a scan rate of 10 mV s^{-1} as compared to g-CN-1, which delivered 165 F g^{-1} under a similar scan rate. Similarly, g-CN-2 retained 60% of its initial specific capacitance when the current density was increased from 0.5 to 4 A g^{-1}, which is much higher than that of g-CN-1 (40%). While the superior capacitance of g-CN-2 is attributed to its distinctive coiled and lamellar structure and higher surface area, which offers a large number of active sites for capacitive storage of ions, the presence of ordered mesopores and a large number of sp^2 domains in g-CN-2 could have facilitated rapid transport of electrons and ions and thus a higher rate capability. Broccoli-like MCN was

https://doi.org/10.1021/acsomega.5c00679
ACS Omega 2025, 10, 18184−18212

synthesized by Cai et al.[88] using a simplified one-step carbonization process of a composite material consisting of a zeolitic imidazolate framework of Zn-based ZIF-8 and melamine. The composite (ZIF-8/melamine) was prepared by suspending 0.5 g of melamine in 10 mL of water, followed by the addition of 2.0 g of ZIF-8 to the mixture, and subsequently sonicated for 1 h before drying in a vacuum at 60 °C for 24 h. The composite powder obtained was placed in a furnace and heated at various temperatures, including 600, 800 and 900 °C, under a nitrogen atmosphere for 3 h. The composite carbonized at 800 °C (ZM-C-800) exhibited a 3D broccoli-like morphology and a high N content of about 28.3%, and thus it delivered a specific capacitance of 359.1 F g^{-1} at a current density of 1 A g^{-1}. Moreover, a symmetric supercapacitor fabricated using ZM-C-800 as the electrode displayed an energy density of 11.4 Wh kg^{-1} at a power density of 498.5 W kg^{-1}.[88] Shen et al.[89] reported the deposition of nickel−cobalt-layered double hydroxide flower-like NSs (f-NiCo-LDH) onto the framework of g-CN using poly(ethylene glycol)-*block*-poly(propylene glycol)-*block*-poly(ethylene glycol) diacrylates (Pluronic F127) as a modulating agent through a refluxing method. The optimized composite having 10 mg of g-CN (f-NiCo-LDH/g-CN2) displayed a hierarchically porous structure and a combination of both macro- and mesopores and thus delivered a high specific capacitance of 2,933.3 F g^{-1} at 0.5 A g^{-1} and retained 75.3% of its initial capacitance after 7,000 charge/discharge cycles. Asymmetric hybrid supercapacitors assembled using the f-NiCo-LDH/g-CN2 composite as the cathode and activated carbon as the anode delivered an energy density of 52.7 Wh kg^{-1} at a current density of 0.5 A g^{-1}. Shen et al.[90] synthesized porous activated CN (ACN) by a one-step pyrolysis/activation method using citric acid and melamine as blowing agent and precursor, respectively. They found that varying the temperature has significant effects on the textural parameters and oxygen/nitrogen content of the final products. The surface area and pore size increased and decreased, respectively, with an increase in the pyrolysis temperature from 500 to 700 °C, which is mainly due to the increase in the surface area contribution from the micropores. In contrast, the nitrogen and oxygen content were found to decrease and increase, respectively, with an increase in the pyrolysis temperature from 500 to 800 °C. Notably, 700 °C was found to be the optimum temperature for the preparation of ACN (ACN-700) with superior textural and nitrogen/oxygen content, which delivered a specific capacitance of 185 F g^{-1} at a current density of 0.5 A g^{-1}. The assembled symmetric supercapacitors based on ACN-700 achieved energy densities of 16.9 Wh kg^{-1} at a power density of 650 W kg^{-1} and 6.2 Wh kg^{-1} at a power density of 300 W kg^{-1} in 2 M 1-butyl-3-methylimidazolium tetrafluoroborate ($[BMIm]BF_4$)/acetonitrile and 6 M KOH, respectively.

The major limitation of carbonaceous materials is inferior energy density, which is primarily attributed to the surface-dependent charge storage mechanism. Heteroatom doping has been identified as a viable option for introducing sites for fast Faradaic reactions, thereby enhancing the overall capacitance. Although MCN possesses high nitrogen content, introducing other heteroatoms such as P, S, B, etc. was found to improve its electrochemical properties. In this regard, our group investigated the effects of phosphorus doping on the composition and capacitance properties of MGCN.[91] It was found that a phosphorus dopant prefers a carbon site for doping, thereby introducing defects into the structural framework of MGCN. An increase in the loading level of the dopant leads to corresponding increases in the oxygen content and surface area, mainly attributed to phosphoric acid activation and incorporation of large atomic radius P into the lattice of MGCN, thereby introducing structural distortion. The doping of MGCN with P creates a new bond configuration in which the P atom is bonded to both O and C (P−C, P−O), thereby breaking the electroneutrality of the carbon host. This is expected to enhance the capacitance properties of MGCN. Furthermore, the structural defects and improved surface area offered by phosphoric acid activation provide ideal sites for charge storage and formation of double layers, respectively. Consequently, all the P-doped MGCN electrodes (MGCN-P-*X*, where *X* denotes the amount of the phosphoric acid used) deliver higher specific capacitance at all the current rates as compared to pristine MGCN. A symmetrical supercapacitor device fabricated with MGCN-P-0.5 delivered an energy density of 17.22 Wh kg^{-1} at a power density of 500 W kg^{-1} and demonstrated excellent rate capability by retaining its energy density up to 9.92 Wh kg^{-1} when the power density was increased by 20 times. Furthermore, the device presented stable cycling stability over 10,000 cycles. Kong et al.[92] used boron doping to enhance the supercapacitive performance of porous CN. Typically, an ionic liquid solvent namely; $BMIBF_4$ was utilized as the source of the boron and a sacrificial template. The optimized as-prepared hierarchically porous boron-doped g-CN (B-g-CN_{800}) NS electrode showed specific capacitance value of 620.0 F g^{-1} at 0.1 A g^{-1} and 312.0 F g^{-1} at 20 A g^{-1}, stable cycling stability after 2,500 charge/discharge cycles and a high energy density of 86.1 Wh kg^{-1} at a power density of 100 W kg^{-1}. The superior electrochemical performance is attributed to the hierarchically porous structure with pore size dominantly in the range of 1−3 nm and high contents of pyrrolic nitrogen (11.12 at%) and boron (8.21%).

Besides heteroatom doping, compositing MCN with other materials has been reported as a facile method to enhance its electrochemical performance. For instance, a composite comprised of $NiCo_2S_4$ NSs and porous g-CN was prepared by Li et al.[93] First, porous g-CN was prepared by calcination of thiourea at 550 °C,[18] followed by hydrothermal treatment of $NiCo_2S_4$ precursors with as-prepared porous g-CN at 180 °C for 12 h. In the composite, g-CN provides structural support, thereby preventing the rapid degradation of $NiCo_2S_4$, and the distinctive "sheets on sheets" architectures shorten the diffusion path lengths for ions and electrons. Accordingly, the colored composite ($NiCo_2S_4$/NSs/P-g-C_3N_4) exhibited a specific capacitance of 506 F g^{-1} at a current density of 1 A g^{-1} and outstanding rate capability and cycling stability. An asymmetrical device constructed using $NiCo_2S_4$/NSs/P-g-C_3N_4 as the anode and activated carbon as a cathode offered an energy density of 16.7 Wh kg^{-1} at a power density of 200 W kg^{-1} as well as retaining 99% of its initial capacitance after 5,000 cycles. Karuppaiah et al.[94] demonstrated the synthesis of uniform hierarchically 3D urchin-like Bi_2S_3@2D-g-CN NSs by a hydrothermal method. The resultant optimized 3D-Bi_2S_3@2D-g-C_3N_4 composite presented a battery-type charge storage mechanism and delivered an aerial capacity of 41.53 μAh cm^{-2} at 1 mA cm^{-2} and an excellent rate capability of 62.77% with a capacity retention of 94.86% after 5,000 cycles. Moreover, when the 3D-Bi_2S_3@2D-g-C_3N_4 composite was employed as an electrode material for the fabrication of symmetric supercapacitors, it delivered an energy density of 3.17 μWh

https://doi.org/10.1021/acsomega.5c00679
ACS Omega 2025, 10, 18184−18212

cm^{-2} at a power density of 1495 $\mu W\ cm^{-2}$ with a good cycling retention of 83.84% after 7,500 cycles in hybrid KOH/poly(vinyl alcohol) (PVA) gel electrolyte. The synergistic effect of the porous structure, abundant electroactive sites and enhanced electronic/ionic conductivities, which decrease the interfacial resistance, is responsible for its fascinating electrochemical performance. A 3D/2D composite made up of MCN and bioderived carbon (Bio-Cx) was investigated as an electrode material for supercapacitors by Taha et al.[95] The composite was prepared by a one-pot thermal polymerization of urea to obtain g-CN,[96] followed by the addition of various amounts of as-prepared biocarbon (GCN/Bio-C*x*, where *x* denotes the amount of biocarbon used during the synthesis). The composite prepared using 20 mg of biocarbon exhibited an enriched number of electrochemically active sites, a larger surface area and distinctive 3D/2D networks and thus demonstrated a high capacitance of 300 F g^{-1} at 1 A g^{-1} in the potential window of 1.2 V in 0.5 M H_2SO_4 electrolyte. The assembled asymmetric supercapacitor device fabricated using the GCN/Bio-C_{20} composite as an anode and mesoporous N-doped carbon (MPNDC) material as the cathode presented an enhanced energy density of 53.72 Wh kg^{-1} at a power density of 900 W kg^{-1} and retained almost 100% of its initial capacitance after 13,000 charge/discharge cycles. Baruah et al.[97] exploited the advantage of the synergistic influence of the enhanced surface area and interfaces, thereby increasing the electroactive sites of the electrode material for supercapacitors. They prepared self-assembled heterostructures of the protonated graphitic carbon nitride (pg-CN) and negatively charged reduced graphene oxide (rGO) and then introduced polypyrrole nanotubes (PPyNTs) via an *in situ* polymerization. The ternary nanocomposite (rGO-pg-CN/PPyNTs) with enhanced microstructures and large surface area displayed an excellent specific capacitance of 803 F g^{-1} at a current density of 0.5 A g^{-1} and good cycling stability of 82% after 5,000 charge/discharge cycles in 1 M KCl electrolyte. Additionally, the symmetric supercapacitor fabricated using rGO-pg-CN/PPyNTs delivered an energy density of 8.063 Wh kg^{-1} at a power density of 125.002 W kg^{-1}.[97] Tahir et al.[98] developed a facile method for the preparation of porous g-CN with a nanofiber morphology as an efficient material for photocatalysis and supercapacitors. The addition of ethanol and 0.2 M HNO_3 during the synthesis resulted in the activation of melamine, thereby forming a bigger unit of heptazine, and the presence of ethanol as a polar solvent in the reaction mixture led to the generation of g-CN with a fibrous structure. The as-prepared 1D g-CN with fibrous structure (GCNNFs), exhibiting a higher nitrogen content, displayed a specific capacitance of 275 F g^{-1} at a current density of 0.5 A g^{-1} in 0.1 M Na_2SO_4 aqueous electrolyte and demonstrated superior cycling stability with 93.6% capacitance retention after 2,000 cycles at a current density of 1 A g^{-1}.

MCN can be used as a sacrificial template and nitrogen source for the preparation of advanced electrode materials. Yang et al.[99] realized the synthesis of nitrogen-rich porous graphene-like carbon sheets (NPGCs) using MCN as both nitrogen source and *in situ* template by a plasma-enhanced chemical vapor deposition method followed by high-temperature pyrolysis. The as-prepared NPGCs demonstrated exciting features, including a conductive interconnected network with an electrical conductivity of 693 S m^{-1}, copious number of mesopores, ultralarge pore volume of 4.35 $cm^3\ g^{-1}$ and high surface area of 1277 $m^2\ g^{-1}$, which are all expected to improve its electrochemical performance. Consequently, NPGCs delivered a specific capacitance of 261 F g^{-1} at 1 A g^{-1} with an exceptional rate capability of 72.41% after the current density was increased to 100 A g^{-1} and presented an outstanding cycling performance with capacitance retention of 97% at 10 A g^{-1} after 20,000 cycles. Furthermore, the assembled symmetric supercapacitors delivered an energy density of 6.53 Wh kg^{-1} at a high power density of 28.4 kW kg^{-1}. A layered conductive bamboo-like carbon nitride (c-CN) was synthesized by Cai et al.[100] using a metal−organic framework (MOF). The as-prepared MOF was annealed under vacuum followed by filtration and drying to obtain c-CN. When used as a negative electrode for flexible supercapacitors, c-CN produced a large capacitance value of 333.8 F g^{-1} at 5 mV s^{-1} and retained over 88% capacitance with retention of cycling stability after 12,000 cycles. A symmetrical device was constructed using a solid-state electrolyte (PVA/KOH gel) by assembling two symmetric c-CN electrodes with a PVA/KOH gel. The device functioned as a flexible EC, which worked under different deformation conditions and delivered an energy density of 5.9 W h kg^{-1} at a power density of 846 W kg^{-1}, thanks to the synergistic effects of high porosity, mechanical flexibility and improved electrical conductive.

3.1.2. Batteries. A battery is an electrochemical energy storage device that converts the chemical energy of the active materials into electrical energy by redox reactions. A battery is considered as two or more galvanic cells coupled in series or in parallel or both. Batteries are the preferred source of energy for portable and mobile applications owing to their high conversion efficiency and because they are user-friendly in terms of shape, size and design. Rapid advancements in the field of materials science and technology has resulted in improvements in the performance of different battery and cell technologies. For instance, over the years, nonrechargeable technologies such as zinc−carbon and alkaline batteru technologies have evolved, and new and exciting rechargeable batteries such as Li-ion, Na-ion, Li-S, etc. are either commercialized or will be available soon. Furthermore, all-solid-state batteries, with the potential to replace traditional batteries based on flammable liquid electrolytes, are gaining momentum.[101] This class of battery technology can be deployed for large-scale energy storage, including power grids and electric vehicles, among others. The performance of various MCN-based materials toward battery applications is summarized in Table 2.

3.1.2.1. Li/Na-Ion Batteries. Among the various batteries, Li-ion batteries (LIBs) are considered the most promising due to their high energy density, low memory effect, good rate capability, etc.[102,103] Although g-CN possesses a suitable interlayer distance that can accommodate both Li and Na ions, the capacities reported for LIBs and Na-ion batteries (NIBs) range from 6 to 182 mAh g^{-1} and from 10 to 100 mAh g^{-1}, respectively.[43,104−106] The obtained limited capacity is mainly attributed to the low electronic conductivity and inferior cycling stability of the g-CN material.[105,107] Furthermore, the limited intercalation kinetics of g-CN has a detrimental impact on Li- and Na-ion storage performance. Over the years, various strategies, such as heteroatom doping, compositing with conductive materials, etc., have been adopted to overcome these issues.[108] In this regard, most of the studies on the application of g-CN for battery applications are based on compositing. Furthermore, the introduction of porous

https://doi.org/10.1021/acsomega.5c00679
ACS Omega 2025, 10, 18184−18212

Table 2. Performance of Various MCN-Based Materials toward Battery Applications

Material	Specific capacity (mAh g^{-1})	C-rate (C)/ Current density (mA g^{-1})	Capacitance retention (%)/number of cycles	Ref
g-CN/N-C	54.9	0.2	200	40
c-CN PP	996.8	2.0	-	100
MCN/S	828.4	0.1/0.5	100	109
MCN-11/MoS_2	193 and 54	100	500	98
Fe_2O_3@g-C_3N_4@ H-MMCN	1115.1/ 998.4	100/2000	100/500	111
g-CN@carbon composite	180	0.5 A g^{-1}	1600	112
g-CN@carbon composite/ $Na_3V_2(PO_4)_3$	136	0.1 A g^{-1}	140	112
α-C_3N_2	2791	-	-	113
CN/MoS_2	605 and 431	100 and 1000	-	114
P-MCN-1	963	1 A g^{-1}	1000	115
S-MCN	413.9	50	10	116
Li_2S/p-C_3N_4/ CNT	997.5	0.2 A g^{-1}	600	118
PTCN/S	504	4	500	119
CN/MoS_2	680	0.5	200	120
C_3N_4/N-rGO/ MoS_2	800	100	100	117
Pt/CNHS	600	100	100	129
NGM-CN-Fe	677	5	100	130
g-CN/N-Cs	54.9	0.2	200	131

networks into the framework of g-CN has been identified to facilitate the efficient transport of ions and chemical species and to provide enough space to accommodate large amounts of active material, thereby mitigating unwanted volume expansion.[109] For instance, Kim et al.[110] reported the Li- and Na-ion storage properties of MCN with a triazole framework coupled with molybdenum sulfide (MCN-11/MoS_2) for the first time. According to density functional theory (DFT) calculations, the reversible adsorption of the Li and Na ions follows the order g-C_3N_4 < C_3N_5 < MCN-11/MoS_2 composite, indicating that the charge transport of both LIBs and NIBs is more facile in the composite than in pristine g-CN and C_3N_5. On the other hand, experimental studies revealed that the optimized composite (MCN-11/MS2) delivered a reversible capacity of 193 and 54 mAh g^{-1} for LIBs and NIBs, respectively, which are 3.86 and 10.80 times higher than that of pristine MCN, which is ascribed to the composite's enriched mesopore channels, extended gallery height and high ion adsorption energy. The low initial Coulombic efficiency witnessed in the material is attributed to the formation of a solid−electrolyte interphase, which is more predominant in a Li environment than Na.[110] In 2021, Jiang et al.[111] synthesized a g-CN honeycomb-shaped meso@mesoporous carbon nanofiber material integrated with homogeneously dispersed ultrafine Fe_2O_3 NPs (Fe_2O_3@g-C_3N_4@H-MMCN) through a multistep synthetic approach. A first cathodic peak at a potential of 1.54 V in the cyclic voltammogram (CV) of the hybrid material revealed the intercalation reaction of Li (Fe_2O_3 changes to $Li_xFe_2O_3$), while the second cathodic peak was attributed to the transformation of Fe^{3+} to Fe^{2+}, an indication that Fe_2O_3 NPs act as hosts for Li ions. On the other hand, the nitrogen doping originating from the g-CN lowered the energy barrier for the intercalation of Li ions, thereby enhancing the surface wettability, whereas the mesoporous structure mitigated the unwanted volume expansion. The as-prepared hybrid material delivered a superior specific capacity of 1510 mAh g^{-1} at a current density of 100 mA g^{-1}. The material still maintained a specific capacity of 782.9 mAh g^{-1} after 500 cycles. Zhou et al.[112] reported the NIB performance of a g-CN@carbon composite prepared by gel coating followed by calcination. During the calcination process, the gel coating was found to play a vital role in the homogeneous dispersion of g-C_3N_4, thereby preventing the aggregation of particles. Owing to the unique structure of the composite, including enhanced pyridinic-N content, high electronic conductivity and conductive porous networks, it delivered a high discharge capacity of 250 mAh g^{-1} at 0.1 A g^{-1} and a long-term cycling performance with 180 mAh g^{-1} over 1600 cycles at 0.5 A g^{-1}. Additionally, the composite material, when used as an anode with $Na_3V_2(PO_4)_3$ as a cathode for a full battery, demonstrated good cycling stability and maintained a specific capacity of 136 mAh g^{-1} over 140 cycles at 0.1 A g^{-1}. Cai et al.[113] investigated the LIB performance of a novel holey α-C_3N_2 monolayer using swarm-intelligence 2D global minimum structure search methods in conjunction with structure design through the assembly of organic unit building blocks. The CN structure developed from a convex hull, based on the relative thermodynamic stabilities, revealed that the α-C_3N_2 exhibited a high porosity structure and improved N content offering multiple pyridinic-N sites. Hence, the material demonstrated enhanced Li adsorption sites and displayed an extremely high theoretical capacity (2791 mAh g^{-1}). Experimentally, high feasibility, a low Li-diffusion energy barrier and a suitable open-circuit voltage are the major attributes of porous α-C_3N_2 that make it a highly promising anode material for LIBs. Furthermore, it has been demonstrated that the α-C_3N_2 framework can be composited with other materials, thereby extending its applications beyond LIB anodes. Kim et al.[114] demonstrated the preparation of MoS_2 coupled with ordered MCN using nanotemplating as a single-step strategy. The nanotemplating process involved the pyrolysis of phosphomolybdic acid hydrate (PMA), dithiooxamide (DTO) and 5-amino-1H-tetrazole (5-ATTZ) precursors in the presence of a 3D mesoporous silica template. During the calcination process, the hybridization of the materials followed by sulfidation and polymerization and thus formation of MoS_2 and CN occured simultaneously inside the meso-channels of the hard template. The prepared CN/MoS_2 hybrid material exhibited a high purity and remarkable degree of crystallinity and thus delivered specific capacities of 605 and 431 mAh g^{-1} at current densities of 100 and 1000 mA g^{-1}, respectively. The preparation of P-doped MCN (P-MCN-1) with ordered porous structures for a high-energy and high-power LIB anode was reported by Kesavan et al.[115] The as-prepared P-MCN-1 material delivered a high reversible discharge capacity of 963 mAh g^{-1} after 1000 cycles at a current density of 1000 mA g^{-1} when used as an anode for LIBs, which is much higher than that of other reported materials like s-triazine ($C_3H_3N_3$, g-C_3N_4), pristine MCN1 and B-MCN-1 subunits. The prediction based on first-principles calculations revealed that P-MCN-1 has a high formation energy, lower bandgap value and high Li-ion adsorption, which results in high lithium storage, stable cycle-life, high power capability and minimal irreversible capacity (IRC) loss.

Although phosphorus doping enhances the NIB performance of MCN, the introduction of heteroatoms with larger

https://doi.org/10.1021/acsomega.5c00679
ACS Omega 2025, 10, 18184−18212

atomic radii such as S could expand the interlayer distance of the MCN, thereby facilitating the facile insertion of a large volume of Na ions. Inspired by this, Cha et al.[116] reported the preparation of sulfur-doped MCN (S-MCN) through a hard template method by using DTO as a single molecular precursor. According to first-principles DFT calculations, the doping of S on MCN increases the high adsorption energy and chemical structure of the composite, thereby optimizing its uptake of Na-ions. Notably, S-MCN prepared at 700 °C possesses the largest surface area and highest number of defect sites, instigating its inherently low crystallinity, facilitating the delivery of a specific discharge capacity of 413.9 mAh g^{-1} at a current density of 50 mA g^{-1} after 10 cycles. The design of N-doped graphene/porous g-CN NSs supported by a layered MoS_2 hybrid (C_3N_4/N-rGO/MoS_2) for use as a LIB anode was reported by Hou et al.[117] A 2D multilayered nanostructure was formed by the dispersion of few-layer MoS_2 NSs onto the N-doped graphene/porous g-C_3N_4 NS matrix using a facile hydrothermal method. The obtained hybrid C_3N_4/N-rGO/MoS_2 NSs displayed a considerably large capacity of more than 800 mAh g^{-1} at 100 mA g^{-1} and high rate capability by retaining 83% of their capacity when the current density was increased from 50 to 500 mA g^{-1}. Furthermore, the hybrid material delivers excellent cycling stability by maintaining 91% of its initial capacity after 100 cycles. The obtained remarkable rate capability and cycling stability of the composite are attributed to the porous networks in g-CN, which provide enriched channels for the facile diffusion of electrolyte ions and restrain the large volume changes of MoS_2 NSs, thereby enabling the material to exhibit superior rate performance and cycling extended stability, respectively.

3.1.2.2. Li-S Batteries. Lithium−sulfur batteries (LSBs) are a new and promising next-generation battery technology, based on elemental sulfur (S_8) as a cathode and Li as an anode. Theoretically, LSBs are expected to deliver a specific capacity of 1675 mAh g^{-1} and a specific energy of 2600 Wh kg^{-1}, which is 2−5 times higher than those of LIBs. Nevertheless, intense shuttling of lithium polysulfides (LiPSs) and slow redox kinetics are among the major limitations of LSBs. MCN, with large surface area, enriched mesopores and high pyridinic nitrogen content, can efficiently enhance the redox kinetics of S species and facilitate rapid redox conversion of LiPSs. Besides, via tailoring the textural properties and morphology and tuning the surface functionalities, including nitrogen content/type, of MCN by doping, compositing could significantly improve its performance toward LSB applications. For instance, Liang et al.[118] reported the synthesis of a 3D lithium sulfide/porous g-CN/carbon nanotube ternary composite (Li_2S/p-C_3N_4/CNT) as a bifunctional host for a Li-S cathode. The composite, prepared by a direct and easy liquid infiltration−evaporation method, delivered an initial discharge capacity of 997.5 mAh g^{-1} at 0.2 A g^{-1} and demonstrated good cycling stability over 600 cycles. The reasonable Li-S performance of the composite is attributed to the ultrafine nature of Li_2S, which ensures material utilization, a highly conductive network of CNTs accelerating the rapid transport of electrons and porous g-CN providing strong polar adsorption capacity for Li_2S. Very recently, the inherently inferior conductivity of g-CN toward LSBs was overcome by exploiting the defect engineering strategy by Ma et al.[119] The etching approach was adopted for the preparation of vertically aligned tubular g-CN with porous structure and low nitrogen content (PTCN). The low nitrogen content in PTCN endows the material with excellent conductivity and superior capability for adsorption of S atoms and enhances the catalytic conversion of LiPSs, where the enriched porous structure and tubular morphology facilitate rapid redox conversion of LiPSs. Consequently, Li-S batteries with PTCN/S cathodes delivered a discharge capacity of 504 mAh g^{-1} at 4 C and a remarkable cycling stability over 500 cycles with minimal capacity fading of 0.0063% per cycle. Angamuthu et al.[120] adopted a hydrothermal method for the preparation of MoS_2 anchored onto the surface of a CN-based nanomaterial (C-N/MoS_2) for LSBs. The as-prepared hybrid material demonstrated improved electrochemical performance, with an initial charge/discharge capacities of 1252 and 1264 mAh g^{-1} at 0.5 C rate and good capacity retention of 680 mAh g^{-1} after 200 cycles. The higher capacity and cyclic stability of CN/MoS_2-based hybrid in comparison with the pure CN are attributed to the uniform formation of a hybrid structure with CN supporting the MoS_2 and enhancing the surface area and porosity of the composite, thereby providing more electrochemical active sites and suppressing the diffusion of dissolved polysulfides. Li et al.[109] reported the efficient synthesis of MCN-based materials as cathode matrixes for advanced LSBs using a hard template method followed by melt-diffusion under a nitrogen atmosphere. The MCN material, with a large surface area and abundant mesopores, provides an effective platform for anchoring S and provides highly conductive channels for the rapid transport of electrons and Li ions while retarding the shuttling of polysulfides during the charge/discharge process. Furthermore, the high nitrogen content in the framework of MCN induces polarization with the framework, thereby allowing the facile chemical adsorption of S. Electrochemical studies revealed that the MCN/S hybrid cathode demonstrated an excellent performance with initial discharge capacities of 1284.5 and 1107.1 mAh g^{-1} for 66.7 wt% active material at 0.1 and 0.5 C, respectively. It also displayed remarkable cycling stability by retaining its initial discharge capacity at 828.4 mAh g^{-1} after 100 cycles. Recently, vacuum annealing of a MOF followed by hydrochloric acid solution treatment was adopted by Cai and co-workers[100] for the preparation of multilayered bamboo-like conductive carbon nitride (c-CN) as an *in situ* interlayer separator−support toward LSB applications. The metallic Ni formed during the high-temperature vacuum calcination acts as a catalyst, which propels the transformation of amorphous carbon into sp^2-C. Subsequently, a tubular-like c-CN material with excellent electronic conductivity, large surface area and ultrahigh nitrogen content was obtained after acid washing. A flexible and high-performance c-CN-based (c-CN PP) separator was prepared via facile vacuum filtration of c-CN and a commercially available Celgard polypropylene (PP) sheet, to fabricate a coil cell LSB in such a way that the c-CN PP separator is facing the cathode side. The CV profile of the fabricated LBS displayed two cathodic peaks at potential ranges of 2.21−2.24 and 1.81−2.07 V, which were assigned to the reduction of S_8 to Li_2S_x ($4 \leq x \leq 8$), followed by the reduction of the byproduct into an insoluble compound. Furthermore, the assembled LSB delivered an initial capacity of 1532.1 mAh g^{-1} at 0.2 C and maintained a capacity of 996.8 mAh g^{-1} when the C rate was increased to 2.0 C, suggesting that the developed separator facilitated the accelerated kinetics of the LiPSs redox reaction.

3.1.2.3. Metal−Air Batteries and Beyond. In metal−air batteries, air and metal are utilized as cathode and anode,

https://doi.org/10.1021/acsomega.5c00679
ACS Omega 2025, 10, 18184−18212

Table 3. Performance of Various MCN-Based Materials toward Electrocatalytic ORR, OER and HER

Electrocatalyst	Onset potential (V vs RHE)	Overpotential (mV)@10 mA cm^{-2}/Current density (mA cm^{-2})	Tafel slope (mV dec^{-1})	Electrolyte	Application	Ref
C-MGCN-0.3	160.1	314.8		0.5 M H_2SO_4	HER	36
g-CN@G MMs	-	219	53	0.5 M H_2SO_4	HER	140
O-Co_3S_4@S-MCN	1.60	370	52	1.0 M KOH	OER	141
g-CN/NiO-7.5%	-	215	95	1.0 M KOH	HER	142
Co_3O_4/P-CN	-	320	66.8	1.0 M KOH	OER	143
Mo_2C@carbon	1.00	-	-	0.5 M H_2SO_4	HER	144
MTiCN	-	37.6	34	0.5 M H_2SO_4	HER	145
MCN-11-G3	0.81	11.1	51.4	0.1 M KOH	ORR	153
C_3N_7	0.81	-	53.8	0.1 M KOH	ORR	154
FePc@MCN	0.93	-	-	0.1 M KOH	ORR	155
Fe_3C@mCN-800	0.90	-	-	0.1 M KOH	ORR	157
CoO_x/mC@MoS_2@g-C_3N_4	0.89	4.53	84	0.1 M KOH	ORR	158
g-CN/C	0.90	23.92	-	0.1 M KOH	ORR	159

respectively. Metal−air batteries exhibit higher energy density than traditional batteries since the ambient air used in the cathode is weightless. The common metals investigated as anode materials include Li, Na, Mg, Al, K, Zn and Fe.[121] Among them, lithium−air batteries (LABs) and zinc−air batteries (ZABs) have received a large amount of scientific interest. The major limitations of LABs and ZABs for practical applications include their inferior cycling stability and efficiency, due to the corrosion of the anode material, and poor capacity and rate capability, due to the large overpotential caused by the sluggish kinetics of the oxygen evolution reaction (OER) and oxygen reduction reaction (ORR) during the charging/discharging process, respectively.[122−126] In recent years, it was identified that developing efficient electrocatalysts could be an ideal strategy for solving the slow kinetics of the ORR and OER, and hence various electrocatalysts have been investigated.[127,128] Owing to their facile synthetic methods, environmental friendliness, large surface areas and enriched mesopores, MCN-based materials have been investigated as electrocatalysts for both LABs and ZABs. For instance, Zhao et al.[129] investigated the preparation of a single-atom Pt catalyst supported on holey ultrathin g-CN NSs (Pt-g-CN) using a facile liquid-phase reaction of g-CN and H_2PtCl_6. They observed that the single-atom Pt NPs could achieve high stability and dispersibility, thereby promoting their full utilization during the electrochemical process, thanks to the support offered by the holey ultrathin g-CN NSs. Incorporating Pt atoms and porous structure g-CN proffer the composite to exhibit excellent electrocatalytic activity when employed as a cathode catalyst for LABs, showing a discharge capacity of 600 mAh g^{-1} after 100 cycles. Wang et al.[130] developed a hydrothermal method for the preparation of heterolayered iron−nitrogen coordination between g-CN and a graphene nanomesh (NGM-CN-Fe) with superior ORR electrocatalytic activity. The optimized composite demonstrated an enhanced ORR performance with an onset potential of 0.5 V, which is 14 times better than that of atomic Fe, and a half-wave potential 20 mV more positive than that of commercial Pt/C. The enhanced ORR electrocatalytic activity of the hybrid is ascribed to the formation of interfacial metal−nitrogen coordination between different 2D materials. Recently, MCN-based materials have been used for other battery technologies, including as separators for aqueous ZIBs, cathode materials for Al-ion batteries (AIBs), etc. For instance, Yang et al.[131] reported a facile drop-casting method for the synthesis of a modified separator based on a composite made up of a layer of g-CN NSs and a commercially available separator for aqueous ZIBs. The 2D porous g-CN NSs facilitate the distribution of electrolyte ions, thereby inducing uniform Zn-ion flux, and thus prevent dendrite growth on the zinc anode, which enhances the reversibility of the battery. A symmetrical ZIB based on Zn||Zn utilizing a g-CN-coated separator delivered a 300-fold enhancement in terms of cycling stability for over 590 h at 3 mA cm^{-2} and a Coulombic efficiency of 99.2% at 1 mA cm^{-2} for over 750 cycles. Li et al.[40] prepared g-CN/N-doped carbon (g-CN/N-C) composites as advanced cathode materials for aqueous AIBs. The optimized composite delivered an initial capacity of ∼54.9 mAh g^{-1} at 0.2 C with a high Coulomb efficiency of ∼99.9% and excellent long-term cycling stability over 200 cycles. The *ex situ* X-ray diffraction and scanning electron microscopy investigation revealed that the charge/discharge process occurring in AIBs involves the removal/addition of Al species, mostly Al^{3+}, $AlCl^{4-}$ and Al_2Cl_7, from/into the g-C_3N_4 crystal lattice with the formation of intermediate $Al_8C_3N_4$ and (ClCN).[3]

Of special interest, all-solid-state batteries with the potential to replace traditional batteries based on flammable liquid electrolytes are receiving a great amount of attention.[101] This class of battery technology can be deployed for large-scale energy storage, including power grids and electric vehicles, among others. Nevertheless, the difficulty in finding a suitable nanosize all-solid-state battery assembly, including a solid electrolyte with superior ionic conductivity, remains a herculean task toward actualizing the full potential of all-solid-state batteries. It is worth mentioning that research is currently ongoing aiming at overcoming the above-mentioned challenges related to this technology.[101]

3.2. Mesoporous Carbon Nitride-Based Materials for Electrochemical Energy Conversion Applications. The performance of various MCN-based materials toward electrocatalytic ORR, OER and HER, as discussed below, is summarized in Table 3.

3.2.1. Electrocatalytic Hydrogen Evolution Reaction and Oxygen Evolution Reaction. Considering its high energy and cleanliness, hydrogen has the potential to be used as an alternative and sustainable energy source for the future economy.[132] At present, a large proportion of H_2 gas is produced by steam reforming of natural gas, which is considered to be nonsustainable as the reserve of hydrocarbons is fast-depleting.[133] Furthermore, the utilization of hydro-

https://doi.org/10.1021/acsomega.5c00679
ACS Omega 2025, 10, 18184−18212

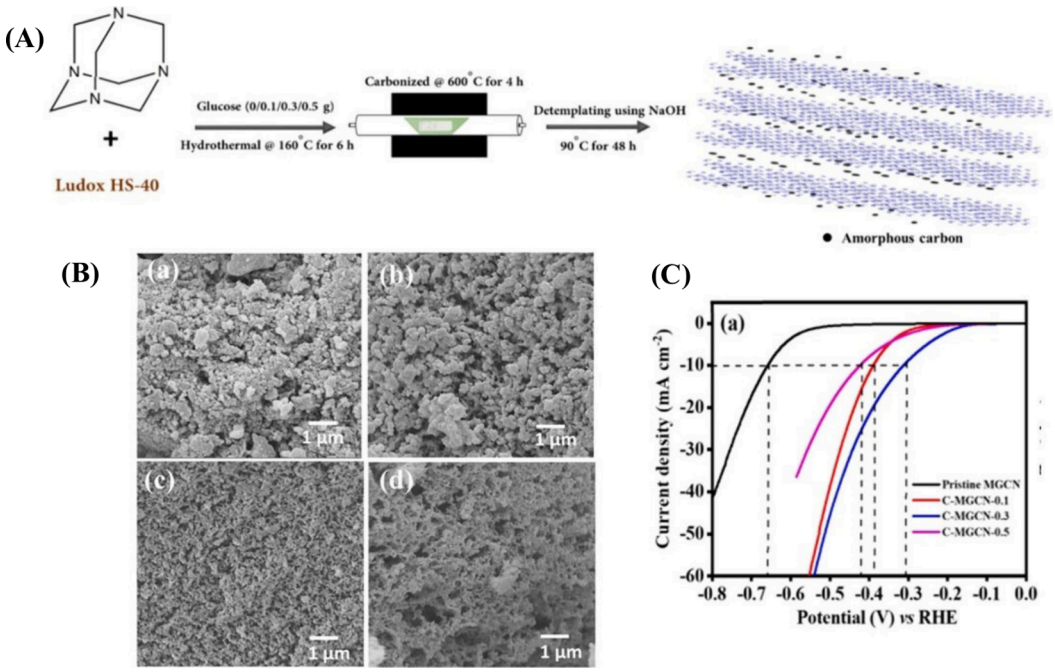

Figure 6. (A) Schematic representation of the synthesis of C-MGCN-*X* samples. (B) SEM images of (a) pristine MGCN, (b) C-MGCN-0.1, (c) C-MGCN-0.3 and (d) C-MGCN-0.5 samples. (C) HER polarization curve recorded at a sweep rate of 20 mV s^{-1} of pristine MGCN and C-MGCN-*X* samples. Reproduced with permission from ref 35. Copyright 2022 Elsevier B.V.

carbons for the production of H_2 gas leads to the release of greenhouse gases (GHGs), which trigger climate changes. In recent decades, electrocatalytic water-splitting has received attention as an efficient and sustainable method for the generation of H_2 gas.[134] During the overall electrocatalytic water-splitting, a hydrogen evolution reaction (HER) and an oxygen evolution reaction (OER) occur at the cathode and anode, respectively. The major limitation of electrocatalytic water-splitting is the slow reaction kinetics associated with both OER and HER, and thus an efficient electrocatalyst is required to reduce the high overpotential of the reactions, thereby increasing the efficiency of the overall process.[135] Though noble metals such as platinum are reported to demonstrate excellent electrocatalytic activity, their high cost and scarcity remain major hurdles from the commercialization point of view.[135−139] Hence, researchers are focused on finding alternative electrocatalysts that are cost-effective and environmentally benign. Accordingly, transition-metal-based materials exhibiting unique chemical and physical properties, including excellent corrosion and chemical stability, high electrical conductivity, etc., have been found to demonstrate an appreciable electrocatalytic HER performance. On the other hand, the direct application of MCN as an electrocatalyst for HER is very limited due to its inferior electrical conductivity. Therefore, compositing it with other materials and heteroatom/carbon doping has been studied to overcome this limitation. For instance, our group reported that the presence of residual carbon in the interlayer of MCN provides a conductive pathway for the transfer of electrons, thereby decreasing the interfacial charge transfer involved in HER.[36] Inspired by this, we deliberately doped MCN with carbon and investigated its influence on the electrocatalytic HER performance.[35] Typically, a sol−gel method was adopted for the introduction of mesoporosity and glucose was utilized as a carbon source (Figure 6A). It was found the residual carbon originated from the thermal decomposition of glucose, which is mainly amorphous, enlarging the interlayer space of MCN, an indication that structural doping of carbon was achieved. Microstructural studies (Figure 6B) revealed that the amount of carbon source used during the synthesis has a significant influence on both the texture and particle size of the as-prepared material. Notably, the particle size was found to decrease with an increase in the amount of carbon source, which was ascribed to the increase in the effective coordination between the precursors. On the other hand, the degree of porosity was found to increase with an increase in the amount of the carbon source, mainly due to the increase in the amount of gas originating from the thermal decomposition of glucose. Among all the samples, MCN prepared using 0.3 g of glucose (C-MGNC-0.3) presented the lowest onset potential of 160.1 mV vs reversible hydrogen electrode (RHE) and required only 314.8 mV to achieve a current density of 10 mA cm^{-2} in 0.5 M H_2SO_4 (Figure 6C). The better HER performance of C-MGCN-0.3 was ascribed to its better textural properties and comparably smaller particle size, which facilitated rapid charge transfer reactions. Han et al.[140] synthesized a mesh-on-mesh g-CN@mesoporous graphene mesh hybrid (g-CN@GMMs) by a facile hydrothermal treatment of presynthesized 2D mesoporous graphene meshes with urea, followed by thermal carbonization at 600 °C under an argon atmosphere. The mesh-on-mesh architecture of the composite, coupled with the strong synergetic influence of g-CN and GMMs, endows it with an enriched surface area and high electrical conductivity, which provide exposed adsorption sites for molecular hydrogen and facile transport of electrons. Consequently, the g-CN@GMMs electrocatalyst demonstrated superior HER activity, with an overpotential of 219 mV at a current density of 10 mA cm^{-2} and a Tafel slope of 53 mV dec^{-1}.

Besides carbon doping, composites made up of transition-metal-based materials and MCN have been prepared for both HER and OER. For example, Signh et al.[141] reported the electrocatalytic performance of sulfur-doped conductive MCN

https://doi.org/10.1021/acsomega.5c00679
ACS Omega 2025, 10, 18184−18212

supported with defect-rich cobalt sulfide (O-Co_3S_4@S-MCN). It was found that the hard template used, namely, MCM-41, could be employed as a porogen and an *in situ* oxygen source. The presence of the porous nanostructures in the as-prepared material offers accessible and abundant active sites for the fast transport of electrons and reactant mass, thereby speeding up the OER. On the other hand, the addition of oxygen into Co_3S_4 results in an improvement in its electrocatalytic performance. Physiochemical studies revealed that the as-prepared O-Co_3S_4@S-MCN material is highly crystalline and consists of Co_3S_4 with abundant defects. The O-Co_3S_4@S-MCN composite showed a low onset potential of 1.6 V at a current density of 10 mA cm^{-2}, a high mass activity of 71 A g^{-1} at 1.7 V, a low Tafel slope of 52 mV dec^{-1} and excellent stability (only a 5% decrease in current density after 2 h of continuous electrolysis) for the electrocatalytic OER in 1.0 M KOH. Chebanenco et al.[142] prepared an exfoliated g-CN/NiO nanocomposite using the thermal pyrolysis of urea followed by ultrasonic exfoliation of g-CN colloidal solution in the presence of nickel acetate. Ultrafine g-CN/NiO nanocomposites with various amounts of NiO (g-CN/NiO-0.0%, g-CN/NiO-2.5%, g-CN/NiO-5.0%, g-CN/NiO-7.5% and g-CN/NiO-10%) were successfully prepared by varying the concentration of nickel acetate. Among all the samples, g-CN/NiO-7.5%, with an optimized amount of NiO NPs, delivered the best performance, showing an overpotential of 215 mV at 10 mA cm^{-2} and a Tafel slope of 95 mV dec^{-1}. Phosphorus-doped g-CN was utilized to overcome the agglomeration and limited conductivity of Co_3O_4 nanocrystals toward OER by Zhu et al.[143] Typically, Co_3O_4 nanocrystals were anchored onto the surface of phosphorus-doped g-CN (P-CN). The X-ray photoelectron spectroscopy studies demonstrated that sintering of the Co_3O_4 nanocrystals and P-CN NSs results in the formation of Co−N bonds, thereby creating an effective route for charge transport and exposing a large number of potential active sites. The OER performance of the as-prepared Co_3O_4/P-CN catalyst exhibited a remarkable overpotential of 320 mV, a Tafel slope of 66.8 mV dec^{-1} and a superior electrochemical active surface area of 133.58 mF cm^{-2}.

Owing to its high nitrogen content and confined pore spaces, MCN has been utilized as a hard reactive template for the preparation of nitrogen-doped nanostructured metal oxides/sulfides for HER. For instance, Alhajri et al.[144] developed molybdenum carbide nanocrystals (Mo_2C) sized within 3 to 20 nm within a carbon matrix using MCN with confined pores as a sacrificial template. Physicochemical analysis revealed that the carbonization temperature used for the thermal decomposition of MCN influences the compositions and surface structures of the final product, which in turn affect their electrocatalytic performance toward HER. Among the samples, the Mo_2C@carbon nanocomposite prepared at 1050 °C exhibited the largest surface area (308 m^2 g^{-1}) and a relatively small particle size (∼8 nm on average) and thus delivered the highest HER activity, with an onset potential of 100 mV vs RHE in 0.05 M H_2SO_4 electrolyte. In 2022, Gujral et al.[145] utilized MCN as a reactive hard template for the preparation of mesoporous titanium carbonitride (MTiCN). The as-synthesized MTiCN materials exhibited a rod-like morphology, abundant mesostructures, high specific surface area and enriched graphitic carbon domains. The ratio between the MCN and titanium chloride precursor was varied from 0.4 to 1.2, and the optimized MTiCN demonstrated an appreciable electrocatalytic HER activity, with a low onset potential of 37.6 mV vs RHE and a Tafel slope of 34 mV dec^{-1}, which is close to that of commercial Pt/C.

3.2.2. Electrocatalytic Oxygen Reduction Reaction. The oxygen reduction reaction (ORR) plays a significant role in various electrochemical energy storage and conversion devices such as fuel cells, metal−air batteries, etc. The strong O═O bond requires energy of 498 kJ mol^{-1}, making ORR kinetically sluggish, thereby resulting in low efficiency of the devices. Thus, electrocatalysts are used to speed the activation and reduction of O_2. Several noble metals and nonprecious transition metal oxides have shown remarkable performance as electrocatalysts, but their low earth-abundance, toxicity and high cost remain major challenges. On the other hand, carbon-based materials such as carbon nanotubes (CNTs), graphene and their analogues are considered attractive electrocatalysts owing to their low cost, good stability, high electrical conductivity and high surface area.[146−150] Additionally, their electronic structures can be easily modified by defect engineering, heteroatom doping or combination with other substrates, thereby achieving higher electrocatalytic ORR activity.[151] MCN, with high inherent nitrogen content, enriched sp^2-hybridized carbon, large surface area and excellent thermal and chemical stabilities could be a promising electrocatalyst for ORR. The high nitrogen content is expected to provide important sites for O_2 adsorption, the enriched sp^2-hybridized carbon will facilitate the flow of electrons, and the large surface area will provide abundant sites for the adsorption of a large volume of reactants. Nevertheless, the ORR performance of pristine MCN is limited mainly due to the difficulties in O_2 adsorption, O═O bond activation/cleavage and oxide removal.[152] Three major strategies were recently adopted to overcome the above limitations, namely, tailoring the nitrogen content and configuration, compositing with other materials and carbon doping. Kim et al.[153] reported tuning of the nitrogen content and configuration of MCN, thereby enhancing its ORR activity. Is is typical, a facile self-assembly of 5-amino-1H-tetrazole (5-ATTZ) was adopted for the preparation of MCN with a combined triazine and triazole framework. Subsequently, the as-prepared MCN with a C_3N_5 stoichiometric ratio was hybridized with graphene by using graphene−mesoporous silica hybrids as a template, thereby tuning the electronic properties of the composite. Among the materials studied, MCN hybridized with an optimized amount of graphene content (2.1 wt% graphene, MCN-11-G3) demonstrated the best onset potential of 0.81 V vs RHE and the lowest Tafel slope of 51.4 mV dec^{-1}. Furthermore, the material exhibited a kinetic current density of 11.1 mA cm^{-2} at 0.60 V. It has been pointed out that the 3D structure of MCN plays a significant role in the removal of the oxide byproduct during the ORR. In another study, Kim et al.[154] prepared thermodynamically stable C_3N_7 and C_3N_6 with ordered mesoporous structures by pyrolysis of 5-ATTZ at two temperatures, namely, 250 and 300 °C. Various physicochemical and DFT studies revealed that the N−N bonds in the C_3N_7 and C_3N_6 are stabilized as tetrazine and/or triazole moieties. Although ordered mesoporous C_3N_6 possesses a larger surface area (167 m^2 g^{-1}) than ordered mesoporous C_3N_7 (114 m^2 g^{-1}), electrocatalytic studies indicated that C_3N_7 displays better ORR performance, with an onset potential of 0.81 V vs RHE, as compared to C_3N_6 (onset potential 0.8 V vs RHE). The better electrocatalytic activity of C_3N_7 is ascribed to its higher number of nitrogen atoms, which provide a greater number of active sites for molecular oxygen adsorption.

https://doi.org/10.1021/acsomega.5c00679
ACS Omega 2025, 10, 18184−18212

Table 4. Performance of Various MCN-Based Materials toward Gas Storage, Separation and Conversion

Material	Application	Surface area ($m^2\ g^{-1}$)	Amount of gas adsorbed (mmol g^{-1})/current density (mA cm^{-2})	Operation temp (°C), pressure (bar)	Ref
gNPCN-130	CO_2 storage	466	23.1	0, 30	170
MCN-8E-150	CO_2 storage		5.63	0, 30	171
DP-CN-1-4	CO_2 and H_2S storage	2036.9	8.3, 13.8	25, 1	172
Pebax/ZIF-8/g-CN-9 MMMs	CO_2/CH_4 separation	278	35.5 ± 0.67	25, 2	173
SEW-MCN-1-130	CO_2 storage	655	11.6	0, 30	55
MCN-3	CO_2 storage	514	1.74	70, 1	176
MCN-1-130	CO_2 storage	678	16.5	0, 30	175
MCN-7-150	CO_2 storage	801.5	11.3	0, 30	177
E-MCN-1-900	CO_2 storage	738	20.1	0, 30	178
CN-C_9N_7	CO_2 storage, CO_2/N_2 and CO_2/CH_4 separation	-	7.06[a]	25, 1	179
Cr-MCN-10-1.5	CO_2 storage	1294	16.8	0, 30	180
20MgO/MCN	CO_2 storage	215	1.15	25, 1.013	181
Porous rGO/CN	CO_2 storage and selectivity	450	0.43[b]	27, 0.1	192
MCN-14-180	CO_2 storage and conversion	244	9.1 and ∼48	0, 30	174
Pd/Cu/g-CN NTs	Electrochemical reduction of CO_2	240	12.5	-	182
Ni-MCN	H_2 storage	1481	1.46%	30, 100	188
ND-MCN	H_2 storage	62.6	0.4%	25, 100	191

[a]Separation factor: CO_2/N_2 and CO_2/CH_4 = 41.43 and 18.67 Barrer. [b]Selectivity factor: $\alpha 12^{ads}$ = 427.

It is worth mentioning that there is a limited amount of research in the area of tailoring the nitrogen content and configuration of MCN for ORR applications, and thus the formation of MCN composites has received the most attention. For instance, Signh et al.[155] reported the ORR activity of MCN-immobilized metal phthalocyanines (MPc, where M = Mn, Fe, Co, Ni, Cu and Zn). Typically, the MCN material was prepared by a hard template method using MCM-41 as the hard template, followed by the immobilization of MPcs. In the composite, MCN is expected to act as a support material, thereby preventing the aggregation of MPc molecules and stabilizing the metal ions through coordination with nitrogen groups. The MPc-incorporated MCN materials (MPc@MCN) were investigated for their electrocatalytic ORR activity in acidic and basic media. Electrocatalytic studies revealed that FePc@MCN and CoPc@MCN materials displayed higher ORR activity than the other composites in 0.1 M KOH. Notably, FePc@MCN follows a direct four-electron oxygen reduction pathway and shows an ORR onset potential of 0.93 V in 0.1 M KOH, comparable to that of Pt/C (1.0 V). Additionally, FePc@MCN exhibited superior stability when subjected to 3000 cycles and showed better methanol tolerance as compared to Pt/C. FePc@MCN was found to have a better methanol tolerance in comparison to Pt/C in the basic medium. On the other hand, CoPc@MCN displayed a favorable two-electron reduction reaction in both acidic and basic media. The superior ORR activity of FePc@MCN is ascribed to the side-on interaction that occurs between the oxygen and Fe in FePc, leading to the concurrent reduction of both oxygen atoms.[156] Liu et al.[157] adopted a colloidal amphiphile-templating method for the synthesis of MCN loaded with Fe_3C (Fe_3C@mCN). Preparation of the composite involved the synthesis of MCN via the colloidal amphiphile (CAM)-templating method, followed by loading of Fe^{3+} into the mesochannels of MCN. Microstructural analysis indicated that the composite prepared using MCN carbonized at 800 °C (Fe_3C@mCN-800) consisted of uniformly distributed nanospheres with an average diameter of 225 nm. Furthermore, nanocrystals of Fe_3C, with an average size of 14 nm, can be seen in the frameworks of MCN. The Fe_3C@mCN-800 electrocatalyst displayed a much higher ORR activity, with an onset potential value of 0.90 V and a half-wave potential ($E_{1/2}$) of 0.81 V, comparable to those of Pt/C. Moreover, the Fe_3C@mCN-800 electrocatalyst demonstrated better durability than the Pt/C catalyst and retained 90% of its initial current density after 10 h. The superior electrocatalytic activity of Fe_3C@mCN-800 is attributed to the higher surface area and higher degree of crystallinity of the ultrafine size Fe_3C, which endow the catalyst with multiple exposed sites that are electrochemically active toward ORR. He et al.[158] reported the bifunctional electrocatalytic activity of a mesoporous cobalt oxide/carbon@molybdenum disulfide@g-CN (CoO_x/mC@MoS_2@g-CN) composite derived from a cobalt-based MOF (ZIF-67) embedded with MoS_2 and melamine. The enhanced HER and ORR activities of CoO and MoS_2, respectively, are exploited in the composite. g-CN provides a conductive network for the rapid transport of electrons and enriches nitrogen dopant for the formation of a Co-N complex, which enhances the overall electrocatalytic activity. Notably, synergistic effects among the different components enables the as-synthesized composite (CoO_x/mC@MoS_2@g-C_3N_4) to exhibit an onset overpotential of 0.89 V and a Tafel slope of 84 mV dec^{-1} in 0.1 M KOH for ORR. Furthermore, the composite displayed a low onset potential of −0.031 V and a Tafel slope of 66 mV dec^{-1} in 0.5 M H_2SO_4 for HER.

Fu et al.[159] overcame the poor electrical conductivity of g-CN by the intentional incorporation of carbon into its structural framework. Following the typical procedure, a 3D hierarchical porous g-CN/carbon (g-CN/C) composite was prepared using glucose as a carbon source. During the carbonization of the precursor, the released ammonia gas generates the pores in the material, which makes the whole process a sustainable and template-free approach. The as-synthesized g-CN/C composite displayed fluffy microspheres, which were linked together and formed 3D structures. Moreover, the as-synthesized g-CN/C composite featured a wide specific surface area of 450 $m^2\ g^{-1}$ as well as multiscale macropores and micropores, providing abundant ORR active

https://doi.org/10.1021/acsomega.5c00679
ACS Omega 2025, 10, 18184−18212

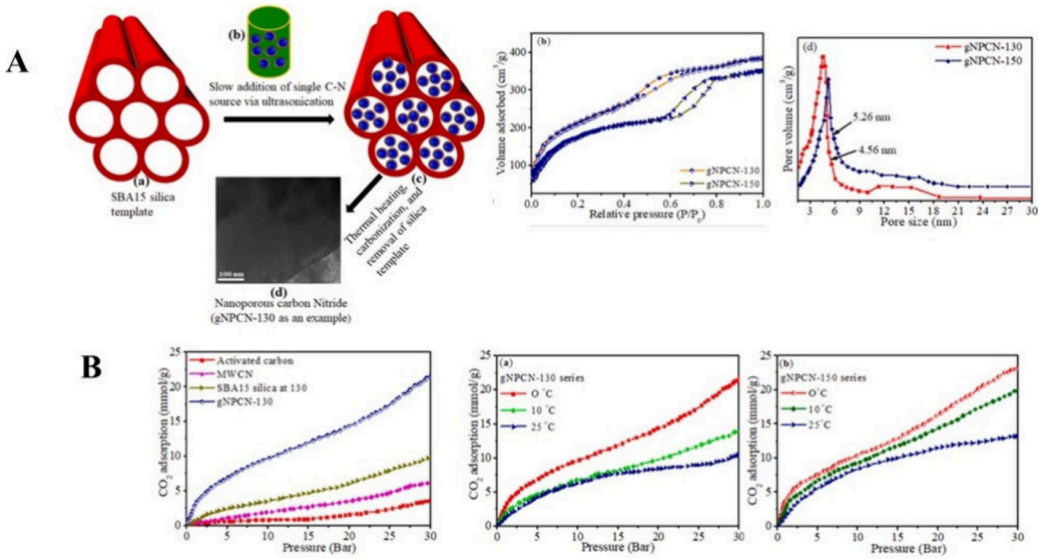

Figure 7. (A) Synthesis scheme for nanoporous carbon nitride materials using guanidine HCl as a single C-N precursor and the SBA-15 silica template, N_2 isotherms of g-NPCN-130 and g-NPCN-150 and pore size distribution curves of g-NPCN-130 and g-NPCN-150. (B) CO_2 adsorption abilities of different materials at 0 °C and CO_2 adsorption abilities at three different temperatures for (a) g-NPCN-130 series and (b) g-NPCN-150 series; pressures were up to 30 bar for both series. Reproduced with permission from ref 170. Copyright 2020 Elsevier B.V.

sites that facilitate charge transfer. The 3D hierarchical composites catalyzed ORR efficiently, with an onset potential of 0.90 V and a current density of 23.92 mA cm^{-2}. These remarkable performances suggest their promise for applications in fuel cells and metal−air batteries.

3.3. Gas Storage. Gas storage using porous materials via adsorption-based technologies has been in existence since the invention of synthetic zeolites in the early 1940s.[160,161] Advancements in the preparation of the existing materials and discovery of new promising porous materials with controlled textural, morphological and surface properties over the years have opened a new direction toward a green and sustainable separation technology. Indeed, the separation and purification of CO_2 and the desulfurization of transportation fuels are among the emerging applications of porous materials. The performance of various MCN-based materials toward gas storage, separation and conversion is summarized in Table 4.

3.3.1. Carbon Dioxide and Hydrogen Sulfide Storage. The accelerated increase in the global energy demand due to rapid population growth and industrialization has dramatically increased the excessive burning of fossil fuels, thereby resulting in the emission of GHGs.[162] Carbon dioxide is among the key components of GHGs, which has several environmental implications such as climatic changes, global warming, deforestation, flooding, etc. The level of CO_2 in the atmosphere has risen steadily from 322 ppm in 1967 to 408 ppm in 2017 and is projected to attain 600 ppm by 2100.[162−164] Hydrogen sulfide is another hazardous gas emitted during the operation of fossil fuel-based machinery. Hence, mitigating the emission rates of CO_2 and H_2S is urgently needed to slow down the impact of global warming and climate change. Over the years, various methods such as physical and chemical absorption,[165−167] adsorption,[168] cryogenic distillation,[169] etc. have been adopted to reduce the concentrations of CO_2 and H_2S in the atmosphere.[162] Among them, adsorptive separation and storage using advanced porous materials are gaining significant interest. MCN, with adjustable textural and environmentally benign properties, excellent thermal and mechanical stability and high basicity, has been studied as an exciting material for CO_2 and/or H_2S adsorption, separation and storage. Wahab et al.[170] reported the preparation of high-nitrogen MCN by a nanoconfined synthesis method using SBA-15 and guanidine hydrochloride as a hard template and single precursor, respectively (Figure 7A). To investigate the influence of textural properties of the MCN toward CO_2 adsorption, the hard template (SBA-15) was prepared at two different hydrothermal temperatures, namely, 130 and 150 °C (SBA-130 and SBA-150). The nanoconfined porous carbon nitride (g-NPCN) was prepared using the as-prepared hard template, and surface area analysis indicated that the surface area and pore volume increased with an increase in the hydrothermal temperature used for the preparation of the hard template (Figure 7A). The CO_2 adsorption capacity of the samples at various temperatures demonstrated that g-NPCN prepared using SBA-130 (g-NPCN-130) outperformed several mesoporous materials possessing higher surface area and pore volume (Figure 7B), indicating the role of the inherent C−N in boosting its adsorption capacity. The acid−base interaction existing in g-NPCN-130 could enhance its CO_2 adsorption capacity. On the other hand, g-NPCN prepared using SBA-150 demonstrates higher CO_2 uptake, which can reach up to 23.1 mmol g^{-1} at 30 bar, compared to g-NPCN-130 (Figure 7B). The difference in the adsorption capacity between g-NPCN-150 and g-NPCN-130 was ascribed to the higher surface area and pore volume of g-NPCN-150. Additionally, the large pore size of g-NPCN-150 and higher nitrogen content could facilitate the adsorption of higher amounts of CO_2.[55]

The preparation of nitrogen-rich MCN materials with abundant −NH- and $-NH_2$-based functionalities is expected to modify their physicochemical and textural properties and thus improve their CO_2 uptake capacity. Park et al.[171] reported the synthesis of highly ordered 3D MCN with high nitrogen content reaching 61%, which is higher than that of ideal g-CN, using an uncalcined KIT-6 template. Owing to the higher nitrogen content, MCN synthesized using KIT-6, prepared at a

https://doi.org/10.1021/acsomega.5c00679
ACS Omega 2025, 10, 18184−18212

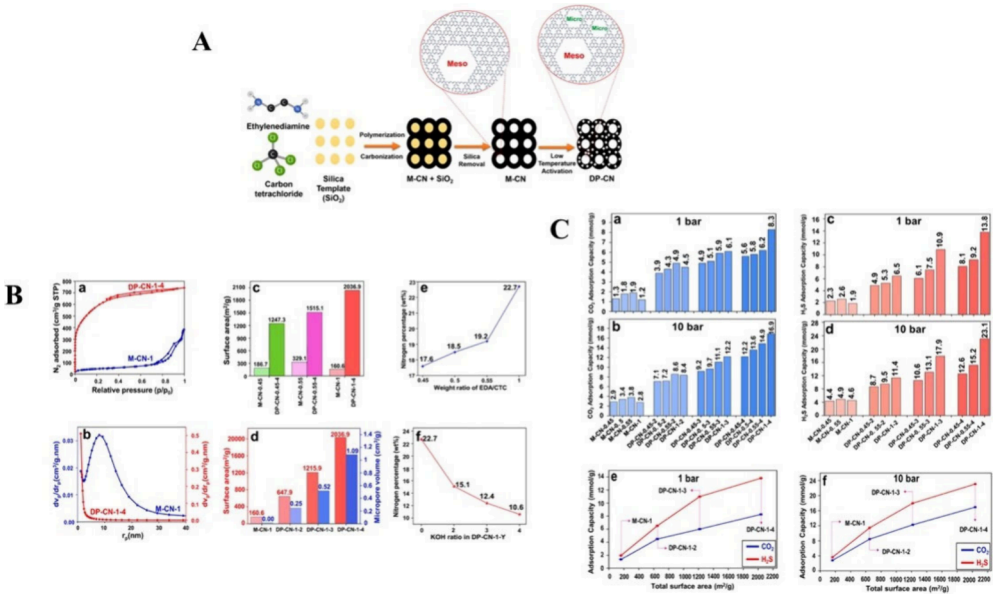

Figure 8. (A) Schematic diagram of the synthesized DP-CN-*X*-*Y*, where *X* and *Y* denote the amounts of MCN and KOH, respectively, used during the synthesis. (B) N_2 adsorption/desorption (a,b) pore size distributions of M-CN-1 and DP-CN-1-4, (c) comparison of surface area among M-CN-*X* and DP-CN-*X*-*Y* (before and after activation with KOH), (d) surface area and micropore volume of M-CN-1 and DP-CN-1-*Y* prepared with different activation ratios (2, 3 and 4), and effects of (e) EDA/CTC ratio on the nitrogen content of M-CN-*X* samples and (f) chemical activation on the nitrogen content of M-CN-1 and DP-CN-1-*Y*. (C) Bar charts of equilibrium (a,b) CO_2 and (c,d) H_2S adsorption capacities of M-CN-*X* and DP-CN-*X*-*Y* at low (1 bar) and medium pressure (10 bar) at 25 °C and (e,f) effect of total surface area on CO_2 and H_2S uptake at 1 and 10 bar (25 °C). Reproduced with permission from ref 172. Copyright 2022 Elsevier B.V.

hydrothermal temperature of 150 °C (MCN-8E-150), exhibited the highest CO_2 adsorption capacity of 5.63 mmol g^{-1} at 0 °C under 30 bar. It is worth mentioning that the reported CO_2 adsorption capacity of MCN-8E-150 is comparably lower than the values reported for 2D MCN possessing higher textural properties but lower nitrogen content, which leads us to speculate that the textural properties of MCN play a more important role toward its CO_2 adsorption capacity.

Tabarkhoon et al.[172] reported the synthesis of porous carbon nitride with dual pores (DP-CN) using a hard template method followed by KOH activation.[172] The hard template method was used to introduce mesoporosity into the frameworks of CN, whereas the low-temperature KOH activation was exploited to create microporosity (Figure 8A). It was observed that the amount of nitrogen in the parent mesoporous CN influenced the surface area, pore volume and pore size of the final material after KOH activation. In other words, the part of the nitrogen presence in the parent MCN reacts with KOH during the thermal activation, leading to the liberation of some gases such as NO_x, NH_3, etc., thereby facilitating the formation of a higher number of micropores and thus increasing the surface area and pore volume. In addition, the ratio between the activating agent and the parent MCN influences the textural properties, and it was found that the surface area contribution increases with an increase in the amount of KOH. Thus, DP-CN prepared using a MCN:KOH ratio of 1:4 (DP-CN-1-4) exhibited the best textural properties (Figure 8B). CO_2 adsorption studies demonstrated that DP-CN-1-4 exhibited the highest CO_2 and H_2S uptake values, 8.3 and 13.8 mmol g^{-1} at 1 bar, respectively. It is worth mentioning that the adsorption capacity of the parent MCN is lower than that of DP-CN-1-4, which indicates the role of microporosity in enhancing the CO_2 and H_2S uptake. On the other hand, the adsorption capacity of H_2S is higher than that of CO_2 at all pressures (Figure 8C), mainly due to the higher polarizability of H_2S (38.0×10^{-25} cm^3) than CO_2 (26.3×10^{-25} cm^3).[167] The higher polarizability results in a stronger electrostatic affinity of the H_2S molecule toward nitrogen-based functionalities on the surface of the DP-CN-1-4 adsorbent. The selectivity of CO_2 and CO_2/CH_4 separation was investigated by Li et al.[173] using high-performance mixed matrix membranes (MMMs) made up of zeolite imidazolate framework-8 (ZIF-8) anchored onto the surface of the porous g-CN. The ZIF-8 was anchored onto the surface of the porous g-CN by the thermal oxidation etching method. In the composite, the interconnected 3D nanopores of ZIF-8 offered the MMMs highly selective nanochannels, whereas the porous g-CN improved the CO_2 adsorption and permeability. The selectivity of the MMMs toward CO_2 and CO_2/CH_4 separation was improved by incorporating Pebax as a nanofiller. Thus, MMMs prepared using 1:9 wt% between the Pebax matrix and ZIF-8/GCN demonstrated the highest separation performance, reaching 553 ± 23 Barrer and 35.5 ± 0.67 for CO_2 permeability and CO_2/CH_4 separation factor, respectively.[173] Removal of the surfactant used to create the porosity in the hard template is an important step, dictating the textural properties of both the template and the daughter MCN.[1,174,175] Although calcination is the most widely adopted method, it is an energy- and time-extensive process. In this regard, Lakhi et al.[55] adopted a calcination-free approach for removing the surfactant from the SBA-15 template and used it to prepare MCN with rod-shaped morphology. The as-prepared MCN showed excellent properties, with the surface area reaching 655 m^2 g^{-1} for SEW-MCN-1-130 prepared using SEW-SBA-15-130 (where SEW and 130 denote static ethanol wash and the hydrothermal temperature used for the preparation of the template). Owing to its higher surface

https://doi.org/10.1021/acsomega.5c00679
ACS Omega 2025, 10, 18184−18212

area and larger percentage of micropores as compared to SEW-MCN-1-150 and SEW-MCN-1-100, SEW-MCN-1-130 displayed the highest CO_2 uptake under identical conditions of temperature and pressure. For instance, SEW-MCN-1-100 and SEW-MCN-1-150 displayed adsorption capacities of 11.6 and 13 mmol g^{-1} at 0 °C and 30 bar, whereas SEW-MCN-1-130 adsorbed 15.4 mmol g^{-1} under identical conditions. The ratio between the ethylenediamine (EDA) and carbon tetrachloride (CTC) was exploited by Khan et al.[176] to tune the nitrogen content and thus CO_2 adsorption and desorption behavior of MCN. It was found that both surface area and pore size decrease with an increase in the ratio of the precursors (1:1 for MCN-1, 1:2 for MCN-2 and 1:3 for MCN-3), whereas the nitrogen content was found to exhibit a reverse direction. The observed slight decreases in the surface area (540, 526 and 514 m^2 g^{-1} for MCN-1, MCN-2 and MCN-3, respectively) and pore size (7.4, 6.9 and 6.1 nm for MCN-1, MCN-2 and MCN-3 respectively) are ascribed to the formation a denser structure with increased nitrogen loading. On the other hand, the increase in the nitrogen content as the ratio between the precursors increases is attributed to the increase in the degree of polymerization of the EDA and CTC, thereby hindering the release of nitrogen atoms during the thermal carbonization. CO_2 adsorption studies revealed that all the as-prepared MCN materials exhibit similar uptake capacity in the range of 2.46−2.51 mmol g^{-1} at room temperature. However, MCN-3, with the highest nitrogen content (26.1%), demonstrated the highest CO_2 uptake (1.74 mmol g^{-1}) when the experimental temperature was increased to 70 °C. The reverse CO_2 uptake capacity of MCN-3 was evaluated using a gravimetric method at two temperatures, namely, 25 and 75 °C, and the results indicated that the adsorption process is completely reversible for up to five cycles. The superior CO_2 adsorption capacity and reversible behavior of MCN-3 are mainly due to its significantly higher initial isosteric heat of adsorptions (Q_{st}) of ∼73 kJ mol^{-1}, which depends on not only the nitrogen content but also the type of nitrogen. In 2015, Lakhi et al.[175] demonstrated that the morphology of the adsorbents has a significant influence on their CO_2 adsorption capacity and an adsorbent with uniform and rectangular-shaped morphology exhibited a better CO_2 adsorption capacity. Typically, a highly ordered MCN (MCN-1-*T*, where *T* is the hydrothermal temperature used for the synthesis of the template) with uniform rod-shaped morphology was prepared using the hard template method. The MCN-1-*T* samples were used as adsorbents for CO_2 capture. Although MCN-1-150 exhibited a higher value of isosteric heat of adsorption, an indication of stronger adsorbate−adsorbent interaction, MCN-1-130 registered the highest CO_2 uptake among all the samples, reaching 16.5 mmol g^{-1} at 0 °C under 30 bar pressure. It was found that the textural properties of the material have a direct relation with its morphology and thus the overall CO_2 adsorption capacity. The adsorbent with uniform morphology (MCN-1-130) exhibited the highest surface area and nitrogen content compared to the other adsorbents (MCN-1-100 and MCN-1-150) and thus demonstrated the highest CO_2 adsorption capacity. Besides the textural and morphological properties and nitrogen content, Lakhi et al.[177] demonstrated the role of high pressure toward increasing the adsorption capacity of an adsorbent. In this regard, they investigated the preparation of a large-pore and 3D cage MCN (MCN-7-*T*, where *T* is the synthesis temperature of the silica template FDU-12). Among the adsorbents, the MCN-7-130 sample showed the highest CO_2 uptake of 13.5 mmol g^{-1}, whereas MCN-7-100 and MCN-7-150 exhibited adsorption capacities of 10.5 and 11.3 mmol g^{-1}, respectively, at 0 °C and 30 bar. The superior adsorption capacity of MCN-7-130 is attributed to its better textural parameters. It was found that the adsorption capacity of MCN-7-130 increases with an increase in the adsorption pressure, with a high isosteric heat of adsorption in the range 34.95−24.3 kJ mol^{-1}.[177] Lakhi et al.[178] investigated the influence of carbonization temperature on the crystallinity, textural parameters and nitrogen contents of MCN and its CO_2 adsorption capacity. The prepolymerized samples were carbonized under various carbonization temperatures in the range of 600−1000 °C. The surface area and pore volume of the MCN material were found to increase with an increase in the carbonization temperature up to 900 °C, beyond which degradation of the mesostructure was witnessed. The increases in the surface area and pore volume of the MCN material with an increase in the carbonization temperature were mainly ascribed to the increase in the percentage surface area contribution from the micropore. On the other hand, the increase in the thermodynamic instability of nitrogen atoms at higher temperatures results in a decrease in the percentage nitrogen content as the carbonization temperature increases. Notably, the nitrogen content reaches the lowest values of 6.3 and 4% at temperatures of 900 and 1000 °C, respectively, a clear indication that the optimum temperature to prepare MCN with considerable nitrogen content is around 850 °C. The CO_2 adsorption capacity studies at various temperatures and pressures revealed that CO_2 uptake of the MCN materials increases with an increase in the carbonization temperature and reaches the highest level at 900 °C. Although MCN prepared at 900 °C exhibits a low nitrogen content, it registered the highest CO_2 adsorption capacity of 20.1 mmol g^{-1} at a temperature of 0 °C and a pressure of 30 bar. This suggests that achieving a superior CO_2 adsorption capacity requires a synergy between the textural parameters, nitrogen content and degree of crystallinity in the MCN-based adsorbent. Very recently, Liu et al.[179] investigated the development of porous CN NSs with C_9N_7 for selective CO_2 adsorption using Grand Canonical Monte Carlo (GCMC) and DFT calculations. The influence of varying slit widths in the range of 0.6 to 1 nm on the selective CO_2 adsorption capacity of the C_9N_7 structure was studied, and C_9N_7 with a slit width of 0.7 nm registered the highest CO_2 adsorption of 7.06 mmol g^{-1} and outstanding CO_2/N_2 and CO_2/CH_4 selectivity of 41.43 and 18.67, respectively, at 25 °C under a pressure of 1 bar. The substantially selective CO_2 adsorption and separation on the C_9N_7 surface are attributed to the strong interaction between the CO_2 and the C_9N_7 surface.

Apart from controlling the textural properties, nitrogen content and experimental pressure, the role of metal oxide NPs in determining the CO_2 adsorption capacity of MCN materials was also investigated. For instance, Joseph et al.[180] functionalized MCN with chromium oxide NPs through a simple and versatile method using a MOF (MIL-100(Cr)) and aminoguanidine hydrochloride (AG) as a template and single molecular precursor, respectively. The use of MIL-100(Cr) as a sacrificial template provides a facile strategy, thereby avoiding the use of corrosive traditional detemplating agents and thus making the whole process scalable. Furthermore, it was found that the textural properties and nitrogen content of the final material can be tailored by adjusting the ratio between

https://doi.org/10.1021/acsomega.5c00679
ACS Omega 2025, 10, 18184−18212

the MIL-100(Cr) and AG. While the surface area and pore volume were seen to decrease with an increase in the amount of AG, the chromium and nitrogen content took reverse trends. Considering that the highest surface area contribution originated from the micropore, the highest surface area was obtained for MCN-functionalized chromium oxide NPs prepared using 1.5 g of AG (Cr-MCN-10-1.5). Among all the samples, Cr-MCN-10-1.5 registered the highest CO_2 adsorption capacity of 16.8 mmol g^{-1} at an adsorption temperature of 0 °C and at 30 bar, which could be attributed to its superior textural properties and abundant nitrogen-based functionalities providing the basic sites. Furthermore, the presence of more chromium oxide NPs in Cr-MCN-10-1.5 could have enhanced its basic character by a synergetic effect, thereby improving the CO_2 uptake.[180] The effects of the NP dispersion on the CO_2 adsorption capacity of MCN were also reported by Refaat et al.[181] A series of MgO-supported MCN materials with varying amounts of MgO in the range of 5−25 wt% was prepared by a sonication-assisted method. The as-prepared MgO-supported MCN (*x*MgO/MCN, where *x* denotes the amount of MgO) was evaluated for CO_2 uptake from a 10 vol% CO_2/N_2 mixture using a fixed-bed adsorber. At 25 °C and under atmospheric pressure, 20MgO/MCN displayed the highest CO_2 adsorption capacity of 1.15 mmol g^{-1}, which is much higher than those of bare MCN (0.99 mmol g^{-1}) and MgO (0.74 mmol g^{-1}) under identical conditions. Furthermore, 20MgO/MCN was found to exhibit superior reusability over five cycles with consistent CO_2 capture capacity. The enhanced CO_2 capture capacity of the 20MgO/MCN nanocomposite is primarily due to the presence of highly dispersed MgO NPs, which can facilitate CO_2 adsorption by acid−base interaction, whereas the excellent reusability is attributed to the inherently reduced energy demands of MgO toward CO_2 regeneration.

Electrochemical conversion of captured CO_2 into valuable feedstocks for fine industry applications is a facile approach toward sustainable energy resource exploitation. Very recently, Kim et al. reported the preparation of nitrogen-rich mesoporous C_3N_5 with tailored pore size, binding energy and basic character for CO_2 capture and conversion.[174] 5-ATTZ and SBA-15 (prepared at various temperatures, *X* = 130, 150 and 180 °C) were utilized as a precursor and hard template, respectively. The as-synthesized MCN-14-*X* material, which is based on triazole structures, is expected to exhibit more basic sites and higher core nitrogen content than traditional g-CN. DFT calculations forecast that C_3N_5 is enclosed by 7 and 10 carbon and nitrogen atoms, respectively, and the CO_2 uptake occurs most likely on the largest hole. Furthermore, as the pore size of MCN increased from 3.5 to 6.1 nm, the basic character and binding energy of CO_2 were found to be in the order MCN-14-130 < MCN-14-150 < MCN-14-180. Thus, MCN-14-180, with optimum pore size, more basic sites and the strongest binding energy of CO_2, registered the highest CO_2 adsorption capacity of 9.1 mmol g^{-1} at 0 °C and 30 bar. Besides, MCN-14-180 demonstrated the highest current density, which is attributed to wider mesoporous channels ensuring rapid transport of gaseous reactant during the CO_2 reduction reactions. In 2019, Eid et al.[182] investigated the electrochemical reduction of CO_2 over Pd/Cu/g-CN nanotubes (Pd/Cu/g-CN NTs). Typically, a melamine precursor was impregnated with metal precursors (Pd and Cu) in the presence of ethylene glycol and HNO_3 solution by stirring at room temperature. Subsequently, the obtained precipitate was annealed at 550 °C for 2 h under a nitrogen atmosphere. The electrochemical reduction activity of Pd/Cu/g-CN NTs was evaluated in CO_2-saturated 0.5 M $NaHCO_3$, demonstrating an appreciable electrochemical CO_2 reduction and delivering a current density of ∼12.5 mA cm^{-2} at a potential of ∼−1 vs Ag/AgCl. The superior electrochemical CO_2 reduction activity of Pd/Cu/g-CN NTs was ascribed to the higher surface area and abundant active sites, which facilitated rapid mass transport and accelerated adsorption/dissociation of O_2.

3.3.2. Hydrogen Storage. Hydrogen is among the potential energy carriers which will not only provide a sustainable solution to the alarming increase in the depletion of fossil fuel sources but also help to realize the green mission of the United Nations. Nevertheless, storing hydrogen gas presents a difficult challenge owing to its lightweight and gaseous nature, and various practical methods have been developed for safe and reliable storage of hydrogen. Over the past few decades, the physisorption of hydrogen using porous materials has received a lot of attention. g-CN with a high degree of crystallinity, and its abundant active edges are expected to act as hosts for hydrogen gas. However, the reported hydrogen storage capacity of BGCN and its composite materials is rather inadequate from the practical point of view, which could be due to the low surface area.[103,183−186] Thus, MCN, with an inherently large surface area, tailored morphology and exposed abundant surface structures, could be an ideal candidate for hydrogen adsorption and storage. Nevertheless, few research groups have reported on potential applications of MCN for hydrogen adsorption. In 2011, Park et al.[187] investigated the hydrogen storage performance of 2D and 3D MCN with high nitrogen content using SBA-15 and cubic meso-SiO_2 as a hard template for the first time. Later, in 2014, Moradi reported the synthesis and hydrogen adsorption capacity of Ni-doped MCN.[188] The ordered MCN was prepared by the thermal polymerization reaction of ethylene diamine and carbon tetrachloride in the presence of mesoporous silica MCM-48 as a hard template. Subsequently, MCN was impregnated with nickel metal by a vacuum decomposition process. Adsorption studies using the pressure−composition−temperature (PCT) method at 100 bar and 303 K revealed that doping MCN with Ni increases its adsorption capacity (MCN, 1 wt% and Ni-MCN, 1.49 wt%). Furthermore, the hydrogen adsorption capacity of undoped MCN is higher than that of mesoporous carbon synthesized under the same reaction conditions. The higher adsorption capacity of Ni-doped MGCN is attributed to a spillover mechanism, and the enhanced adsorption arises from the strong affinity for hydrogen of Ni.[189,190] On the other hand, the larger uptake capacity of undoped MGCN as compared to mesoporous carbon is related to the stronger interaction of hydrogen gas on the C−N bond. It is worth mentioning that both the surface area and pore volume of mesoporous carbon (1530 m^2 g^{-1}, 0.73 cm^3 g^{-1}) are higher than those of Ni-doped MCN (1481 m^2 g^{-1}, 0.64 cm^3 g^{-1}) and undoped MCN (1501 m^2 g^{-1}, 0.71 cm^3 g^{-1}), a clear indication of the role the surface functional groups plays toward the hydrogen storage performance of porous materials. The role of defect engineering in tuning the surface and bulk properties of g-CN and thus its hydrogen adsorption capacity was explored by Wang and his co-workers.[191] They proposed the preparation of nitrogen-deficient porous CN (ND-MCN) by acid-assisted pyrolysis of melamine as a template-free, green and scalable method for the synthesis of nitrogen-deficient

https://doi.org/10.1021/acsomega.5c00679
ACS Omega 2025, 10, 18184−18212

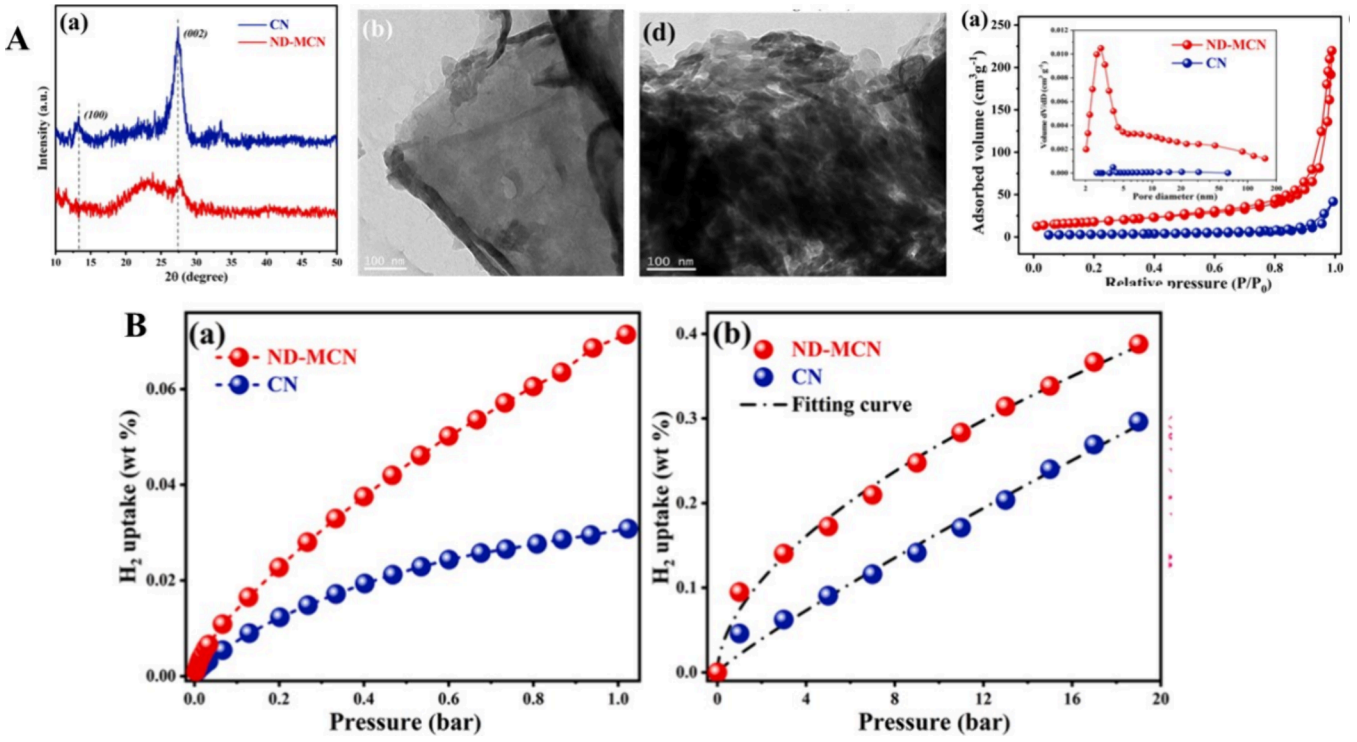

Figure 9. (A) XRD patterns, TEM images and nitrogen adsorption/desorption isotherms and pore size distributions of CN and ND-MCN. (B) Hydrogen adsorption isotherms at various temperatures for CN and ND-MCN. Reproduced with permission from ref 191. Copyright 2021 Elsevier B.V.

MCN. HCl is used as both a porosity and a nitrogen-vacancy-generating agent, thereby resulting in the formation of nitrogen-deficient and porous CN (Figure 9A). Hydrogen adsorption studies conducted at 77 and 298 K under 100 bar indicated that ND-MCN exhibited higher hydrogen uptake at both temperatures (Figure 9B). The observed higher hydrogen adsorption capacity of ND-MCN as compared to BGCN could be due to the enhanced textural properties in addition to abundant vacancies generated by nitrogen deficiency. The large surface area and pore volume of ND-MCN provide more active sites for the adsorption of hydrogen molecules, while the mesoporous structures facilitate the rapid and facile diffusion of hydrogen gas into the inner channel of the material, thereby increasing the percentage utilization of the interior surface area. Furthermore, modulation of the electronic properties of the ND-MCN by the nitrogen vacancy could have increased the adsorption energy of hydrogen molecules on its surface, thus leading to the higher hydrogen storage density of 6.39×10^{-3} wt%·g m^{-2}.

4. CONCLUSION, FUTURE OUTLOOK AND PROSPECTS

The fascinating properties of MCN-based materials, such as tailored morphology, high nitrogen content, improved textural parameters, enriched surface functionalities, etc., have enabled them to demonstrate a promising performance for various applications. In this Review, we have discussed the recent research trends involving MCN in the areas of electrochemical energy storage and conversion and gas storage, as highlighted in Tables 1−4. The structure−property relationships of MCN-based materials in the above-mentioned applications were discussed in detail. Emphasis was given to the role of the synthetic approach adopted and the nature of the precursor(s) used in controlling the textural and morphological properties and chemical composition of MCN-based materials toward obtaining the final product with improved performance. Moreover, the key impacts that MCN modifications have on the final material's electrochemical performance were discussed. Nevertheless, several challenges need to be overcome to pave the way for the potential utilization of MCN-based materials for the development of next-generation energy storage and conversion devices. The challenges and future research directions associated with MCN-based materials toward electrochemical energy storage and conversion and gas storage are as follows:

1. At present, MCN with controlled properties has only been prepared using hard template methods which involve the use of corrosive and hazardous detemplating agents, thereby making the whole process expensive and time-consuming. Therefore, developing a greener, time- and energy-efficient method for the preparation of MCN with tailored properties is key toward its potential commercialization in the area of energy storage and conversion and gas storage. Although biotemplate approaches were recently introduced, it is rather difficult to control the textural properties and chemical composition of the final product, which could inevitably negate their performance toward the final applications. Therefore, a detailed understanding of the nucleation mechanism between the biotemplate and the precursor(s) could be a turning point in overcoming this challenge.
2. Although MCN-based materials offer an impressive capacitance performance, as highlighted in Table 1, their utilization as electrode materials is still at a nascent stage, and the reported energy density is still far from the

https://doi.org/10.1021/acsomega.5c00679
ACS Omega 2025, 10, 18184−18212

requirement for practical applications. One major limitation of MCN-based materials toward electrochemical energy storage and conversion applications is their low electrical conductivity. Therefore, future research is expected to tailor the surface chemistry of MCN through surface functionalization with conductive substrates, thereby improving both ionic and electrical conductivity. Also, surface defect engineering and nanostructuring could be viable options in tuning the overall capacitance properties of MCN-based material. Ionic and solid-state electrolytes possessing a wider potential window are emerging platforms for the fabrication of superconductor (SC) devices with enhanced energy density. Surprisingly, little attention has been devoted toward investigating the capacitance performance of MCN-based materials; instead, aqueous-based electrolytes were predominantly explored. Hence, future studies are expected to focus not only on the utilization of ionic and solid-state electrolytes in MCN-based SC devices but also on their detailed charge storage mechanisms.

3. Although theoretical calculations have shown that pristine MCN could be used as the anode for various rechargeable batteries, most of the reported studies are based on composite and heteroatoms doping. Yet, the detailed structure−property relationships of the reported MCN-based composite and heteroatoms doping for the associated performance remain subjects of investigation. Therefore, a detailed theoretical understanding of the role of each component in the heterostructure is necessary to further enhance their performance. Moreover, gaining a deeper understanding of the electrode−electrolyte interaction and the associated electrochemical reactions is crucial in optimizing the design and performance of MCN-based rechargeable batteries. Furthermore, the formation of composites of MCN with other functional materials, including MXenes,[193−195] COFs, MOFs,[196,197] etc., would address the poor electrical conductivity of MCN and thus provide an avenue for improving its electrochemical energy storage and conversion performance.
4. As highlighted in Table 3, MCN-based materials were widely utilized as electrocatalysts for various electrochemical energy conversions. It was found that various modifications, such as tailoring the nitrogen content and configuration, compositing with other materials and carbon doping, etc., improve the adsorption of reactants and accelerate the kinetics of the overall reaction in MCN-based electrocatalysts. Given this, future research should be directed toward the synthesis of MCN-based materials with controllable surface defects and enhanced surface textural properties, thereby improving the rate of mass-transfer reactions during electrocatalytic transformations. The preparation of single-layered MCN materials with tailored nitrogen contents is expected to provide an efficient platform for various types of electrochemical energy conversion. Furthermore, strategic doping of p-block elements into the structural framework of MCN materials, particularly at edge sites, would provide a greater number of active sites for the adsorption reaction. Finally, a deeper theoretical understanding of the basic mechanisms associated with various electrochemical interactions of MCN-based electrocatalysts (i.e., the mechanism of electrocatalyst/electrolyte) and the roles of defects would help in further improving their electrocatalytic performance.
5. MCN-based materials with adjustable textural and environmentally benign properties, excellent thermal and mechanical stability and high basicity have been studied as exciting materials for gas separation, storage and conversion. Apart from controlling the textural properties and nitrogen content, the incorporation of various materials has been reported to further enhance their performance. Although there are a number of reports on the utilization of MCN-based materials for CO_2 adsorption, their potential applications in hydrogen storage and electrochemical conversion of CO_2 are still areas of ongoing scientific endeavors. This suggests that there is a need to understand the inherent properties of MCN-based materials in terms of their adsorptive H_2 uptake, molecular CO_2 diffusion and bond cleavage.
6. Although MCN exhibits fascinating textural properties and structural tunability, which could be explored for storage of various gases including ammonia, it is surprising to find out that research in this direction is lacking. Therefore, it is expected that future research should be directed toward the utilization of MCN as a metal-free material for storage of ammonia and other emerging gases.
7. The future outlook and prospects for MCN-based materials for electrochemical energy storage and conversion and gas storage applications require a triple helix of collaborative efforts, i.e., among academia, industry and government. Academia is expected to drive the advancement of both fundamental and applied research toward the large-scale synthesis of MCN-based materials with improved and tailored properties, which could be achieved through endowed interdisciplinary collaboration. On the other hand, entrepreneurial investment in the various electrochemical energy storage and conversion devices based on MCN materials would foster the establishment of large-scale manufacturing facilities, whereas government intervention and fair regulation would catalyze the mass adoption of unveiled technologies, ensuring economic and societal development.

AUTHOR INFORMATION

Corresponding Author

Mustapha Balarabe Idris − *Institute of Nanotechnology and Water Sustainability, College of Science, Engineering and Technology, University of South Africa, Johannesburg 1710, South Africa;* orcid.org/0000-0002-0188-2792; Email: idrisbm@unisa.ac.za

Authors

Zaharaddeen Musa Mohammed − *Materials Electrochemistry and Electrochemical Energy Storage Laboratory, Department of Chemistry, Faculty of Physical Sciences, Federal University Dutse, Jigawa 7156, Nigeria; Department of Physical and Chemical Science, Faculty of Science, Federal University of Health Sciences, Ila-Orangun, Ogun State 204, Nigeria*

Sadiya Nuhu − *Materials Electrochemistry and Electrochemical Energy Storage Laboratory, Department of Chemistry, Faculty of Physical Sciences, Federal University Dutse, Jigawa 7156, Nigeria*

https://doi.org/10.1021/acsomega.5c00679
ACS Omega 2025, 10, 18184−18212

Halima Aliyu − *Materials Electrochemistry and Electrochemical Energy Storage Laboratory, Department of Chemistry, Faculty of Physical Sciences, Federal University Dutse, Jigawa 7156, Nigeria*

Habu Abba − *Materials Electrochemistry and Electrochemical Energy Storage Laboratory, Department of Chemistry, Faculty of Physical Sciences, Federal University Dutse, Jigawa 7156, Nigeria; Department of Chemistry, Faculty of Science, Yobe State University, Damaturu 1144, Nigeria*

Bhekie B. Mamba − *Institute of Nanotechnology and Water Sustainability, College of Science, Engineering and Technology, University of South Africa, Johannesburg 1710, South Africa;* orcid.org/0000-0003-2534-2579

Devaraj Sappani − *Centre for Energy Storage & Conversion, School of Chemical and Biotechnology, SASTRA Deemed University, Thanjavur 613401, India;* orcid.org/0000-0001-7735-4315

Fuku Xolile − *Institute of Nanotechnology and Water Sustainability, College of Science, Engineering and Technology, University of South Africa, Johannesburg 1710, South Africa*

Complete contact information is available at: https://pubs.acs.org/10.1021/acsomega.5c00679

Notes

The authors declare no competing financial interest.

■ ACKNOWLEDGMENTS

The authors thank the University of South Africa, the Institute for Nanotechnology and Water Sustainability (iNanoWS), College of Science, Engineering, and Technology for funding and research facilities.

■ REFERENCES

(1) Lakhi, K. S.; Park, D.-H.; Al-Bahily, K.; Cha, W.; Viswanathan, B.; Choy, J.-H.; Vinu, A. Mesoporous carbon nitrides: synthesis, functionalization, and applications. *Chem. Soc. Rev.* **2017**, *46* (1), 72−101.

(2) Teter, D. M.; Hemley, R. J. Low-compressibility carbon nitrides. *Science* **1996**, *271* (5245), 53−55.

(3) Thomas, A.; Fischer, A.; Goettmann, F.; Antonietti, M.; Müller, J.-O.; Schlögl, R.; Carlsson, J. M. Graphitic carbon nitride materials: variation of structure and morphology and their use as metal-free catalysts. *J. Mater. Chem.* **2008**, *18* (41), 4893−4908.

(4) Liu, A. Y.; Cohen, M. L. Prediction of new low compressibility solids. *Science* **1989**, *245* (4920), 841−842.

(5) Wang, X.; Maeda, K.; Chen, X.; Takanabe, K.; Domen, K.; Hou, Y.; Fu, X.; Antonietti, M. Polymer semiconductors for artificial photosynthesis: hydrogen evolution by mesoporous graphitic carbon nitride with visible light. *J. Am. Chem. Soc.* **2009**, *131* (5), 1680−1681.

(6) Wang, X.; Maeda, K.; Thomas, A.; Takanabe, K.; Xin, G.; Carlsson, J. M.; Domen, K.; Antonietti, M. A metal-free polymeric photocatalyst for hydrogen production from water under visible light. *Nat. Mater.* **2009**, *8* (1), 76.

(7) Galan, L.; Montero, I.; Rueda, F. An X-ray photoelectron spectroscopy study of carbon nitride films grown by low energy ion implantation. *Surf. Coat. Technol.* **1996**, *83* (1−3), 103−108.

(8) Hoffman, A.; Gouzman, I.; Brener, R. Possibility of carbon nitride formation by low-energy nitrogen implantation into graphite: In situ electron spectroscopy studies. *Appl. Phys. Lett.* **1994**, *64* (7), 845−847.

(9) Goettmann, F.; Fischer, A.; Antonietti, M.; Thomas, A. Chemical Synthesis of Mesoporous Carbon Nitrides Using Hard Templates and Their Use as a Metal-Free Catalyst for Friedel−Crafts Reaction of Benzene. *Angew. Chem., Int. Ed.* **2006**, *45* (27), 4467−4471.

(10) Li, H.; Wang, L.; Liu, Y.; Lei, J.; Zhang, J. Mesoporous graphitic carbon nitride materials: synthesis and modifications. *Res. Chem. Intermed.* **2016**, *42* (5), 3979−3998.

(11) Zhang, H.; Zuo, X.; Tang, H.; Li, G.; Zhou, Z. Origin of photoactivity in graphitic carbon nitride and strategies for enhancement of photocatalytic efficiency: insights from first-principles computations. *Phys. Chem. Chem. Phys.* **2015**, *17* (9), 6280−6288.

(12) Qiu, Y.; Gao, L. Chemical synthesis of turbostratic carbon nitride, containing C−N crystallites, at atmospheric pressure. *Chem. Commun.* **2003**, *18*, 2378−2379.

(13) Haque, E.; Jun, J. W.; Talapaneni, S. N.; Vinu, A.; Jhung, S. H. Superior adsorption capacity of mesoporous carbon nitride with basic CN framework for phenol. *J. Mater. Chem.* **2010**, *20* (48), 10801−10803.

(14) Vinu, A. Two-Dimensional Hexagonally-Ordered Mesoporous Carbon Nitrides with Tunable Pore Diameter, Surface Area and Nitrogen Content. *Adv. Funct. Mater.* **2008**, *18* (5), 816−827.

(15) Vinu, A.; Ariga, K.; Mori, T.; Nakanishi, T.; Hishita, S.; Golberg, D.; Bando, Y. Preparation and characterization of well-ordered hexagonal mesoporous carbon nitride. *Adv. Mater.* **2005**, *17* (13), 1648−1652.

(16) Gonçalves, R.; Lima, T. M.; Paixão, M. W.; Pereira, E. C. Pristine carbon nitride as active material for high-performance metal-free supercapacitors: simple, easy and cheap. *RSC Adv.* **2018**, *8* (61), 35327−35336.

(17) Gong, Y.; Li, M.; Wang, Y. Carbon nitride in energy conversion and storage: recent advances and future prospects. *ChemSusChem* **2015**, *8* (6), 931−946.

(18) Das, H. T.; Babu, S. P.; Mondal, A.; Naresh, N.; Balaji, T. E.; Das, N. 2D-layered graphitic carbon nitride nanosheets for electrochemical energy storage applications. *J. Power Sources* **2024**, *603*, 234374.

(19) Chaluvachar, P.; Mahesha, G. T.; Sudhakar, Y. N.; Nair, V.; Pai, D. A Review on Graphitic Carbon Nitride and Conducting Polymer Nanocomposite Electrodes for Supercapacitors. *Eng. Proc.* **2023**, *59* (1), 154.

(20) Thomas, S. A.; Pallavolu, M. R.; Khan, M. E.; Cherusseri, J. Graphitic carbon nitride (g-C3N4): Futuristic material for rechargeable batteries. *J. Energy Storage* **2023**, *68*, 107673.

(21) Sajid, M.; Chandio, Z. A.; Hwang, B.; Yun, T. G.; Cheong, J. Y. Graphitic carbon nitrides as electrode supporting materials for lithium-ion batteries: what lies ahead in view of the current challenges? *Front. Energy Res.* **2023**, *11*, 1285044.

(22) Iqbal, O.; Ali, H.; Li, N.; Al-Sulami, A. I.; Alshammari, K. F.; Abd-Rabboh, H. S.; Al-Hadeethi, Y.; Din, I. U.; Alharthi, A. I.; Altamimi, R. J. M. T. P. A review on the synthesis, properties, and characterizations of graphitic carbon nitride (g-C3N4) for energy conversion and storage applications. *Mater. Today Phys.* **2023**, *34*, 101080.

(23) Safaei, J.; Mohamed, N. A.; Noh, M. F. M.; Soh, M. F.; Ludin, N. A.; Ibrahim, M. A.; Isahak, W. N. R. W.; Teridi, M. A. M. Graphitic carbon nitride (gC 3 N 4) electrodes for energy conversion and storage: a review on photoelectrochemical water splitting, solar cells and supercapacitors. *J. Mater. Chem. A* **2018**, *6* (45), 22346−22380.

(24) Ghaemmaghami, M.; Mohammadi, R. Fuels, Carbon nitride as a new way to facilitate the next generation of carbon-based supercapacitors. *Sustainable Energy Fuels* **2019**, *3* (9), 2176−2204.

(25) Govindaraju, V. R.; Sureshkumar, K.; Ramakrishnappa, T.; Muralikrishna, S.; Samrat, D.; Pai, R. K.; Kumar, V.; Vikrant, K.; Kim, K.-H. Graphitic carbon nitride composites as electro catalysts: Applications in energy conversion/storage and sensing system. *J. Cleaner Production* **2021**, *320*, 128693.

(26) Pachaiappan, R.; Rajendran, S.; Kumar, P. S.; Vo, D.-V. N.; Hoang, T. K.A.; Cornejo-Ponce, L. Recent advances in carbon nitride-based nanomaterials for hydrogen production and storage. *Int. J. Hydrogen Energy* **2022**, *47* (88), 37490−37516.

(27) Tang, S.; Xing, Y.; Wang, Y.; Wei, G. J. N. Recent advances in graphitic carbon nitride-based nanocomposites for energy storage and conversion applications. *Nanotechnology* **2025**, *36*, 122002.

(28) Ajmal, Z.; Tu, X.; Abbas, W.; Ibrahim, E. H.; Ali, H.; Hussain, I.; Al-Muhana, M. K.; Khered, M.; Iqbal, A.; Rahaman, S. J. F.; et al. Recent advances in Carbon-nitride based advance materials: Synthesis, characterization and Photo-electrochemical Energy Application: Key Challenges and Prospects. *Fuel* **2024**, *378*, 132903.
(29) Patel, V.; Baskar, A.; Tiburcius, S.; Morrison, B.; Mod, B.; Tanwar, P. S.; Kumar, P.; Karakoti, A.; Singh, G.; Vinu, A. Mesoporous carbon nitrides as emerging materials: Nanoarchitectonics and biosensing applications. *Adv. Sensor Res.* **2023**, *2* (9), 2300024.
(30) Zhang, H.; Zuo, X.; et al. Origin of photoactivity in graphitic carbon nitride. *Phys. Chem. Chem. Phys.* **2015**, *17*, 6280−6288.
(31) Tahir, M.; Cao, C.; Butt, F. K.; Idrees, F.; Mahmood, N.; Ali, Z.; Aslam, I.; Tanveer, M.; Rizwan, M.; Mahmood, T. Tubular graphitic-C 3 N 4: a prospective material for energy storage and green photocatalysis. *J. Mater. Chem. A* **2013**, *1* (44), 13949−13955.
(32) Wang, X.; Blechert, S.; Antonietti, M. Polymeric graphitic carbon nitride for heterogeneous photocatalysis. *ACS Catal.* **2012**, *2* (8), 1596−1606.
(33) Zheng, Y.; Liu, J.; Liang, J.; Jaroniec, M.; Qiao, S. Z. Graphitic carbon nitride materials: controllable synthesis and applications in fuel cells and photocatalysis. *Energy Environ. Sci.* **2012**, *5* (5), 6717−6731.
(34) Vinoth, S.; Devi, K. S.; Pandikumar, A. A comprehensive review on graphitic carbon nitride based electrochemical and biosensors for environmental and healthcare applications. *TrAC: Trends Anal. Chem.* **2021**, *140*, 116274.
(35) Idris, M. B.; Subramaniam, T.; Sappani, D.; Materials, R. Tailoring the electrocatalytic activity of mesoporous graphitic carbon nitride towards hydrogen evolution reaction by incorporation of amorphous carbon. *Diamond Relat. Mater.* **2022**, *129*, 109359.
(36) Idris, M. B.; Devaraj, S. Mesoporous graphitic carbon nitride synthesized using biotemplate as a high-performance electrode material for supercapacitor and electrocatalyst for hydrogen evolution reaction in acidic medium. *J. Energy Storage* **2019**, *26*, 101032.
(37) Kumar, Y. A.; Vignesh, S.; Ramachandran, T.; Kumar, K. D.; Al-Sehemi, A. G.; Moniruzzaman, M.; Oh, T. H. Solidifying the future: Metal-organic frameworks in zinc battery development. *J. Energy Storage* **2024**, *97*, 112826.
(38) Mortazavi, B.; Cuniberti, G.; Rabczuk, T. Mechanical properties and thermal conductivity of graphitic carbon nitride: A molecular dynamics study. *Comput. Mater. Sci.* **2015**, *99*, 285−289.
(39) Fang, L.; Ohfuji, H.; Shinmei, T.; Irifune, T. Experimental study on the stability of graphitic C3N4 under high pressure and high temperature. *Diamond Related Mater.* **2011**, *20* (5−6), 819−825.
(40) Li, J.; Ma, D.; Lu, G.; Fu, D.; de Leon, C. P.; Pan, J. H. Correlations of Precursor and Carbon Coating with Electrochemical Property of 2D Graphitic Carbon Nitride (g-C3N4) Nanosheets as High-Reversibility Cathode of Nonaqueous Al-Ion Batteries. *J. Phys. Chem. C* **2023**, *127* (10), 4862−4871.
(41) Sun, S.; Wu, Y.; Zhu, J.; Lu, C.; Sun, Y.; Wang, Z.; Chen, J. Stabilizing plasma-induced highly nitrogen-deficient g-C3N4 by heteroatom-refilling for excellent lithium-ion battery anodes. *Chem. Eng. J.* **2022**, *427*, 131032.
(42) Idris, M. B.; Sappani, D. Unveiling Mesoporous Graphitic Carbon Nitride as a High Performance Electrode Material for Supercapacitors. *ChemistrySelect* **2018**, *3* (40), 11258−11269.
(43) Adekoya, D.; Gu, X.; Rudge, M.; Wen, W.; Lai, C.; Hankel, M.; Zhang, S. Carbon nitride nanofibres with exceptional lithium storage capacity: from theoretical prediction to experimental implementation. *Adv.Funct.Mater.* **2018**, *28* (50), 1803972.
(44) Bafekry, A.; Faraji, M.; Fadlallah, M. M.; Sarsari, I. A.; Jappor, H. R.; Fazeli, S.; Ghergherehchi, M. Two-dimensional porous graphitic carbon nitride C_6N_7 monolayer: First-principles calculations (vol 119, 142102 2021). *Appl. Phys. Lett.* **2022**, *120* (18), 096428.
(45) Hou, J. F.; Zheng, S.; Zhu, D. Q. Highly effective catalytic peroxymonosulfate activation on mesoporous carbon nitride for o-phenylphenol degradation. *Abstracts of Papers of the American Chemical Society*, 255th National Meeting and Exposition, New Orleans, LA, March 18−22, 2018.
(46) Liu, J.; Zhang, T.; Wang, Z.; Dawson, G.; Chen, W. Simple pyrolysis of urea into graphitic carbon nitride with recyclable adsorption and photocatalytic activity. *J. Mater. Chem.* **2011**, *21* (38), 14398−14401.
(47) Wang, Q.; Yan, J.; Fan, Z. J. E. Carbon materials for high volumetric performance supercapacitors: design, progress, challenges and opportunities. *Energy Environ. Sci.* **2016**, *9* (3), 729−762.
(48) Zhang, L.; Xia, Z. Mechanisms of oxygen reduction reaction on nitrogen-doped graphene for fuel cells. *J. Phys. Chem. C* **2011**, *115* (22), 11170−11176.
(49) Chebanenko, M. I.; Lobinsky, A. A.; Nevedomskiy, V. N.; Popkov, V. I. NiO-decorated graphitic carbon nitride toward electrocatalytic hydrogen production from ethanol. *Dalton Trans.* **2020**, *49* (34), 12088−12097.
(50) Chen, T.; Dai, L. Carbon nanomaterials for high-performance supercapacitors. *Mater. Today* **2013**, *16* (7−8), 272−280.
(51) Hooch Antink, W.; Choi, Y.; Seong, K.-d.; Kim, J. M.; Piao, Y. Recent progress in porous graphene and reduced graphene oxide-based nanomaterials for electrochemical energy storage devices. *Adv. Mater. Interfaces* **2018**, *5* (5), 1701212.
(52) Chen, T. W.; Kalimuthu, P.; Veerakumar, P.; Lin, K. C.; Chen, S. M.; Ramachandran, R.; Mariyappan, V.; Chitra, S. Recent Developments in Carbon-Based Nanocomposites for Fuel Cell Applications: A Review. *Molecules* **2022**, *27* (3), 761.
(53) Peng, X.; Peng, L.; Wu, C.; Xie, Y. Two dimensional nanomaterials for flexible supercapacitors. *Chem. Soc. Rev.* **2014**, *43* (10), 3303−3323.
(54) Zheng, S. Q.; Lim, S. S.; Foo, C. Y.; Haw, C. Y.; Chiu, W. S.; Chia, C. H.; Khiew, P. S. J. F. i. M. Recent progress on the applications of carbonaceous and metal-organic framework nanomaterials for supercapacitors. *Front.Mater.* **2021**, *8*, 777149.
(55) Lakhi, K. S.; Park, D.-H.; Singh, G.; Talapaneni, S. N.; Ravon, U.; Al-Bahily, K.; Vinu, A. Energy efficient synthesis of highly ordered mesoporous carbon nitrides with uniform rods and their superior CO_2 adsorption capacity. *J. Mater. Chem. A* **2017**, *5* (31), 16220−16230.
(56) Sathish, C. I.; Kothandam, G.; Selvarajan, P.; Lei, Z. H.; Lee, J.; Qu, J. T.; Al-Muhtaseb, A. H.; Yu, X. J.; Breese, M. B. H.; Zheng, R. K.; Yi, J. B.; Vinu, A. Ordered Mesoporous Boron Carbon Nitrides with Tunable Mesopore Nanoarchitectonics for Energy Storage and CO_2 Adsorption Properties. *Adv. Sci.* **2022**, *9* (16), 2105603.
(57) González, A.; Goikolea, E.; Barrena, J. A.; Mysyk, R. Review on supercapacitors: technologies and materials. *Renewable Sustainable Energy Rev.* **2016**, *58*, 1189−1206.
(58) Ramachandran, T.; Raji, R. K.; Palanisamy, S.; Renuka, N.; Karuppasamy, K. The role of in situ and operando techniques in unraveling local electrochemical supercapacitor phenomena. *J. Ind. Eng. Chem.* **2025**, *145*, 144.
(59) Bharathidasan, P.; Idris, M. B.; Kim, D.-W.; Sivakkumar, S.; Devaraj, S. Enhanced capacitance properties of nitrogen doped reduced graphene oxide obtained by simultaneous reduction and nitrogen doping. *FlatChem* **2018**, *11*, 24−31.
(60) Patiño, J.; et al. Phosphorus-doped carbon−carbon nanotube hierarchical monoliths as true three-dimensional electrodes in supercapacitor cells. *J. Mater. Chem. A* **2016**, *4*, 1251−1263.
(61) Conway, B. E. Transition from "supercapacitor" to "battery" behavior in electrochemical energy storage. *J. Electrochem. Soc.* **1991**, *138* (6), 1539−1548.
(62) Conway, B. E. *Electrochemical supercapacitors: scientific fundamentals and technological applications*; Springer Science & Business Media, 2013.
(63) Li, H.-c.; Shen, H.-r.; Shi, Y.; Wen, L.; Li, F. Progress and prospects of graphene for in-plane micro-supercapacitors. *New Carbon Mater.* **2022**, *37* (5), 781−801.
(64) Mouli, K. V. C.; Kalla, R. M. N.; Ramachandran, T.; Kumar, Y. A.; Moniruzzaman, M.; Lee, J. Cutting-edge advancements in HOFs-derived materials for energy storage supercapacitor application. *Int. J. Hydrogen Energy* **2024**, *90*, 1−24.

https://doi.org/10.1021/acsomega.5c00679
ACS Omega 2025, 10, 18184−18212

(65) Bharathidasan, P.; Idris, M. B.; Kim, D.-W.; Sivakkumar, S.; Devaraj, S. Exploiting the chemistry of redox active compounds to enhance the capacitance of reduced graphene oxide. *FlatChem* **2019**, *15*, 100108.
(66) Idris, M. B.; Nuhu, S.; Mohammed, Z. M.; Aliyu, H.; Abba, H.; Xolile, F.; Devaraj, S. Progress in metal-organic frameworks and their carbon-based composites for supercapacitor. *J. Energy Storage* **2024**, *93*, 112322.
(67) Kumar, Y. A.; Vignesh, S.; Ramachandran, T.; Fouda, A. M.; Hegazy, H.; Moniruzzaman, M.; Oh, T. H. Advancements in novel electrolyte materials: Pioneering the future of supercapacitive energy storage. *J. Ind. Eng. Chem.* **2025**, *145*, 191.
(68) Borenstein, A.; Hanna, O.; Attias, R.; Luski, S.; Brousse, T.; Aurbach, D. Carbon-based composite materials for supercapacitor electrodes: a review. *J. Mater. Chem. A* **2017**, *5* (25), 12653−12672.
(69) Palem, V. V.; Idris, M. B.; Subramaniam, T.; Sappani, D. The Charge Storage Mechanism of $MnCO_3$ in Aqueous Electrolytes. *ChemistrySelect* **2020**, *5* (17), 5316−5322.
(70) Anil Kumar, Y.; Koyyada, G.; Ramachandran, T.; Kim, J. H.; Sajid, S.; Moniruzzaman, M.; Alzahmi, S.; Obaidat, I. M. J. N. Carbon materials as a conductive skeleton for supercapacitor electrode applications: a review. *Nanomaterials* **2023**, *13* (6), 1049.
(71) Ramachandran, T.; Roy, N.; Hegazy, H.; Yahia, I.; Kumar, Y. A.; Moniruzzaman, M.; Joo, S. W. From graphene aerogels to efficient energy storage: current developments and future prospects. *J. Alloys Compds.* **2025**, *1010*, 177248.
(72) Vardhan, P. V.; Idris, M. B.; Liu, H. Y.; Sivakkumar, S. R.; Balaya, P.; Devaraj, S. Tuning the Capacitance Properties of Nanocrystalline MnCO3 by the Effect of a Carbonizing Agent. *J. Electrochem. Soc.* **2018**, *165* (9), A1865−A1873.
(73) Vardhan, P. V.; Idris, M. B.; Ramanathan, V.; Devaraj, S. Electrodeposited MnCO3 as a high performance electrode material for supercapacitor. *ChemistrySelect* **2018**, *3* (24), 6775−6778.
(74) Vardhan, P. V.; Idris, M. B.; Liu, H. Y.; Sivakkumar, S. R.; Balaya, P.; Devaraj, S. Tuning the Capacitance Properties of Nanocrystalline $MnCO_3$ by the Effect of a Carbonizing Agent. *J. Electrochem. Soc.* **2018**, *165* (9), A1865−A1873.
(75) Zheng, S. Q.; Lim, S. S.; Foo, C. Y.; Haw, C. Y.; Chiu, W. S.; Chia, C. H.; Khiew, P. S. Recent progress on the applications of carbonaceous and metal-organic framework nanomaterials for supercapacitors. *Front. Mater.* **2021**, *8*, 777149.
(76) Kumar, Y. A.; Alagarasan, J. K.; Ramachandran, T.; Rezeq, M.; Bajaber, M. A.; Alalwiat, A. A.; Moniruzzaman, M.; Lee, M. The landscape of energy storage: Insights into carbon electrode materials and future directions. *J. Energy Storage* **2024**, *86*, 111119.
(77) Kumar, Y. A.; Roy, N.; Ramachandran, T.; Hussien, M.; Moniruzzaman, M.; Joo, S. W. Shaping the future of energy: The rise of supercapacitors progress in the last five years. *J. Energy Storage* **2024**, *98*, 113040.
(78) Idris, M. B.; Sappani, D. Unveiling Mesoporous Graphitic Carbon Nitride as a High Performance Electrode Material for Supercapacitors. *ChemistrySelect* **2018**, *3* (40), 11258−11269.
(79) Idris, M. B.; Devaraj, S. Tuning the chemical composition, textural and capacitance properties of mesoporous graphitic carbon nitride. *Electrochim. Acta* **2019**, *303*, 219.
(80) Xu, Z. Y.; Kong, L. R.; Wang, H.; Ma, Q.; Shen, X. P.; Wang, J. Y.; Premlatha, S. Soft-template assisted preparation of hierarchically porous graphitic carbon nitride layers for high-performance supercapacitors. *J. Appl. Polym. Sci.* **2022**, *139* (39), 52947.
(81) Idris, M. B.; Sakthivel, G.; Devaraj, S. Textural properties dependent supercapacitive performances of mesoporous graphitic carbon nitride. *Materials Today Energy* **2018**, *10*, 325−335.
(82) Nazari, M.; Rahmanifar, M. S.; Noori, A.; Li, W. J.; Zhang, C.; Mousavi, M. F. The ordered mesoporous carbon nitride-graphene aerogel nanocomposite for high-performance supercapacitors. *J. Power Sources* **2021**, *494*, 229741.
(83) Idris, M. B.; Devaraj, S. Few-layered mesoporous graphitic carbon nitride: a graphene analogue with high capacitance properties. *New J. Chem.* **2019**, *43* (29), 11626−11635.
(84) Lu, C.; Yang, Y.; Chen, X. Ultra-thin conductive graphitic carbon nitride assembly through van der Waals epitaxy toward high-energy-density flexible supercapacitors. *Nano Lett.* **2019**, *19* (6), 4103−4111.
(85) Zhu, S.; Li, J.; Ma, L.; Guo, L.; Li, Q.; He, C.; Liu, E.; He, F.; Shi, C.; Zhao, N. Three-dimensional network of N-doped carbon ultrathin nanosheets with closely packed mesopores: controllable synthesis and application in electrochemical energy storage. *ACS Appl. Mater. Interfaces* **2016**, *8* (18), 11720−11728.
(86) Wang, H.; Liu, Y.; Kong, L.; Xu, Z.; Shen, X.; Premlatha, S. Porous graphitic carbon nitride nanosheets with three-dimensional interconnected network as electrode for supercapacitors. *J. Energy Storage* **2023**, *63*, 106935.
(87) Shwetha, K.; Divakara, S.; Kamath, M. S.; Gupta, T. Synthesis and electrochemical characterization of mesoporous graphitic carbon nitride for super capacitor applications. *Mater. Today: Proc.* **2023**, *76*, 219−226.
(88) Cai, C. L.; Zou, Y. J.; Xiang, C. L.; Chu, H. L.; Qiu, S. J.; Sui, Q. L.; Xu, F.; Sun, L. X.; Shah, A. Broccoli-like porous carbon nitride from ZIF-8 and melamine for high performance supercapacitors. *Appl. Surf. Sci.* **2018**, *440*, 47−54.
(89) Xu, Z. Y.; Kong, L. R.; Wang, H.; Shen, X. P.; Premlatha, S. Flower-like nickel-cobalt-layered double hydroxide nanosheets deposited on hierarchically porous graphitic carbon nitride for enhanced electrochemical energy storage. *J. Energy Storage* **2022**, *51*, 104541.
(90) Shen, C.; Li, R. Z.; Yan, L. J.; Shi, Y. X.; Guo, H. T.; Zhang, J. H.; Lin, Y.; Zhang, Z. K.; Gong, Y. Y.; Niu, L. Y. Rational design of activated carbon nitride materials for symmetric supercapacitor applications. *Appl. Surf. Sci.* **2018**, *455*, 841−848.
(91) Idris, M. B.; Sai, G. H.; Hemalatha, D.; Sakthivel, G.; Devaraj, S. The effect of phosphorous doping on the composition and capacitance properties of mesoporous graphitic carbon nitride. *J. Electrochem. Soc.* **2019**, *166* (12), A2409.
(92) Kong, L. R.; Chen, Q. R.; Shen, X. P.; Xia, C.; Ji, Z. Y.; Zhu, J. Ionic Liquid Templated Porous Boron-Doped Graphitic Carbon Nitride Nanosheet Electrode for High-Performance Supercapacitor. *Electrochim. Acta* **2017**, *245*, 241−249.
(93) Li, Z. C.; Wu, L.; Wang, L. B.; Gu, A. J.; Zhou, Q. F. Nickel cobalt sulfide nanosheets uniformly anchored on porous graphitic carbon nitride for supercapacitors with high cycling performance. *Electrochim. Acta* **2017**, *231*, 617−625.
(94) Karuppaiah, M.; Benadict Joseph, X.; Wang, S.-F.; Sriram, B.; Antilen Jacob, G.; Ravi, G. Engineering architecture of 3D-urchin-like structure and 2d-nanosheets of Bi2S3@ g-C3N4 as the electrode material for a solid-state symmetric supercapacitor. *Energy Fuels* **2021**, *35* (15), 12569−12580.
(95) Taha, M. M.; Ghanem, L. G.; Hamza, M. A.; Allam, N. K. Highly stable supercapacitor devices based on three-dimensional bioderived carbon encapsulated g-C3N4 nanosheets. *ACS Appl. Energy Mater.* **2021**, *4* (9), 10344−10355.
(96) Hashem, E. M.; Hamza, M. A.; El-Shazly, A. N.; Abd El-Rahman, S. A.; El-Tanany, E. M.; Mohamed, R. T.; Allam, N. K. Novel Z-Scheme/Type-II CdS@ ZnO/g-C3N4 ternary nanocomposites for the durable photodegradation of organics: Kinetic and mechanistic insights. *Chemosphere* **2021**, *277*, 128730.
(97) Baruah, K.; Sarmah, D.; Kumar, A. Ternary hybrid nanocomposites of polypyrrole nanotubes with 2D self-assembled heterostructures of protonated g-C_3N_4-rGO as supercapacitor electrodes. *Ionics* **2021**, *27* (7), 3153−3168.
(98) Tahir, M.; Cao, C.; Mahmood, N.; Butt, F. K.; Mahmood, A.; Idrees, F.; Hussain, S.; Tanveer, M.; Ali, Z.; Aslam, I. Multifunctional g-C3N4 nanofibers: a template-free fabrication and enhanced optical, electrochemical, and photocatalyst properties. *ACS Appl. Mater. Interfaces* **2014**, *6* (2), 1258−1265.
(99) Yang, W.; Hou, L. Q.; Xu, X. W.; Li, Z. H.; Ma, X. L.; Yang, F.; Li, Y. F. Carbon nitride template-directed fabrication of nitrogen-rich porous graphene-like carbon for high performance supercapacitors. *Carbon* **2018**, *130*, 325−332.

https://doi.org/10.1021/acsomega.5c00679
ACS Omega 2025, 10, 18184−18212

(100) Cai, J. S.; Song, Y. Z.; Chen, X.; Sun, Z. T.; Yi, Y. Y.; Sun, J. Y.; Zhang, Q. MOF-derived conductive carbon nitrides for separator-modified Li-S batteries and flexible supercapacitors. *J. Mater. Chem. A* **2020**, *8* (4), 1757−1766.
(101) Kumar, Y. A.; Roy, N.; Ramachandran, T.; Assiri, M. A.; Rao, S. S.; Moniruzzaman, M.; Joo, S. W. Revolutionizing energy storage: exploring the nanoscale frontier of all-solid-state batteries. *Dalton Trans.* **2024**, *53* (30), 12410−12433.
(102) Cai, X. Y.; Yi, W. C.; Chen, J.; Lu, L. G.; Sun, B.; Ni, Y. X.; Redfern, S. A. T.; Wang, H. Y.; Chen, Z. F.; Chen, Y. Z. A novel 2D porous C_3N_2 framework as a promising anode material with ultra-high specific capacity for lithium-ion batteries. *J. Mater. Chem. A* **2022**, *10* (12), 6551−6559.
(103) Gorai, D. K.; Kundu, T. K. Modelling, Lithium and phosphorus-functionalized graphitic carbon nitride monolayer for efficient hydrogen storage: A DFT study. *J. Mol. Graph. Modelling* **2023**, *122*, 108493.
(104) Veith, G. M.; Baggetto, L.; Adamczyk, L. A.; Guo, B.; Brown, S. S.; Sun, X.-G.; Albert, A. A.; Humble, J. R.; Barnes, C. E.; Bojdys, M. J.; Dai, S.; Dudney, N. J. Electrochemical and solid-state lithiation of graphitic C3N4. *Chem. Mater.* **2013**, *25* (3), 503−508.
(105) Hankel, M.; Ye, D.; Wang, L.; Searles, D. J. Lithium and sodium storage on graphitic carbon nitride. *J. Phys. Chem. C* **2015**, *119* (38), 21921−21927.
(106) Weng, G.-M.; Xie, Y.; Wang, H.; Karpovich, C.; Lipton, J.; Zhu, J.; Kong, J.; Pfefferle, L. D.; Taylor, A. D. A promising carbon/g-C3N4 composite negative electrode for a long-life sodium-ion battery. *Angew. Chem.* **2019**, *131* (39), 13865−13871.
(107) Zeng, Z.; Su, Y.; Quan, X.; Choi, W.; Zhang, G.; Liu, N.; Kim, B.; Chen, S.; Yu, H.; Zhang, S. Single-atom platinum confined by the interlayer nanospace of carbon nitride for efficient photocatalytic hydrogen evolution. *Nano Energy* **2020**, *69*, 104409.
(108) Moniruzzaman, M.; Reddy, G. R.; Ramachandran, T.; Kumar, Y. A.; Bajaber, M. A.; Alalwiat, A. A.; Joo, S. W. Sodium symphony: Crafting the future of energy storage with sodium-ion capacitors. *J. Energy Storage* **2024**, *95*, 112566.
(109) Li, X. L.; Xu, C. S.; Zhao, K.; Wang, Y. Y.; Pan, L. S. Carbon nitride based mesoporous materials as cathode matrix for high performance lithium-sulfur batteries. *RSC Adv.* **2016**, *6* (16), 13572−13580.
(110) Kim, S.; Hankel, M.; Cha, W.; Singh, G.; Lee, J. M.; Kim, I. Y.; Vinu, A. Theoretical and experimental investigations of mesoporous C3N5/MoS2 hybrid for lithium and sodium ion batteries. *Nano Energy* **2020**, *72*, 104702.
(111) Jiang, L.; Zhang, Z.; Liang, F. H.; Wu, D. N.; Wang, K.; Tang, B. H. J.; Rui, Y. C.; Liu, F. J. Superior lithium-storage properties derived from a g-C_3N_4-embedded honeycomb-shaped meso@mesoporous carbon nanofiber anode loaded with Fe_2O_3 for Li-ion batteries. *Dalton Trans.* **2021**, *50* (28), 9775−9786.
(112) Zhou, P.; Hou, L.; Song, T.; Wang, X.; Yang, J.; Wu, X.; Long, B.; Wu, Y. Tuning N-species of graphitic carbon nitride for high-performance anode in sodium ion battery. *ACS Appl. Energy Mater.* **2022**, *5* (8), 9286−9291.
(113) Cai, X.; Yi, W.; Chen, J.; Lu, L.; Sun, B.; Ni, Y.; Redfern, S. A. T.; Wang, H.; Chen, Z.; Chen, Y. A novel 2D porous C3N2 framework as a promising anode material with ultra-high specific capacity for lithium-ion batteries. *J. Mater. Chem. A* **2022**, *10* (12), 6551−6559.
(114) Kim, S.; Cha, W.; Ramadass, K.; Singh, G.; Kim, I. Y.; Vinu, A. Single-Step Synthesis of Mesoporous Carbon Nitride/Molybdenum Sulfide Nanohybrids for High-Performance Sodium-Ion Batteries. *Chem.-Asian J.* **2020**, *15* (12), 1863−1868.
(115) Kesavan, T.; Partheeban, T.; Vivekanantha, M.; Prabu, N.; Kundu, M.; Selvarajan, P.; Umapathy, S.; Vinu, A.; Sasidharan, M. Design of P-Doped Mesoporous Carbon Nitrides as High-Performance Anode Materials for Li-Ion Battery. *ACS Appl. Mater. Interfaces* **2020**, *12* (21), 24007−24018.
(116) Cha, W.; Kim, I. Y.; Lee, J. M.; Kim, S.; Ramadass, K.; Gopalakrishnan, K.; Premkumar, S.; Umapathy, S.; Vinu, A. Sulfur-Doped Mesoporous Carbon Nitride with an Ordered Porous Structure for Sodium-Ion Batteries. *ACS Appl. Mater. Interfaces* **2019**, *11* (30), 27192−27199.
(117) Hou, Y.; Li, J.; Wen, Z.; Cui, S.; Yuan, C.; Chen, J. N-doped graphene/porous g-C3N4 nanosheets supported layered-MoS2 hybrid as robust anode materials for lithium-ion batteries. *Nano Energy* **2014**, *8*, 157−164.
(118) Liang, S.; Chen, J.; Zhou, N.; Hu, L.; Liu, L.; Wang, L.; Liang, D.; Yu, T.; Tian, C.; Liang, C. CNT threaded porous carbon nitride nanoflakes as bifunctional hosts for lithium sulfide cathode. *J. Alloys Compd.* **2021**, *887*, 161356.
(119) Ma, H.; Liu, X.; Liu, N.; Zhao, Y.; Zhang, Y. G.; Bakenov, Z.; Wang, X. Defect-rich porous tubular graphitic carbon nitride with strong adsorption towards lithium polysulfides for high-performance lithium-sulfur batteries. *J. Mater. Sci. Technol.* **2022**, *115*, 140−147.
(120) Angamuthu, G.; Babu, D. B.; Ramesha, K.; Rangarajan, V. MoS2 anchored carbon nitride based mesoporous material as a polysulfide barrier for high capacity lithium-sulfur battery. *J. Electroanal. Chem.* **2019**, *843*, 37−46.
(121) Davari, E.; Ivey, D. G. Bifunctional electrocatalysts for Zn−air batteries. *Sustainable Energy Fuels* **2018**, *2* (1), 39−67.
(122) Eftekhari, A.; Ramanujam, B. In pursuit of catalytic cathodes for lithium−oxygen batteries. *J. Mater. Chem. A* **2017**, *5* (17), 7710−7731.
(123) Wu, J.; Liu, B.; et al. Carbon-based cathode materials for rechargeable zinc-air batteries: From current collectors to bifunctional integrated air electrodes. *Carbon Energy* **2020**, *2*, 370−386.
(124) Yang, D.; Chen, D.; et al. Carbon-based materials for all-solid-state zinc−air batteries. *Carbon Energy* **2021**, *3*, 50−65.
(125) Ahmed, S.; Shim, J.; Sun, H.-J.; Park, G. Enhanced performance of carbon-coated manganese catalysts derived from metal-organic framework for rechargeable zinc-air batteries. *Surf. Coat. Technol.* **2021**, *408*, 126786.
(126) Ao, K.; Daoud, W. A. Facile controlled formation of CoNi alloy and CoO embedded in N-doped carbon as advanced electrocatalysts for oxygen evolution and zinc-air battery. *Electrochim. Acta* **2021**, *395*, 139204.
(127) Chen, Y.; Wang, H.; Ji, S.; Pollet, B. G.; Wang, R. Toward high performance of zinc-air battery using hydrophobic carbon foam-based diffusion electrode. *J. Ind. Eng. Chem.* **2019**, *71*, 284−292.
(128) Zahoor, A.; Ghouri, Z. K.; Hashmi, S.; Raza, F.; Ishtiaque, S.; Nadeem, S.; Ullah, I.; Nahm, K. S. Electrocatalysts for lithium−air batteries: current status and challenges. *ACS Sustainable Chem. Eng.* **2019**, *7* (17), 14288−14320.
(129) Zhao, W.; Wang, J.; Yin, R.; Li, B.; Huang, X.; Zhao, L.; Qian, L. Single-atom Pt supported on holey ultrathin g-C3N4 nanosheets as efficient catalyst for Li-O2 batteries. *J. Colloid Interface Sci.* **2020**, *564*, 28−36.
(130) Wang, C.; Zhao, H.; Wang, J.; Zhao, Z.; Cheng, M.; Duan, X.; Zhang, Q.; Wang, J.; Wang, J. Atomic Fe hetero-layered coordination between gC3N4 and graphene nanomeshes enhances the ORR electrocatalytic performance of zinc−air batteries. *J. Mater. Chem. A* **2019**, *7* (4), 1451−1458.
(131) Yang, Y.; Chen, T.; Yu, B.; Zhu, M.; Meng, F.; Shi, W.; Zhang, M.; Qi, Z.; Zeng, K.; Xue, J. Manipulating Zn-ion flux by two-dimensional porous g-C3N4 nanosheets for dendrite-free zinc metal anode. *Chem. Eng. J.* **2022**, *433*, 134077.
(132) Ramachandran, T.; Butt, H.; Zheng, L.; Rezeq, M. A review of 2D metal boride-derived nanostructures: From synthesis to energy storage and conversion applications. *J. Energy Storage* **2024**, *99*, 113425.
(133) Chen, W.-F.; Muckerman, J. T.; Fujita, E. Recent developments in transition metal carbides and nitrides as hydrogen evolution electrocatalysts. *Chem. Commun.* **2013**, *49* (79), 8896−8909.
(134) Ito, Y.; Cong, W.; Fujita, T.; Tang, Z.; Chen, M. High catalytic activity of nitrogen and sulfur co-doped nanoporous graphene in the hydrogen evolution reaction. *Angew. Chem., Int. Ed.* **2015**, *54* (7), 2131−2136.

https://doi.org/10.1021/acsomega.5c00679
ACS Omega 2025, 10, 18184−18212

(135) Subbaraman, R.; Tripkovic, D.; Strmcnik, D.; Chang, K.-C.; Uchimura, M.; Paulikas, A. P.; Stamenkovic, V.; Markovic, N. M. Enhancing hydrogen evolution activity in water splitting by tailoring Li+-Ni (OH) 2-Pt interfaces. *Science* **2011**, *334* (6060), 1256−1260.
(136) Alhajri, N. S.; Yoshida, H.; Anjum, D. H.; Garcia-Esparza, A. T.; Kubota, J.; Domen, K.; Takanabe, K. Synthesis of tantalum carbide and nitride nanoparticles using a reactive mesoporous template for electrochemical hydrogen evolution. *J. Mater. Chem. A* **2013**, *1* (40), 12606−12616.
(137) Trasatti, S Work function, electronegativity, and electrochemical behaviour of metals: III. Electrolytic hydrogen evolution in acid solutions. *J. Electroanal. Chem. Interfacial Electrochem.* **1972**, *39* (1), 163−184.
(138) Greeley, J.; Jaramillo, T. F.; Bonde, J.; Chorkendorff, I.; Nørskov, J. K. Computational high-throughput screening of electrocatalytic materials for hydrogen evolution. *Nat. Mater.* **2006**, *5* (11), 909−913.
(139) Santos, E.; Schmickler, W. d-Band catalysis in electrochemistry. *ChemPhysChem* **2006**, *7* (11), 2282−2285.
(140) Han, Q.; Cheng, Z. H.; Gao, J.; Zhao, Y.; Zhang, Z. P.; Dai, L. M.; Qu, L. T. Mesh-on-Mesh Graphitic-C_3N_4@Graphene for Highly Efficient Hydrogen Evolution. *Adv. Funct. Mater.* **2017**, *27* (15), 1606352.
(141) Singh, D. K.; Ganesan, V.; Yadav, D. K.; Yadav, M. Facile synthesis of sulfur-doped mesoporous carbon nitride supported defect-rich cobalt sulfide for electrocatalytic water oxidation. *Cryst. Growth Des.* **2020**, *20* (10), 6321−6328.
(142) Chebanenko, M. I.; Lobinsky, A. A.; Nevedomskiy, V. N.; Popkov, V. I. NiO-decorated graphitic carbon nitride toward electrocatalytic hydrogen production from ethanol. *Dalton Trans.* **2020**, *49* (34), 12088−12097.
(143) Zhu, M.; Yu, S.; Ge, R.; Feng, L.; Yu, Y.; Li, Y.; Li, W. Cobalt oxide supported on phosphorus-doped g-C3N4 as an efficient electrocatalyst for oxygen evolution reaction. *ACS Appl. Energy Mater.* **2019**, *2* (7), 4718−4729.
(144) Alhajri, N. S.; Anjum, D. H.; Takanabe, K. Molybdenum carbide−carbon nanocomposites synthesized from a reactive template for electrochemical hydrogen evolution. *J. Mater. Chem. A* **2014**, *2* (27), 10548−10556.
(145) Gujral, H. S.; Singh, G.; Yang, J. H.; Sathish, C. I.; Yi, J. B.; Karakoti, A.; Fawaz, M.; Ramadass, K.; Al-Muhtaseb, A. H.; Yu, X. J.; Breese, M. B. H.; Vinu, A. Mesoporous titanium carbonitride derived from mesoporous C_3N_5 for highly efficient hydrogen evolution reaction. *Carbon* **2022**, *195*, 9−18.
(146) Wen, L.; Li, F.; Cheng, H.-M. Carbon nanotubes and graphene for flexible electrochemical energy storage: from materials to devices. *Adv. Mater.* **2016**, *28* (22), 4306−4337.
(147) Cui, H.; Zhou, Z.; Jia, D. Heteroatom-doped graphene as electrocatalysts for air cathodes. *Mater. Horiz.* **2017**, *4* (1), 7−19.
(148) Kessler, F. K.; Zheng, Y.; Schwarz, D.; Merschjann, C.; Schnick, W.; Wang, X.; Bojdys, M. J. Functional carbon nitride materials−design strategies for electrochemical devices. *Nat. Rev. Mater* **2017**, *2*, 17030.
(149) Tu, Y.; Deng, D.; Bao, X. Nanocarbons and their hybrids as catalysts for non-aqueous lithium−oxygen batteries. *J. Energy Chem.* **2016**, *25* (6), 957−966.
(150) Li, J.-C.; Hou, P.-X.; Liu, C. Heteroatom-doped carbon nanotube and graphene-based electrocatalysts for oxygen reduction reaction. *Small* **2017**, *13* (45), 1702002.
(151) Liu, X.; Dai, L. Carbon-based metal-free catalysts. *Nat. Rev. Mater.* **2016**, *1* (11), 1278.
(152) Kim, I. Y.; Kim, S.; Jin, X. Y.; Premkumar, S.; Chandra, G.; Lee, N. S.; Mane, G. P.; Hwang, S. J.; Umapathy, S.; Vinu, A. Ordered Mesoporous C_3N_5 with a Combined Triazole and Triazine Framework and Its Graphene Hybrids for the Oxygen Reduction Reaction (ORR). *Angew. Chem., Int. Ed.* **2018**, *57* (52), 17135−17140.
(153) Kim, I. Y.; Kim, S.; Jin, X.; Premkumar, S.; Chandra, G.; Lee, N.-S.; Mane, G. P.; Hwang, S.-J.; Umapathy, S.; Vinu, A. Ordered mesoporous C3N5 with a combined triazole and triazine framework and its graphene hybrids for the oxygen reduction reaction (ORR). *Angew. Chem.* **2018**, *130* (52), 17381−17386.
(154) Kim, I. Y.; Kim, S.; Premkumar, S.; Yang, J.-H.; Umapathy, S.; Vinu, A. Thermodynamically stable mesoporous C3N7 and C3N6 with ordered structure and their excellent performance for oxygen reduction reaction. *Small* **2020**, *16* (12), 1903572.
(155) Singh, D. K.; Ganesan, V.; Yadav, D. K.; Yadav, M. Metal (Mn, Fe, Co, Ni, Cu, and Zn) phthalocyanine-immobilized mesoporous carbon nitride materials as durable electrode modifiers for the oxygen reduction reaction. *Langmuir* **2020**, *36* (41), 12202−12212.
(156) Singh, D. K.; Ganesan, V.; Yadav, D. K.; Yadav, M. Metal (Mn, Fe, Co, Ni, Cu, and Zn) Phthalocyanine-Immobilized Mesoporous Carbon Nitride Materials as Durable Electrode Modifiers for the Oxygen Reduction Reaction. *Langmuir* **2020**, *36* (41), 12202−12212.
(157) Liu, B.; Yao, H.; Daniels, R. A.; Song, W.; Zheng, H.; Jin, L.; Suib, S. L.; He, J. A facile synthesis of Fe_3C@ mesoporous carbon nitride nanospheres with superior electrocatalytic activity. *Nanoscale* **2016**, *8* (10), 5441−5445.
(158) He, L.; Cui, B.; Liu, J.; Wang, M.; Zhang, Z.; Zhang, H. Fabrication of porous CoO x/mC@ MoS2 composite loaded on g-C3N4 nanosheets as a highly efficient dual electrocatalyst for oxygen reduction and hydrogen evolution reactions. *ACS Sustainable Chem. Eng.* **2018**, *6* (7), 9257−9268.
(159) Fu, X. R.; Hu, X. F.; Yan, Z. H.; Lei, K. X.; Li, F. J.; Cheng, F. Y.; Chen, J. Template-free synthesis of porous graphitic carbon nitride/carbon composite spheres for electrocatalytic oxygen reduction reaction. *Chem. Commun.* **2016**, *52* (8), 1725−1728.
(160) Rouquerol, F., Rouquerol, J.; Sing, K. *Adsorption by Powders and Porous Solids−Principles Methodology and Applications*; Academic Press: London, 1999; p 467.
(161) Xu, R.; Pang, W.; Yu, J.; Huo, Q.; Chen, J. *Chemistry of Zeolites and Related Porous Materials: Synthesis and Structure*; John Wiley & Sons (Asia) Pet Ltd.: Singapore, 2007.
(162) Leung, D. Y.; Caramanna, G.; Maroto-Valer, M. M. An overview of current status of carbon dioxide capture and storage technologies. *Renewable Sustainable Energy Rev.* **2014**, *39*, 426−443.
(163) *The Paris Agreement*; United Nations Climate Change ConferenceCOP21 or CMP11, Paris, France, Nov 30−Dec 12, 2015.
(164) IPCC. *Climate Change 2014: Synthesis Report. Contribution of Working Groups I, II and III to the Fifth Assessment Report of the Intergovernmental Panel on Climate Change*; Pachauri, R. K.; Meyer, L. A., Eds.; IPCC: Geneva, 2014.
(165) Wang, M.; Lawal, A.; Stephenson, P.; Sidders, J.; Ramshaw, C. design, Post-combustion CO_2 capture with chemical absorption: A state-of-the-art review. *Chem. Eng. Res. Des.* **2011**, *89* (9), 1609−1624.
(166) Taheri, M.; Zhu, R.; Yu, G.; Lei, Z. Ionic liquid screening for CO_2 capture and H2S removal from gases: The syngas purification case. *Chem. Eng. Sci.* **2021**, *230*, 116199.
(167) Alivand, M. S.; Tehrani, N. H. M. H.; Shafiei-Alavijeh, M.; Rashidi, A.; Kooti, M.; Pourreza, A.; Fakhraie, S. Synthesis of a modified HF-free MIL-101 (Cr) nanoadsorbent with enhanced H2S/CH4, CO_2/CH4, and CO_2/N2 selectivity. *J. Environ. Chem. Eng.* **2019**, *7* (2), 102946.
(168) Alivand, M. S.; Najmi, M.; Tehrani, N. H. M. H.; Kamali, A.; Tavakoli, O.; Rashidi, A.; Esrafili, M. D.; Ghasemy, E.; Mazaheri, O. Tuning the surface chemistry and porosity of waste-derived nanoporous materials toward exceptional performance in antibiotic adsorption: Experimental and DFT studies. *Chem. Eng. J.* **2019**, *374*, 274−291.
(169) Song, C.; Liu, Q.; Deng, S.; Li, H.; Kitamura, Y. J. R. Cryogenic-based CO_2 capture technologies: State-of-the-art developments and current challenges. *Renewable Sustainable Energy Rev.* **2019**, *101*, 265−278.
(170) Wahab, M. A.; Na, J.; Masud, M. K.; Hossain, M. S. A.; Alothman, A. A.; Abdala, A. Nanoporous carbon nitride with a high content of inbuilt N site for the CO_2 capture. *J. Hazard. Mater.* **2021**, *408*, 124843.

https://doi.org/10.1021/acsomega.5c00679
ACS Omega 2025, 10, 18184−18212

(171) Park, D. H.; Lakhi, K. S.; Ramadass, K.; Kim, M. K.; Talapaneni, S. N.; Joseph, S.; Ravon, U.; Al-Bahily, K.; Vinu, A. Energy Efficient Synthesis of Ordered Mesoporous Carbon Nitrides with a High Nitrogen Content and Enhanced CO_2 Capture Capacity. *Chem.—Eur. J.* **2017**, *23* (45), 10753−10757.
(172) Tabarkhoon, F.; Abolghasemi, H.; Rashidi, A.; Bazmi, M.; Alivand, M. S.; Tabarkhoon, F.; Farahani, M. V.; Esrafili, M. D. Synthesis of novel and tunable Micro-Mesoporous carbon nitrides for Ultra-High CO_2 and H2S capture. *Chem. Eng. J.* **2023**, *456*, 140973.
(173) Li, X. Q.; Lv, X.; Ding, S. Y.; Huang, L.; Wei, Z. Mixed matrix membranes containing composite nanosheets with three-dimensional nanopores for efficient CO_2 separation. *Int. J. Greenhouse Gas Control* **2022**, *117*, 103658.
(174) Kim, S.; Singh, G.; Sathish, C. I.; Panigrahi, P.; Daiyan, R.; Lu, X. Y.; Sugi, Y.; Kim, I. Y.; Vinu, A. Tailoring the Pore Size, Basicity, and Binding Energy of Mesoporous C_3N_5 for CO_2 Capture and Conversion. *Chem.-Asian J.* **2021**, *16* (23), 3999−4005.
(175) Lakhi, K. S.; Baskar, A. V.; Zaidi, J. S. M.; Al-Deyab, S. S.; El-Newehy, M.; Choy, J. H.; Vinu, A. Morphological control of mesoporous CN based hybrid materials and their excellent CO_2 adsorption capacity. *RSC Advances* **2015**, *5* (50), 40183−40192.
(176) Khan, M. A.; Javed, A. H.; Qammar, M.; Hafeez, M.; Arshad, M.; Zafar, M. I.; Aldawsari, A. M.; Shah, A.; ur Rehman, Z.; Iqbal, N. Nitrogen-rich mesoporous carbon for high temperature reversible CO_2 capture. *J. CO_2 Util.* **2021**, *43*, 101375.
(177) Lakhi, K. S.; Cha, W. S.; Joseph, S.; Wood, B. J.; Aldeyab, S. S.; Lawrence, G.; Choy, J.-H.; Vinu, A. Cage type mesoporous carbon nitride with large mesopores for CO_2 capture. *Catal. Today* **2015**, *243*, 209−217.
(178) Lakhi, K. S.; Park, D. H.; Joseph, S.; Talapaneni, S. N.; Ravon, U.; Al-Bahily, K.; Vinu, A. Effect of Heat Treatment on the Nitrogen Content and Its Role on the Carbon Dioxide Adsorption Capacity of Highly Ordered Mesoporous Carbon Nitride. *Chem.-Asian J.* **2017**, *12* (5), 595−604.
(179) Liu, Z. L.; Li, X.; Shi, D.; Guo, F. Z.; Zhao, G.; Hei, Y. X.; Xiao, Y. F.; Zhang, X.; Peng, Y. L.; Sun, W. C. Superior Selective CO_2 Adsorption and Separation over N2 and CH4 of Porous Carbon Nitride Nanosheets: Insights from GCMC and DFT Simulations. *Langmuir* **2023**, *39* (18), 6613−6622.
(180) Joseph, S.; Kempaiah, D. M.; Benzigar, M.; Baskar, A. V.; Talapaneni, S. N.; Jhung, S. H.; Park, D. H.; Vinu, A. Metal organic framework derived mesoporous carbon nitrides with a high specific surface area and chromium oxide nanoparticles for CO_2 and hydrogen adsorption. *J. Mater. Chem. A* **2017**, *5* (40), 21542−21549.
(181) Refaat, Z.; El Saied, M.; El Naga, A. O. A.; Shaban, S. A.; Hassan, H. B.; Shehata, M. R.; El Kady, F. Y. Mesoporous carbon nitride supported MgO for enhanced CO_2 capture. *Environ. Sci. Pollut. Res.* **2023**, *30* (18), 53817−53832.
(182) Eid, K.; Sliem, M. H.; Jlassi, K.; Eldesoky, A. S.; Abdo, G. G.; Al-Qaradawi, S. Y.; Sharaf, M. A.; Abdullah, A. M.; Elzatahry, A. A. Precise fabrication of porous one-dimensional gC_3N_4 nanotubes doped with Pd and Cu atoms for efficient CO oxidation and CO_2 reduction. *Inorg. Chem. Commun.* **2019**, *107*, 107460.
(183) Guo, R.; Arkhurst, B.; Fan, X.; Lee, M.-w.; Lin, W.-j.; Shih, Y.-H.; Rokh, G. B.; Li, H.; Sasmita, S.; Zhou, Y.; Chan, S. L. I. Unveiling room temperature hydrogen storage in tubular graphitic carbon nitride with diverse morphologies. *Energy Conversion Management* **2023**, *20*, 100496.
(184) Bucuci, M.; Ungureanu, Ş.; Miron, A.; Cziker, A. C. Hydrogen Storage Potential of the Graphitic Carbon Nitride. In *2023 10th International Conference on Modern Power Systems (MPS)*; IEEE, 2023; pp 1−6. DOI: 10.1109/MPS58874.2023.10187412
(185) Arkhurst, B.; Guo, R.; Rokh, G. B.; Chan, S. L. I. Hydrogen Storage Properties of Graphitic Carbon Nitride Nanotube Synthesized by Mix-Grind Technique. In *TMS Annual Meeting & Exhibition*; Springer, 2023; pp 223−231. DOI: 10.1007/978-3-031-22638-0_22
(186) Guo, R.; Tseng, Y.-S.; Retita, I.; Bahmanrokh, G.; Arkhurst, B.; Chan, S. J. M. T. C. A detailed experimental comparison on the hydrogen storage ability of different forms of graphitic carbon nitride (bulk, nanotubes and sheets) with multiwalled carbon nanotubes. *Mater. Today Chem.* **2023**, *30*, 101508.
(187) Park, S. S.; Chu, S.-W.; Xue, C.; Zhao, D.; Ha, C.-S. Facile Synthesis of Mesoporous Carbon Nitrides Using the Incipient Wetness Method and the Application as Hydrogen Adsorbent. *J. Mater. Chem.* **2011**, *21*, 10801−10807.
(188) Moradi, S. E. Highly-ordered Metal-modified Mesoporous Carbon Nitride: As a Novel Hydrogen Adsorbent. *Chem. Biochem. Eng. Q.* **2014**, *28* (3), 267−272.
(189) Conner, W. C.; Falconer, J. L. Spillover in heterogeneous catalysis. *Chem. Rev.* **1995**, *95* (3), 759−788.
(190) Lueking, A. D.; Yang, R. T. Erratum: Hydrogen Spillover from a Metal Oxide Catalyst onto Carbon Nanotubes–Implications for Hydrogen Storage. *J. Catal.* **2002**, *211*, 565.
(191) Wang, P. G.; Xia, K. S.; Chen, Y. R.; Tian, Q. F.; Xiong, R.; Han, B.; Gao, Q.; Zhou, C. G.; Yu, D. Acid-assisted synthesis of nitrogen-deficient mesoporous graphitic carbon nitride for hydrogen storage. *Mater. Lett.* **2021**, *301*, 130347.
(192) Oh, Y.; Le, V. D.; Maiti, U. N.; Hwang, J. O.; Park, W. J.; Lim, J.; Lee, K. E.; Bae, Y. S.; Kim, Y. H.; Kim, S. O. Selective and Regenerative Carbon Dioxide Capture by Highly Polarizing Porous Carbon Nitride. *ACS Nano* **2015**, *9* (9), 9148−9157.
(193) Ramachandran, T.; Mourad, A.-H. I.; ElSayed, M. S. A. Nb2CTx-based MXenes most recent developments: from principles to new applications. *Energies* **2023**, *16* (8), 3520.
(194) Kumar, Y. A.; Kalla, R. M. N.; Ramachandran, T.; Fouda, A. M.; Hegazy, H.; Moniruzzaman, M.; Lee, J. Mxene mastery: Transforming supercapacitors through solid-solution innovations. *J. Ind. Eng. Chem.* **2025**, *145*, 216.
(195) Kumar, Y. A.; Raorane, C. J.; Hegazy, H. H.; Ramachandran, T.; Kim, S. C.; Moniruzzaman, M. 2D MXene-based supercapacitors: A promising path towards high-performance. *J. Energy Storage* **2023**, *72*, 108433.
(196) Ramachandran, T.; Hamed, F.; Kumar, Y. A.; Raji, R. K.; Hegazy, H. H. Multifunctional covalent-organic frameworks (COFs)-2D MXenes composites for diverse applications. *J. Energy Storage* **2023**, *73*, 109299.
(197) Kumar, Y. A.; Reddy, G. R.; Ramachandran, T.; Kulurumotlakatla, D. K.; Abd-Rabboh, H. S.; Hafez, A. A. A.; Rao, S. S.; Joo, S. W. Supercharging the future: MOF-2D MXenes supercapacitors for sustainable energy storage. *J. Energy Storage* **2024**, *80*, 110303.

https://doi.org/10.1021/acsomega.5c00679
ACS Omega 2025, 10, 18184−18212